

https://dspace.org/

Treatment of stored radioactive liquid organic waste at NECSA prior to disposal

Topkin, James Lamont

2011-07-07
http://hdl.handle.net/10539/10283

Downloaded from a DSpace repository. https://dspace.org/

TREATMENT OF STORED RADIOACTIVE LIQUID ORGANIC WASTE AT NECSA PRIOR TO DISPOSAL

A dissertation submitted to the Faculty of Science, University of the Witwatersrand, in fulfilment of the requirements for the degree of Master of Science.

By

James Lamont Topkin

Supervisor:

Prof. **Ewa M. Cukrowska** (School of Chemistry, Wits)

DECLARATION

I, James Lamont Topkin, declare that this dissertation, submitted to the University of the Witwatersrand Johannesburg, is my own, unaided work. It has not been presented before for any degree or examination to any other university.

_____

James Lamont Topkin

November 2010

ABSTRACT

Liquid radioactive waste containing small quantities of organic compounds are stored in high density polyethylene (HDPE) drums at the South Africa Nuclear Energy Corporation (Necsa). These wastes were not encapsulated into cement like other waste streams due to the possibility that the organic compounds in the waste can act as plasticizer that will retard and prevent the curing of a cement matrix.

Results from this study indicated that combined treatment technologies such as polymeric resin absorption, ozone purging and UV radiation are necessary in order to successfully encapsulate this type of waste into a specialised matrix that will fulfil the waste disposal requirements of the Vaalputs waste disposal site. The use of a polymeric absorbent utilised as a filter has the possibility of reducing the absorbent costs significantly.

ACKNOWLEDGEMENTS

I would like to convey a special thank you to Dr. W.C.M.H. Meyer, research advisor at Necsa, for all his assistance and advice.

I am very grateful to Prof Ewa Cukrowska for her support and Wits University for allowing me to do my dissertation at their institute.

I sincerely thank Dr J.R. Zeevaart for his support of my studies.

I also am sincerely thankful to Necsa for allowing me to submit this work as well as my colleagues for their input.

Also thank you to my Creator, God, and lastly to my wife and kids for their support.

CHAPTER 1 INTRODUCTION **1**

CHAPTER 2 LIQUID ORGANIC WASTE **4**

2.1 Sampling of Liquid Waste **4**

2.2 The Processes in Nuclear Industry That Generated Organic Waste **6**

2.2.1 PUREX process 6

2.2.2 Liquid organic waste generated in nuclear laboratories 8

2.2.3 Organic complexation agents used for decontamination 9

2.3 Treatment of Liquid Organic Waste **11**

2.4 Non-thermal processes to destroy the organic constituents in waste **13**

2.4.1 Alkaline hydrolysis process 13

2.4.2 Hydrogen peroxide 15

2.4.3 Potassium permanganate 15

2.4.4 Ozone 16

2.4.5 Peroxydisulphate oxidation of organic waste 19

2.4.6 Acid digestive organic destructive technology 20

2.4.7 Organic destruction by ultraviolet radiation 20

2.4.8 Silver (II) process as an electrochemical method to destroy organic compounds 23

2.4.9 Solvate electron oxidation 24

2.4.10 Drying, evaporation and distillation 24

2.4.11 Biological treatment 24

2.5 Thermal Methods for Treatment of Organic Waste **25**

2.5.1 Incineration 25

2.5.2 Plasma treatment of organic waste 26

2.5.3 Microwave treatment of organic waste 28
2.5.4 Molten salt oxidation of organic waste..... 28
2.5.5 Supercritical water oxidation..... 29

2.6 Solidifying Techniques as Treatment for Organic Waste..... 29
2.6.1 Polymeric resins used as sorbents for treatment of organic waste 30
2.6.2 Direct immobilization with cement 32

2.7 Conclusion 33

2.8 Objectives of Research 34

CHAPTER 3 METHODS AND TECHNIQUES USED..... 35

3.1 Sampling of Liquid Waste in Carboys..... 35
3.1.1 Safety requirements to collect samples from radioactive waste drums..... 35
3.1.2 Sampling procedure..... 35

3.2 Experimental Procedure for Alkaline Hydrolysis of Organic Waste 37

3.3 Experimental Procedure for Ozone Degradation..... 38

3.4 Experimental Procedure for UV and Ozone Destruction..... 39

3.5 Plasma Destruction Technique..... 40

3.6 In Line Filter Sorption 42

3.7 Encapsulation of the Nochar Resin into Cement..... 45
3.7.1 Analysing for sorptivity..... 47
3.7.2 Leaching analysis 48

3.8 Instruments Used in Study 50
3.8.1 Gas chromatography analysis method..... 50
3.8.2 Gas chromatogram mass spectrometry (GC-MS) 53

3.8.3 Ultra violet visible spectrophotometry method 54
3.8.4 Infrared spectrophotometer analyses 57
3.8.5 Gamma spectrophotometry 59

CHAPTER 4 RESULTS AND DISCUSSIONS 61

4.1 Extraction of a Representative Sample 61

4.2 Alkaline Hydrolysis Treatment Method on the Test Mix Components 67

4.3 Non Thermal Treatment of the Components of the Test Mixture 74
4.3.1 Ozone and UV Treatment 74
4.3.2 Stability and UV Lamp Tests 74
4.3.3 Scintillation Liquid 76
4.3.4 Contrad 81
4.3.5 Acetone 86

4.4 Treatment of the Organic Test Mixture with the Non Transfer DC Thermal Plasma 92
4.5 Absorption of Organic Components onto Nochar N910, Polymeric Resins. 95
4.5.1 Absorbance of Contrad detergent on Nochar resin 95
4.5.2 Absorbance of scintillation liquid on Nochar resin 97
4.5.3 Absorbance of acetone on Nochar resin 97
4.5.4 Absorption of TBP Diluted in Acetone onto Nochar 98
4.5.4 Stability of the TBP-Nochar complex 99

4.6 Encapsulation of the TBP / Kerosene Mixture by PPC Cement in Combination with Poly Acrylonitrile Fibres and Polyvinyl Alcohol Fibres 102

CHAPTER 5 SUMMARY OF RESULTS 107

CHAPTER 6 RECOMMENDATIONS 109

APPENDIXES 111

APPENDIX 1 111

APPENDIX 2 112

APPENDIX 3 113

APPENDIX 4 114

APPENDIX 5 115

APPENDIX 6 116

APPENDIX 7 117

APPENDIX 8 118

APPENDIX 9 120

APPENDIX 12 126

APPENDIX 13 127

APPENDIX 14 128

APPENDIX 15 129

REFERENCES 130

LIST OF FIGURES

Figure 1.1 South African Nuclear Energy Corporation situated close to Hartebeespoortdam 1

Figure 1.2 Storage of radioactive liquid organic waste in high density polyethylene containers in a secure area with liquid containment facilities 2

Figure 2.1 Sampling hazardous liquid waste according to procedure of the US army corps of engineers (2001) 5

Figure 2.2 Principle of the PUREX process (European Nuclear Society, 2010) 6

Figure 2.3 Scintillation reactions (Kirsten, 1999) 8

Figure 2.4 Detergent molecules surround organic matter and form a micelle in water 10

Figure 2.5 Commonly used detergents displaying their long organic structures 10

Figure 2.6 Alkaline hydrolyses process (Manohar et al., 1999) 13

Figure 2.7 Hydrolysis reactions of TBP 14

Figure 2.8 Example of direct oxidation of thio-ethers by ozone 17

Figure 2.9 Example of double bond cleavage with ozone 18

Figure 2.10 Silver (II) process 23

Figure 2.11 Plasma torch used for organic destruction at Necsa 27

Figure 2.12 Influence of 70 Million Rad gamma radiation on Nochar encapsulated oil 31

Figure 2.13 Cumulative amount of 2-chloroaniline released during the dynamic leach test 33

Figure 3.1 Schematic representation of the stirring of the liquid organic waste 36

Figure 3.2 Schematic representation of the sampling setup for the liquid organic waste 36

Figure 3.3 Experimental setup for the alkaline hydrolysis process 37

Figure 3.4 Ozone / UV degradation experimental setup 38

Figure 3.5 Schematic representation of the ozone degradation experimental. 39

Figure 3.6 Schematic representation of the experimental setup of ozone combined with UV degradation 40

Figure 3.7 Plasma torch used for destruction of test mixture 41

Figure 3.8 Resin absorption experimental set up 43

Figure 3.9 Sorptivity measurements with bottom side and top sides of samples not coated with vacuum grease 48

Figure 3.10 Leaching tests on samples containing radioactive nuclides (LEU) 49

Figure 3.11 Gas chromatography schematically represented 50

Figure 3.12 Open tubular capillary tubing 51

Figure 3.13 GC chromatogram of a standard solution of organic substances dissolved in heptane 52

Figure 3.14 GC Mass spectrometry 53

Figure 3.15 Cary 100 UV-visible spectrophotometer 55

Figure 3.16 UV-visible absorbance spectra of 0.5% acetone in deionised water 56

Figure 3.17 Scanning kinetics (acetone degradation) detected by UV-visible instrument 57

Figure 3.18 Scanning kinetics from UV-visible spectra at 270 nm 57

Figure 3.19 FTIR instrument with ATR diamond crystal for quick and rapid sample analyses 58

Figure 3.20 FTIR transmissions scan of TBP 59

Figure 4.1 Sampling equipment 61

Figure 4.2 Sampling 100 ml of waste solution demonstrating that all components in the test mixture can be sampled 62

Figure 4.3 UV-visible spectra of waste samples (H014 RARW140 and RARW167) 64

Figure 4.4 UV-visible spectrum of 0.6% Contrad standard 64

Figure 4.5 Calibration curve for Contrad standards 65

Figure 4.6 Infrared analyses (absorption) of the sampled waste solutions compared to Contrad detergent 66

Figure 4.7 FTIR spectra of analytical grade TBP (blue) and TBP that underwent alkaline hydrolysis (red) 68

Figure 4.8 GC-MS analysis of an alkaline hydrolysed 30% TBP-kerosene solution 69

Figure 4.9 FTIR spectra of TBP with 5% Contrad detergent before (blue) and after alkaline hydrolyses (red) 70

Figure 4.10 TBP Kerosene (30/70%) standard mixture 71

Figure 4.11 Scintillation liquid 71

Figure 4.12 GC-MS analysis of an alkaline hydrolysed organic test mixture without 10% Contrad detergent 72

Figure 4.13 GC-MS analysis of the organictest mixture with additional 10% Contrad in the water 73

Figure 4.14 Stability test for scintillation liquid (20 ppm) 75

Figure 4.15 Stability tests on deionised water when purged with ozone to evluate the influence on the baseline 75

Figure 4.16 Determination of the emissions of the UV lamp 76

Figure 4.17 Scintillation liquid, 10 ppm, purged with ozone 76

Figure 4.18 Degradation rates for 10 ppm scintillation liquid 77

Figure 4.19 Degradation with UV radiation of scintillation liquid (20 ppm) 78

Figure 4.20 Degradation rate of UV on scintillation liquid 78

Figure 4.21 Influence of ozone purging combined with UV radiation on scintillation liquid (40 ppm) 79

Figure 4.22 Degradation rates of scintillation liquid at 240 nm for UV and ozone 80

Figure 4.23 UV and ozone degradation rates of scintillation liquid 80

Figure 4.24 Stability tests for experimental setup with a 0.2% Contrad solution 81

Figure 4.25 Ozone degradation of Contrad soap (0.2%) 82

Figure 4.26 Ozone degradation rate of Contrad soap (0.2%) at 220 nm 82

Figure 4.27 UV degradation of Contrad (0.2%) 83

Figure 4.28 Degradation rate of Contrad (UV radiation) 84

Figure 4.29 Contrad degraded by UV radiation and ozone purging 85

Figure 4.30 Degradation rate of Contrad because of UV radiation and ozone purging 85

Figure 4.31 Comparison of degradation rates of Contrad detergent 86

Figure 4.32 Acetone Stability tests 87

Figure 4.33 UV spectra of ozone degradation of acetone 87

Figure 4.34 Degradation rate of ozone on (0.6%) acetone 88

Figure 4.35 UV spectra of acetone radiated with UV light 89

Figure 4.36 Degradation rates of acetone with UV light 89

Figure 4.37 UV spectra of degradation of acetone by UV radiation and ozone purging 90

Figure 4.38 Degradation rate of acetone with UV radiation and ozone purging 91

Figure 4.39 Comparison of degradation rates of acetone 91

Figure 4.40 GC results of gaseuos sample from plasma experiment on the test mixture 1st run 93

Figure 4.41 GC results of gaseous sample from plasma experiment on the test mixture 2nd run 94

Figure 4.42 UV-visible spectrum of Contrad 10% (initial solution) 95

Figure 4.43 UV-visible spectrum of Contrad 12% (initial solution C2 after K_D tests) 96

Figure 4.44 UV-visible spectrum of Contrad 15% (initial solution C3 after K_D tests) 96

Figure 4.45 UV-visible spectraof scintilation liquid (10 ppm) before and after it has been filtered through a Nochar filter 97

Figure 4.46 UV-visible spectrum showing the absorption of acetone on Nochar 910 resin 98

Figure 4.47 GC analysis of TBP in acetone absorbed onto Nochar resin 99

Figure 4.48 Sorptivity results 103

Figure 4.49 Photos of the Fibre reinforced oil – N 910 encapsulated bricks. 105

Figure 4.50 Temperature stability of oil absorbed onto Nochar 106

Figure 6.1 Schematic diagram for the proposed treatment of mixed liquid waste 109

LIST OF TABLES

Table 2.1 Main bonds broken in radiolyses of pure organic compounds 9

Table 2.2 Possible applicability of destructive techniques (IAEA, 1989) 12

Table 2.3 Formation enthalpies for ozone (Horvath et al., 1980) 19

Table 2.4 Redox potentials for chemical oxidants (Horvath et al., 1980) 19

Table 2.5 Dissociation energies of organic bonds measured in nm wavelength 21

Table 2.6 UV initiated reactions of peroxide in water (Song et al., 2008) 22

Table 2.7 Properties of the 30% TBP with kerosene mixture used in liquid reprocessing plants 29

Table 3.1 Tracer samples prepared 43

Table 3.2 Sorption tests of Contrad and acetone on N910 44

Table 3.3 Sample compositions without uranium 46

Table 3.4 Composition of samples containing uranium 46

Table 4.1 GC-MS analyses results of samples taken from carboys 63

Table 4.2 Nochar in line filter activity counts 100

Table 4.3 Uranium activity in liquid after 5 minutes 100

Table 4.4 Uranium activity when Contrad detergent is present 101

Table 4.5 Sorption coefficients for the different matrixes 104

Terminology

Abs	Absorbance
ATR	Attenuated transmission spectroscopy
Carboys	20 Litre high density polyethylene drums
DC	Direct Current
DBP	Dibutyl phosphate
eV	Electron Volt
FTIR spectroscopy	Fourier transform infrared spectroscopy
GC	Gas chromatography
HDPE	High density polyethylene
IAEA	International Atomic Energy Association
IR spectroscopy	Infrared Spectroscopy
kPa	Kilo pascal
LLW	Low level waste
LEU	Low enriched uranium
nm	Nanometer
PAN	Polyacrylonitrile
PE	Polyethylene
ppm	Parts per million
PUREX	Plutonium – Uranium Extraction Process
$PVA_{(OH)}$	Polyvinyl alcohol
RAD	Radiation measurement unit
RPO	Radiation protection officer
SAE	Society for Automotive engineers
TBP	Tributyl phosphate
UV-vis	Ultraviolet visible spectroscopy
WAC	Waste acceptance criteria

Chapter 1 INTRODUCTION

During research on reprocessing of spent fuel at the Atomic Energy Corporation (AEC) of South Africa (Figure 1.1) renamed South Africa Nuclear Energy Corporation (Necsa), various types of liquid organic waste solutions were generated. The generated organic waste consists mostly of organic solvents, scintillation liquid as well as Contrad detergent that was used for decontamination.



Figure 1.1 South African Nuclear Energy Corporation situated close to Hartebeespoortdam

The treatment of these radioactive organic waste solutions for encapsulation prior to disposal was deferred in the 1970s due to the low volumes generated. The waste was stored under controlled conditions in metal drums. After 10 years of storage, the

metal drums started to corrode and the radioactive organic waste were transferred from these metal drums into twenty litres high density polyethylene drums (HDPE) known as “carboys” as shown in Figure 1.2. Carboys are still used in radiological laboratories for the accumulation of liquid radioactive waste. The re-storage of mixed radioactive organic waste into HDPE drums was preferred as HDPE is resistant against most organic liquids. Unfortunately, the HDPE drums, currently in the dry store are deteriorating due to UV light and radiation interaction.



Figure 1.2 Storage of radioactive liquid organic waste in high density polyethylene containers in a secure area with liquid containment facilities

New Necsa policy dictates that storage is no longer an option and all organic liquid waste must be treated and solidified for disposal at Vaalputs. Solidification is

necessary as the Waste Acceptance Criteria (WAC) of the South African disposal site called Vaalputs (Beyleveld and Truter, 2005) is licensed only to accept solidified waste.

The direct solidification of organic waste into cement matrixes is not feasible as organic components in the waste can act as plasticizers preventing curing of a cement matrix. The use of sorbents prior to encapsulation (Sora et al., 2002) can be considered.

Disposal of stored tributyl phosphate (TBP), an organic solvent, that are used to extract uranium from liquid solutions during the fuel re-processing cycle, cannot be done due to the possible presence of uranium and /or plutonium complexes. Another problem is that degraded components of TBP, dibutyl phosphate (DBP), also forms complexes with most metal radioisotopes. The direct encapsulation of TBP into cement will result in the leaching of organic TBP constituents through the matrix, thereby facilitating the migration of radionuclides into the environment. Internationally TBP is hydrolysed with alkaline solutions in order to destroy the TBP-uranium complexes and after purification, the resulting liquid can then be encapsulated into cement.

Chapter 2 LIQUID ORGANIC WASTE

2.1 Sampling of Liquid Waste

The sampling of hazardous waste must be approached with outmost caution as described in the available literature (US Army Corps of Engineers Manual, 2001). Similar deliberations must be taken when considering the information available in the Technical Notes 414 (Innis, 2004) for sampling hazardous waste from drums. The containers, according to these sources, must firstly be inspected to evaluate their integrity. Bulging of a closed container indicate for instance high internal pressures and should only be sampled when the pressure is equilibrated with the outside pressure. Air monitoring during extraction in the sampling vicinity is compulsory to determine possible inhalation of airborne organic compounds. Sampling of a stored container has the possibility of consisting of different layers due to settling and sampling devices such as a stratified sample thief is therefore recommended (Figure 2.1). This sampling device would not suffice for Necsa, as the possibility of contact with radioactive nuclides and volatile organic components formed from radiolysis could be troublesome as most drums have been standing for more than 10 years. Settling of different layers of the organic liquids due to different densities as well as the possibility of precipitants could result in an inhomogeneous sample.

As the liquid organic waste at Necsa contains radioactive nuclides together with hazardous chemicals, a safe sampling method from brittle containers to produce representative samples are crucial for this work and was therefore investigated.

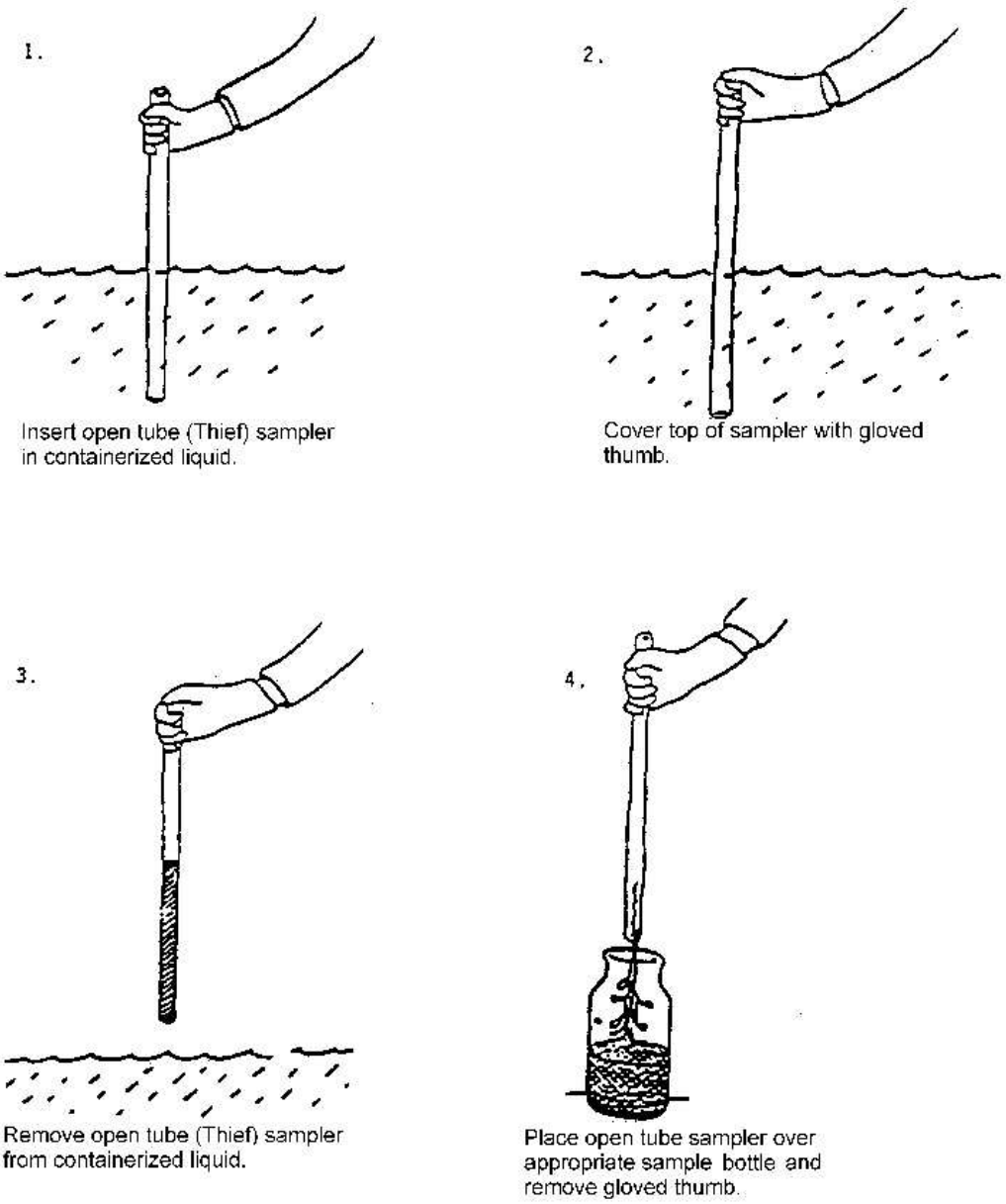

Figure 2.1 Sampling hazardous liquid waste according to procedure of the US army corps of engineers (2001)

2.2 The Processes in Nuclear Industry That Generated Organic Waste

2.2.1 PUREX process

The PUREX process is used at most major plants for the reprocessing of spent nuclear fuel to separate uranium and plutonium from the fission products and from one another (Appendix 1). Following the dissolution of the irradiated fuel in aqueous nitric acid, uranium and plutonium are transferred to an organic phase by intensive mixing with an organic solvent extraction of 30% TBP in kerosene (as organic solvent) while the fission products remain in the aqueous nitric phase (Figure 2.2). Further process steps (not applicable to this study) enable the subsequent separation of uranium and plutonium from one another (Horwitz and Schulz, 1986).

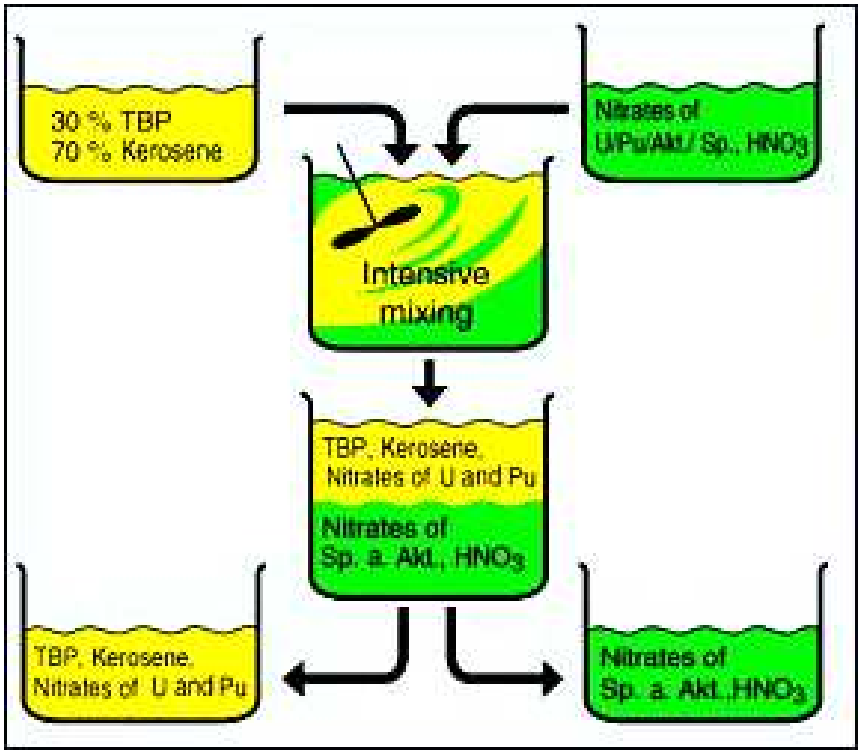

Figure 2.2 Principle of the PUREX process (European Nuclear Society, 2010)

TBP is an organic phosphorus compound with the formula, $(CH_3CH_2CH_2CH_2O)_3PO$ and is the extractant of choice in spent nuclear fuel reprocessing. It can exist in different states that are dictated by the conditions of the solution for example TBP can dimerise in solution, $2TBP \leftrightarrows (TBP)_2$.

During the uranium extraction process, uranium (VI) reacts with nitrates to form uranyl nitrate (Morss et al, 2006). This uranyl nitrate transfers into the organic TBP phase and complexes as follows:

$$UO_2^{2+}(aq) + 2NO_3^-(aq) + 2TBP \leftrightarrows UO_2(NO_3)_2(TBP)_2 \quad (1)$$

The higher the concentration of nitrate ions in the organic aqueous mixture, the more uranium complexes with TBP in the organic phase occurs. Radiolysis of the different organic compounds used in the PUREX process will result in the possible formation of hydrocarbon gases and other organic compounds. Radiolysis can also induce reactive centres for cross-linking reactions and this will result in the formation of organic compounds with increased viscosity, reduced oxidative stability and decreased flash points. TBP itself is a phosphate ester that converts into dibutyl phosphate (DBP) during radiation whereas kerosene forms aliphatic chains of different chain lengths under radiation. The net result is an increase in viscosity (Bolt and Carrol, 1963). DBP forms complexes with many metals and these metals cannot be extracted. This is a drawback and necessitates a scrubbing plant for DBP in all industries that use TBP as extraction medium. The stored drums at Necsa therefore contain DBP, TBP and a range of organic structures resulting from the radiolysis of these organic compounds.

2.2.2 Liquid organic waste generated in nuclear laboratories

Radioactive research and quality control laboratories at Necsa are using scintillation liquid for radioactivity measurements and after analysis it is discarded into the carboys. Scintillation liquid consists of a mixture of substances such as solvents, emulsifiers and fluorescence producing substances. These substances in the scintillation liquid absorb the kinetic energy of particles produced by radioactive decay and transform this absorbed energy into a fluorescence signal (Figure 2.3) measured by sensitive photo multiplier detectors.

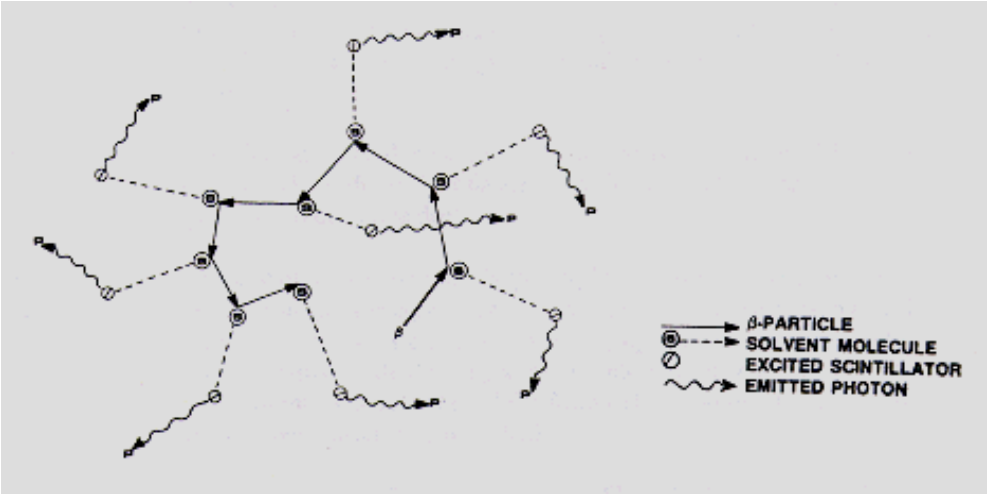

Figure 2.3 Scintillation reactions (Kirsten, 1999)

The scintillation liquid used at Necsa is Ultima Gold AB supplied by Perkin Elmer. The composition of this scintillation liquid consists of six components, namely nonylfenolethoxylaat, 2-(butoxyethoxy) ethanol, diisopropyl naphthalene isomers, 2,5-diphenyloxazole, 1,4-bis(2-methylstyryl)-benzene and nonyl-phenyl polyoxyethylene ether phosphate. The flashpoint of this mixture starts at 140 ˚C and

therefore the mixture cannot auto ignite at room temperature. Radiolysis of these polyphenyl type organic molecules causes a preferential break of the C-H bond (Table 2.1) compared to the rupture of the benzene ring (Bolt and Carrol, 1963). As Necsa's carboys contain scintillation liquid generated in the analytical laboratories, it can contain organic compounds as mentioned in Table 2.1.

Table 2.1 Main bonds broken in radiolyses of pure organic compounds (Bolt and Carrol, 1963)

Compound type	Main attack site
Saturated hydrocarbons	C-H, C-C
Unsaturated hydrocarbons	C-H C-C, polymerisation or cross-linking
Aromatic	C-H, side chain C-C
Alcohols	C-COH, H-COH
Ethers	C-H, C-OR
Aldehydes and ketones	C-H, OC-OR
Esters	C-H, OC-COOR
Carboxylic acids	C-H, OC-COOH
Fluorides	C-H, C-C

2.2.3 Organic complexation agents used for decontamination

Work surfaces contaminated with radioisotopes are decontaminated at Necsa with detergents called "Contrad". This detergent can be classified as an EDTA type organic compound specifically for the complexation of metals. This detergent consists of a water soluble polar segment attached to a hydrocarbon chain as well as a water insoluble component that acts as a solvent for organic liquids. This structure

facilitates the absorption of organic material into water as a micelle (Kevelam, 1999) with the polar part of the detergent associating with the water molecules as shown in Figure 2.4 and Figure 2.5 (Misra et al., 2009). The presence of micelles in the carboys complicates the treatment of organic waste in radioactive solutions.

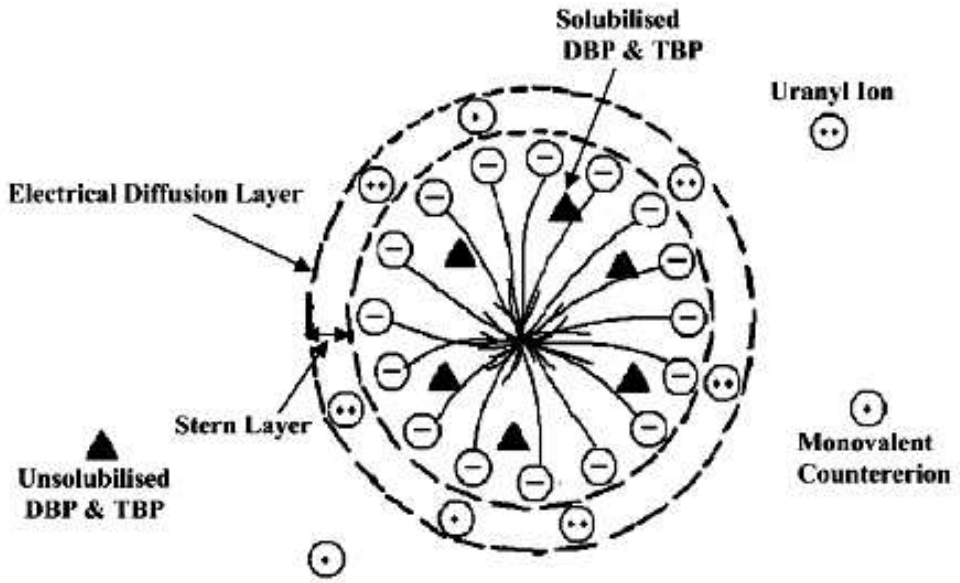

Figure 2.4 Detergent molecules surround organic matter and form a micelle in water (Misra et al., 2009)

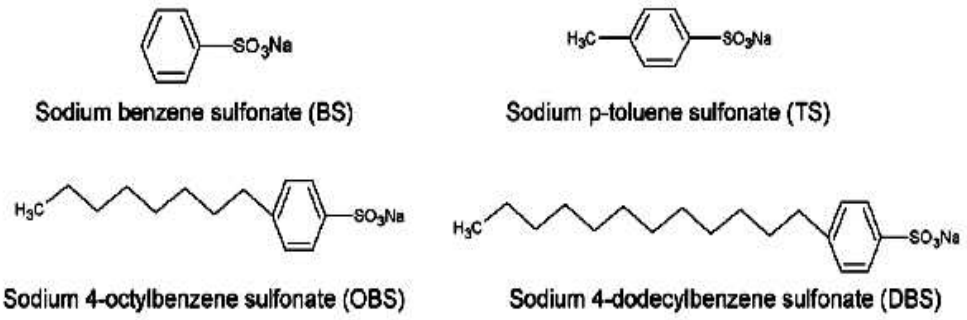

Figure 2.5 Commonly used detergents displaying their long organic structures (Kevelam, 1999)

2.3 Treatment of Liquid Organic Waste

Selection of a specific treatment technology for liquid organic waste are dictated by the economics (Gomez, 2009) of the process, waste volume reduction required, complexity of technology, level of process development and regulatory requirements (IAEA, 1989:10). Treatment and conditioning techniques of organic waste can be grouped into thermal and non-thermal destructive techniques.

Thermal destruction of liquids and solids produces huge volumes of gas that require additional treatment prior to releasing it into the environment (for example wet oxidation with hydrogen peroxide). Although the modern type incinerator design at present meets strict regulatory requirements for destruction and removal efficiency, public concerns still exist. Another drawback of incinerators is the formation of dioxins and furans, gaseous acids that can liberate radionuclides, and other volatile organic matter.

The degradation products of organic constituents in a radioactive environment increase the risks and difficulty of treatment of these constituents. The radiolytical degradation products could be for instance unknown heat generators and flammable components that could pose a danger to the workforce and environment during treatment of these waste streams (IAEA, 1989:35). Non-thermal techniques are widely researched and used in industry. Table 2.2 is a summary of the possible non-thermal technologies that can be considered for the treatment of Necsa's organic waste.

Table 2.2 Possible applicability of destructive techniques (IAEA, 1989)

Technique	Mixed Solids	Lubricants	Organic Solvents	Other Liquids
Electrochemical	N		Y	Y
Direct chemical oxidation			Y	
Acid digestion	Y		Y	
Ozonolysis*		Y	Y	Y
Wet oxidation		Y	Y	Y
Advanced oxidation*				Y
Supercritical water oxidation	Y		Y	
Biological treatment				
Thermo chemical treatment				
Microwave treatment				Y
Incineration	Y	Y	Y	Y
Alkaline hydrolysis*			Y	
Plasma treatment*	Y	Y	Y	Y
Molten salt oxidation			Y	

Y= Known to be appropriate: N = Not appropriate: Blank = Unknown

* - Chosen techniques evaluated at Necsa

2.4 Non-thermal processes to destroy the organic constituents in waste

2.4.1 Alkaline hydrolysis process

This process is a well known treatment for destruction of organic waste preferentially for TBP degradation products such as dibutyl phosphoric acid, DBP, mono-butyl phosphoric acid, H_2MBP, and phosphoric acid. The alkaline hydrolysis process is used specifically for treatment of spent PUREX solvent in India (Raj et al., 2006). The diluent kerosene, used in combination with TBP, is however resistant to alkaline hydrolyses reactions. In the alkaline hydrolyses process (Figure 2.6).

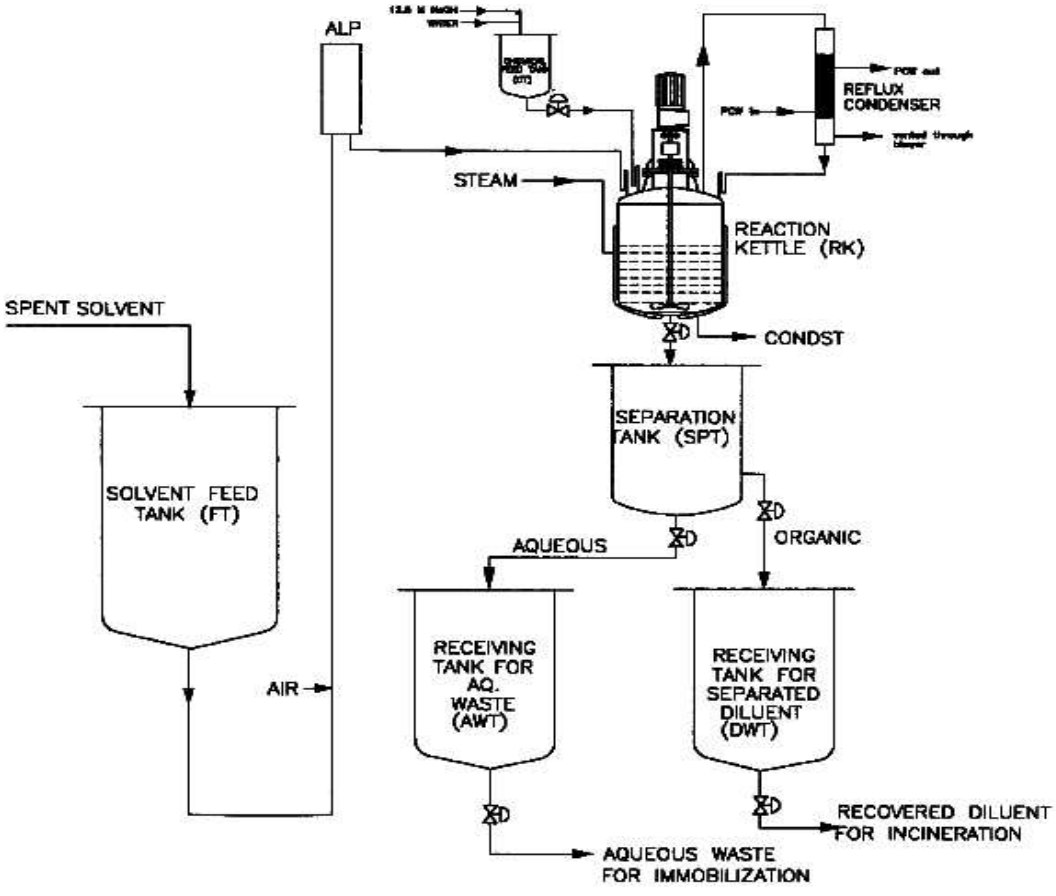

Figure 2.6 Alkaline hydrolyses process (Manohar et al., 1999)

TBP, DBP and other organic compounds are hydrolysed when subjected to 12.5 M NaOH at 125 ˚C. During the hydrolysis process of TBP (Figure 2.7) sodium salts of dibutyl phosphoric acid (NaDBP) forms in the aqueous phase while butanol as a reaction product, remains in the organic top phase. The organic layer containing butanol is incinerated in a furnace while the water phase containing the radioactive nuclides and NaDBP is solidified (Manohar et al., 1999) into cement.

Both acid and alkaline hydrolysis is possible, but in industry the alkaline reaction is favoured as described in equation 2.

$$(C_4H_9O)_3PO + NaOH \rightarrow (C_4H_9O)_2POONa + C_4H_9OH \qquad (2)$$

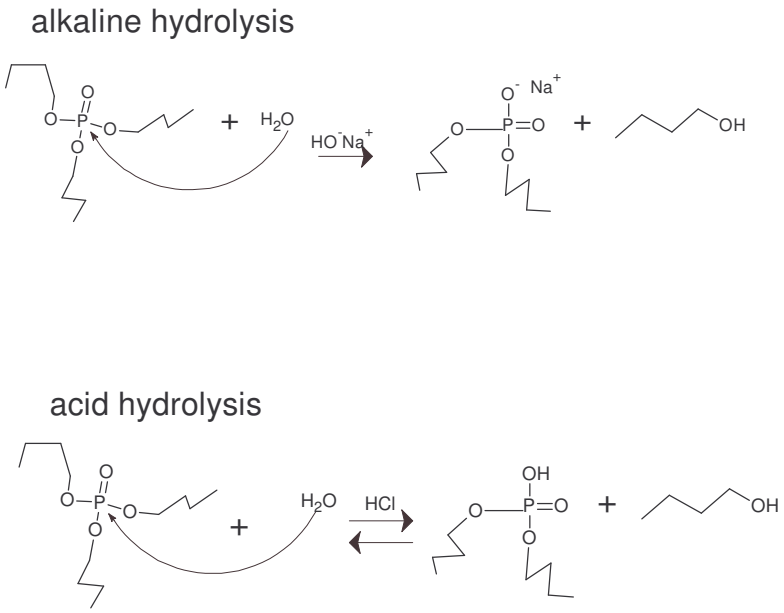

Figure 2.7 Hydrolysis reactions of TBP

The alkaline process is an irreversible process and the hydroxide ion promotes the reaction, thereby increasing the rate of hydrolyses over the acid hydrolysis of the

ester (Paula et al., 2008). The suitability of this process for the treatment of historical waste at Necsa was researched as part of this thesis.

2.4.2 Hydrogen peroxide

Chemical oxidation processes are used in the treatment of radioactive liquid waste to reduce odours, decolourizes effluent, destroy organic matter and improve precipitation and flocculation (Kidd, 1995:7). Addition of liquid hydrogen peroxide (H_2O_2) in the presence of ferrous iron (Fe^{2+}) produces Fenton's Reagent which yields free hydroxyl radicals ($^{\cdot}OH$). These hydroxyl radicals abstract hydrogen atoms from organic carbon structures (Gunale et al., 2009) creating double bonds in the organic structure as well as organic radicals. The ferrous iron stabilizes the organic radicals preventing recombination thereby increasing the quantity of hydroxyl radicals. Oxidation with Fenton's reagent is most effective under acidic conditions (e.g. pH 2 to 4) and becomes ineffective under moderate to strongly alkaline conditions. These reactions are extremely rapid and follow second-order kinetics. This technique for treatment of organic liquid waste at Necsa was not considered as large volumes of hydrogen peroxide (36%) is required in a ratio of 20:1 hydrogen peroxide to waste (Nardi, 1989). Using this technique would increase the volume of secondary waste.

2.4.3 Potassium permanganate

The reaction of another typical chemical oxidizing agent, permanganate ($KMnO_4$), is complex (also available in Na, Ca, or Mg salts). As the manganese ion has multiple valence states it can participate in numerous side reactions. The oxidation reactions proceed at a somewhat slower rate than peroxide and ozone reactions. Depending on the pH (El-Dessouky et al., 2001), the reaction mechanism includes a direct electron transfer or free radical mechanism. Although permanganate reactions are effective over a wide pH range (between 3.5 and 12), the increased volumes created by using

this technique is unfavourable for application at Necsa.

2.4.4 Ozone

Ozone is one of the strongest oxidizing agents that can interact with organic liquids as the structure of ozone is such that an oxygen atom can easily be detached, yielding a free oxygen radical to interact with the organic material (Horvath et al., 1980).

The reaction of ozone and organic substances can be written as a first order kinetic equation

$$Ln(C/C_0) = -kt \qquad (3)$$

Where k is the reaction rate constant, C_0 the initial organic constituent concentration, and C the final organic concentration. Typical rate values from $4x10^{-3}$ s^{-1} to $4x10^{-4}$ s^{-1} was found in laboratories (Klasson, 2002).

The reaction mechanism of ozone with organic substances can be via radical or an electrophyllic / nucleophyllic attack. The ozone reacts with the aqueous medium resulting in the formation of degradation products and hydroxyl radicals (equation 4). This formed hydroxyl radicals can then react with organic substances in the aqueous medium as described in equation 5. The combined rate equation for the two mechanisms can be described as indicated in equation 6.

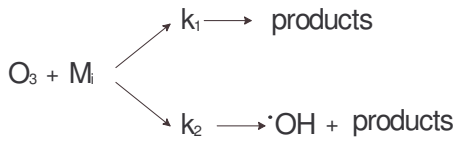

(4)

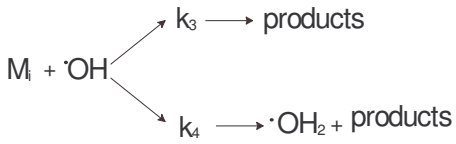

(5)

$$d[M_i]/d_t = (k_1+k_2)[O_3][M_i] + (k_3+k_4)[OH][M_i] \quad (6)$$

Where $[M_i]$ is the concentration of the organic pollutant, $[O_3]$ the ozone concentration, and [OH] the radical concentration (Bruno, 1991).

Ozone can react as an electrophilic reactant or as a nucleophilic reactant (Figure 2.8). From the schematic presentations in Figures 2.8 and 2.9 it is clear that ozone reactions with organic molecules follow three different pathways. Firstly, a common oxidation reaction of ozone is attaching to organic structures, secondly the formation of ozonides and thirdly, the development of peroxide compounds as presented in Figure 2.8 and Figure 2.9.

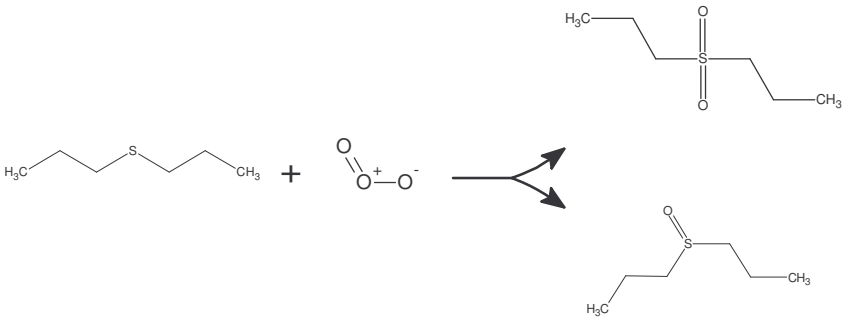

Figure 2.8 Example of direct oxidation of thio-ethers by ozone

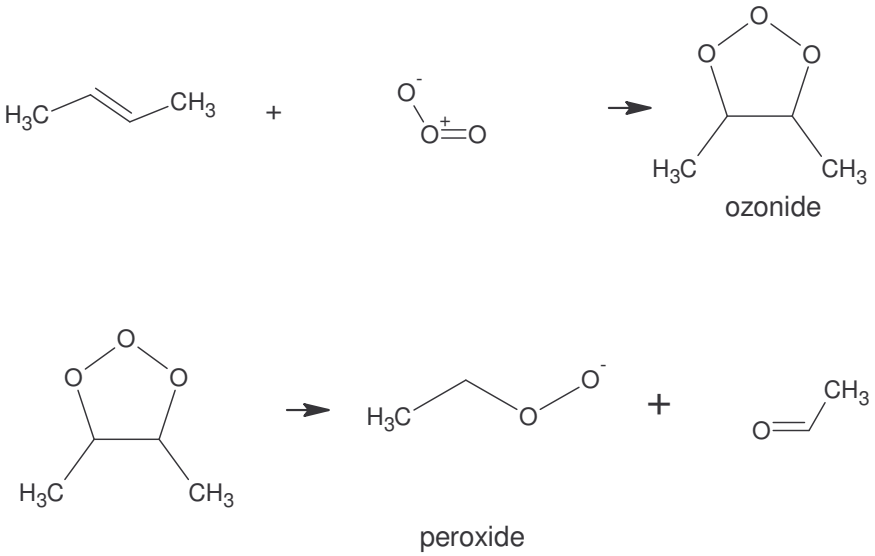

Figure 2.9 Example of double bond cleavage with ozone

Ozone can be manufactured from dry air or oxygen using an electric field to generate corona discharges between electrodes. Like peroxide oxidation, ozone reactions are effective in systems with a neutral or alkaline pH. In acidic conditions the $^{\cdot}OH$ radicals recombine to form water (Table 2.3) thereby reducing the effectiveness of this technique.

When comparing the chemical reactivity of chemical oxidants (Table 2.4), the reaction rates of ozone with organic components are fast therefore ozone is the preferred technique is in the water purifying industry for organic destruction.

Table 2.3 Formation enthalpies for ozone (Horvath et al., 1980)

Chemical reaction	Formation Enthalpies (ΔH_f^0)
$O + O \rightarrow O_2$	-494.9 kJ mol^{-1}
$O + O_2 \rightarrow O_3$	-106.3 kJ mol^{-1}
$O + O + O \rightarrow O_3$	-601.2 kJ mol^{-1}
$\therefore O + O_2 \rightarrow O_3$	**- 126.9 kJ mol^{-1}**

Table 2.4 Redox potentials for chemical oxidants (Horvath et al., 1980)

Redox systems	Normal redox potentials (V)
F_2 (gaseous) / 2 F^-	+2.85
$O_3 + 2\ H^+ / O_2 + H_2O$	+2.07
$MnO^-_4 + 4H^+ / MnO_2 + 2H_2O$	+1.69
Cl_2 / 2 Cl^-	+1.36
Fe^{3+} / Fe^{2+}	+0.77

Ozone oxidation is currently used in Japan (Appendix 4) and will be tested for the possible destruction of organic waste at Necsa (minimum volume increase).

2.4.5 Peroxydisulphate oxidation of organic waste

Oxidation reactions in aqueous systems can be increased with the use of sodium or ammonium peroxydisulphate (IAEA, 2004:54). Peroxydisulphate is a strong oxidant, operating at temperatures between 80 and 90 °C, without a catalyst. This technique has been demonstrated on laboratory scale. The increased sulphate concentration generated with this process could negatively influence the final encapsulation of waste.

2.4.6 Acid digestive organic destructive technology

This technique uses strong mineral acids at elevated temperatures, around 250 °C, to oxidize organic structures (IAEA, 2004:55). Depending on the waste, the reaction could produce sludge, inorganic oxides and / or gases like sulphur and nitrogen oxides. The restrictions are that the equipment must be manufactured from highly resistant material and the extensive off-gas scrubbing system required makes this technique unfavourable for the treatment of organic waste at Necsa.

2.4.7 Organic destruction by ultraviolet radiation

Photolysis of organic compounds is the reaction with photons produced by a light source which leads to the destruction of chemical bonds and formation of less hazardous organic by-products. The light source must emit photons at a wavelength in the UV region so that it can be absorbed by the organic molecule for the chemical bonds to break (Phillips, 1983). Table 2.5 shows the energies required for dissociation of specific bonds. A useful property of UV light is that it has radiation properties sufficient to excite atoms and molecules. These excited molecules may release energy by either returning to the ground state or by participating in chemical reactions or in a chemical change through intermolecular or intramolecular rearrangements.

Table 2.5 Dissociation energies of organic bonds measured in nm wavelength (Phillips, 1983)

Bond	Dissociation Energy ($kcal.mol^{-1}$)	Maximum wavelength for dissociation (nm)
C-C	82.6	346.1
C=C	145.8	196.1
C≡C	199.6	143.2
C-F	116.0	246.5
C-H	98.7	289.7
C=N	72.8	194.5
C≡N	147.0	134.5
C-O	85.5	334.4
C=O aldehydes	176.0	162.4
C=O ketones	179.0	159.7
C-S	65.0	439.9
C=S	166.0	172.2
H-H	104.2	274.4
N-N	52.0	549.8
N=N	60.0	476.5
N≡N	226.0	126.6
N-H	85.0	336.4
N-H (NH_3)	102.2	280.3
N-O	48.0	595.6
O-O (O_2)	119.1	240.1
-O-O-	47.0	608.3
O-H (Water)	117.5	243.3
S-H	83.0	344.5
S-N	115.2	248.6
S-O	119.0	240.3

Destruction of the organic bonds is therefore achieved by an indirect photochemical process that uses UV energy to generate hydroxyl radicals (Table 2.6) from hydrogen peroxide in the mixed aqueous solution. These radicals then oxidize the organic species in the water to produce carbon dioxide, water, and some reaction by-products.

Table 2.6 UV initiated reactions of peroxide in water (Song et al., 2008)

Initiation	$H_2O_2 + hv$	$\longrightarrow 2HO^{\cdot}$
Propagation	$H_2O_2 + HO^{\cdot}$	$\longrightarrow HO^{\cdot}_2 + H_2O$
	$H_2O_2 + HO^{\cdot}_2$	$\longrightarrow HO^{\cdot} + H_2O + O_2$
Termination	$2HO^{\cdot}$	$\longrightarrow H_2O_2$
	$2HO^{\cdot}_2$	$\longrightarrow H_2O_2 + {}^{-}O^{\cdot}_2$
	$HO^{\cdot} + HO^{\cdot}_2$	$\longrightarrow H_2O + O_2$
Decomposition	$RH + HO^{\cdot}$	$\longrightarrow$ Products
	$RH + HO^{\cdot}_2$	$\longrightarrow$ Products

The generation of UV radiation can be done with a combination of different light sources. These different light sources are for example medium and low pressure mercury lamps (Appendix 3), xenon lamps and laser beams. This technique will be considered for Necsa because it complies with strict regulatory requirements and most organic compounds can be oxidised by choosing a UV region corresponding with the organic waste type.

2.4.8 Silver (II) process as an electrochemical method to destroy organic compounds

This method uses highly reactive ions and their properties to break organic bonds and destroy the organic material. For instance, Ag^{2+} ions in an electrochemical cell, known as the silver (II) process (Judd, 2001), are commonly used (Figure 2.10) in the destruction of organic compounds. The mechanism is that a feedstock of Ag^{+} in nitric acid is circulated in the cell where Ag^{+} is transformed to Ag^{2+} ions. Organic matter is then broken down by the Ag^{2+} ions into carbon dioxide, insoluble inorganic salts and water which migrate through a membrane. During the interaction with the organic waste, the Ag^{2+} ions is reduced to Ag^{+} and can be recycled. Insoluble inorganic precipitates are extracted from the anolyte circuit using for example a hydrocyclone. No low molecular volatile compounds are formed in the process during the destruction of the organic structures. The reaction can be performed at low temperatures and the reaction rate is easily controllable with an electric current. Unfortunately it is complex technology with high capital-operating costs. As equipment was not available at Necsa this technique was not considered at this stage, however this technique will be tested in the future for waste minimization.

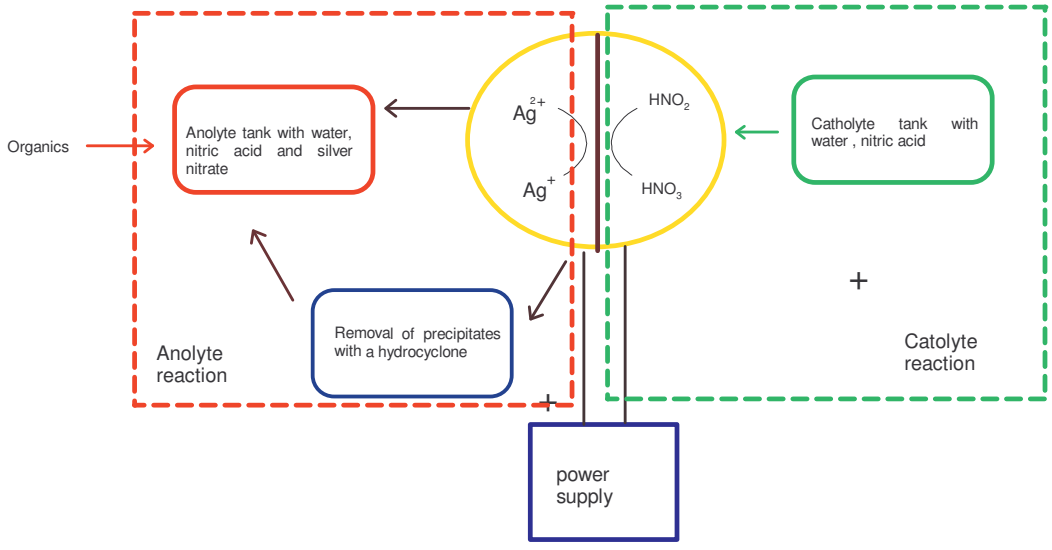

Figure 2.10 Silver (II) process

2.4.9 Solvate electron oxidation

This is a new technique still in development that uses the powerful reducing properties of free electrons to destroy functional groups on organic structures. The electrons are produced by dissolving sodium metal in liquid ammonia. The process is patented therefore not considered for this study.

2.4.10 Drying, evaporation and distillation

Drying, evaporation and distillation technologies are normally used as a pre-treatment technique for reducing the volume of organic material as shown in Appendix 2. Drying will result in the formation of solids or sludges. The evaporated component can be recovered (IAEA, 2004:21). This technique needs advanced equipment for large scale application and was not considered for the organic waste at Necsa as no operating license for such an organic destruction facility was granted by the NNR (National Nuclear Regulator) at the time of research.

2.4.11 Biological treatment

The biological treatment uses bacteria to metabolize and digest organic components in waste. In an oxygen rich environment, carbon dioxide is mainly produced whereas in an anaerobic environment methane is produced. This technique was not considered for Necsa, as bacteria are substrate specific (IAEA, 2004:60), and digestion rates are very slow.

2.5 Thermal Methods for Treatment of Organic Waste

Section 2.3 dealt with the destruction of organic waste by non-thermal methods. The following subsections discuss the destruction of organic waste by thermal methods.

2.5.1 Incineration

Conventional incineration uses heat and oxygen to combust organic waste. Since organic waste is combustible, it can provide sufficient heat to maintain the incineration reaction. The products from complete incineration are carbon dioxide, water, oxides from combustion products and metals. In all incineration processes of organic waste containing radioactive nuclides, a final product with higher radionuclide content is produced.

Pyrolysis is an incineration technique without the presence of oxygen. It usually operates at a lower temperature than conventional incineration, producing organic waste divided into primarily carbon monoxide and hydrogen. Pyrolysis is especially used for destruction of organic waste that generates toxic compounds upon conventional incineration (Schwinkendorf et al., 1997). These advantages of pyrolysis over conventional incineration are offset by additional pre-treatment such as ion exchange resins required for certain waste types.

The advantages of incineration are that it leads to complete destruction of the organic material to inorganic residues. The volume-mass reduction is high and applicable to solid and liquid materials. Ash residues produced are easily immobilized into cement matrixes for long term storage. The disadvantages are relative high capital costs, maintenance costs and the off-gas products.

Incineration is also not favourably perceived by the public and currently Necsa has no license to operate such a facility. At present TBP is not incinerated because of the

corrosion difficulties associated with the formation of phosphoric acid during decomposition of TBP at high temperatures.

2.5.2 Plasma treatment of organic waste

The plasma state can be generally described as consisting of a gaseous mixture of oppositely charged particles with an approximate zero net charge (Denes and Sorin, 2004). The gaseous mixture can be ionized either by high energy radiation, electric fields, or heat. The energy levels of the gas that gets exposed to these high energy sources increases significantly. The results are electrons being released from the gas to form heavy charged particles. The most suited plasma forming materials are thermally stable in solid, liquid and gaseous states. Plasmas can be divided in two main types, hot plasmas and cold plasmas. Hot plasmas or near equilibrium plasmas are categorized by the very high temperatures of the electrons and heavy particles with close to 100% ionization. Cold plasmas, also called non-equilibrium plasmas, consist of low temperature particles and relative high temperature electrons with low degrees of ionization. Plasmas constantly lose their energy to their surroundings by collisions and radiation and require a continuous energy supply. The easiest means of creating plasmas in a laboratory environment is by constantly supplying electrical energy to inorganic, thermally stable gaseous materials.

A non-transferred dc arc type of plasma (Figure 2.11) can be described as an electrical arc confined in a small circular cross section that can generate very high temperatures in the presence of a gas flowing in a specifically designed nozzle. The nozzle channels the plasma fluid in a certain required direction. In a non-transferred plasma set up, the gas flow rates are higher and the energy is dissipated into the gas flow. The plasma torch consists of a nozzle with a cone shaped cathode located inside the cylindrical anode that extends beyond the inner cathode. Inert thermally stable gases flows in this nozzle around the cone shaped cathode exiting the anode,

therefore in between the electrodes. The inert gases are instantly ionized during operation of the plasma device creating the plasma flame at the anode exit. The electrodes are cooled with water to avoid it melting down. The generation of the electric arc is a result of a high voltage impulse and a steady high intensity current.

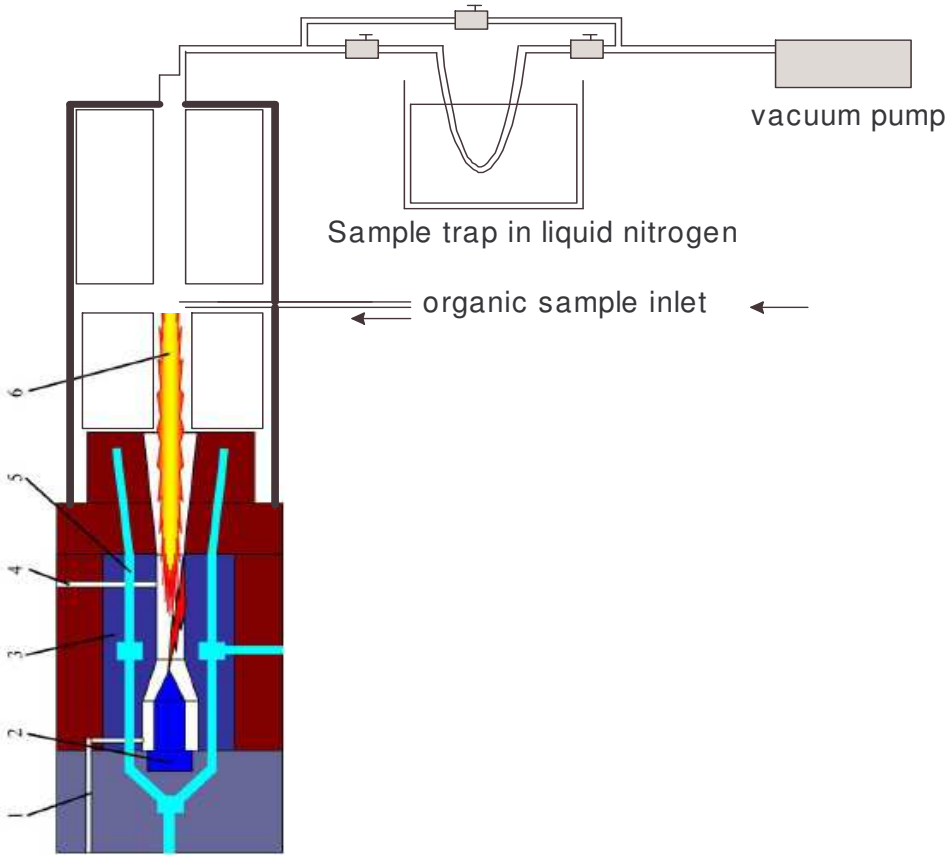

Figure 2.11 Plasma torch used for organic destruction at Necsa showing the flame path way; 1-gas inlet; 2-cathode; 3-anode; 4-sample injection port; 5-cooling system; 6-plasma jet

The use of plasmatechnologies was considered for the minimization of organic waste at Necsa and results will be discussed.

2.5.3 Microwave treatment of organic waste

Applied microwave energy could be used to disintegrate organic waste by destroying the chemical bonds within the organic structure. Heat is generated from vibrations induced by the microwaves in dipolar molecules. Microwave oxidation technology can handle only small volumes of organic waste and the encapsulations of the solid product formed as well as the resulting gases, require further treatment. This process is not recommended for large scale organic waste treatment (Wagner, 1997) as the cost of microwave technology is huge and this technology has not been commercially proved for large scale operations.

2.5.4 Molten salt oxidation of organic waste

The molten salt technology uses a bath of molten alkaline salts at temperatures between 500 and 950 °C to oxidize organic waste. The organic waste reacts with oxygen in the excess salt mixture to produce carbon dioxide, water and inorganic residues (Adamson et al., 1998). Corrosive gases produced during the oxidation processes are neutralized and the radionuclides are trapped inside the molten alkali. These accumulated residues can only be removed when the remaining salts from the process are recycled. Operation of a molten salt system occurs at temperatures hundreds of degrees lower than conventional incineration conditions. The molten salt technique is not considered for treating radioactive organic waste mixtures because of the possibility of explosive organic constituents existing inside the Necsa waste as indicated in (Table 2.7).

Table 2.7 Properties of the 30% TBP with kerosene mixture used in liquid reprocessing plants

Property	Kerosene ($C_6 – C_{16}$)	TBP($C_{12}H_{27}O_4P$)
Flashpoint (°C)	37 - 65	120
Boiling point (°C)	150 -275	298
Auto ignition temperature (°C)	220	482
Density ($g.cm^{-3}$)	0.78	0.97
Water solubility ($mg.L^{-1}$)	0	400 at 20 °C

2.5.5 Supercritical water oxidation

When water is above its critical temperature and pressure (374 °C and 22 MPa) it acts like a non-polar fluid solvating all organic material (Schwinkendorf et al., 1997). Organic constituents are oxidized to carbon dioxide, water and insoluble inorganic salts. These high temperatures and pressures require high capital input for research and bigger plants. This technique shows huge potential for extracting uranium with minimal use of organic extractants and will be investigated at a later stage when equipment becomes available.

2.6 Solidifying Techniques as Treatment for Organic Waste

In case of the organic waste at Necsa not being able to be treated successfully, encapsulation is the only viable option. Encapsulation possibilities are as follows.

2.6.1 Polymeric resins used as sorbents for treatment of organic waste

2.6.1.1 Petroset II

Fluid Tech, Inc manufactures an absorbent called Petroset, to solidify waste (Meyer, 2009) products. Petroset II is an organophillic absorbent that could absorb most organic liquids, such as oils and other hydrocarbon solutions. Polar activators are needed to accelerate the curing of Petroset II, and low-molecular weight alcohols such as methanol, propanol, or isopropyl alcohol can be used. By mixing organic waste and Petroset II at lower temperatures, a solid product is set irreversibly. Petroset II cure into a stiff putty-like form within twenty-four hours, depending on the contents of the waste and the solidification matrix

2.6.1.2 Nochar absorbents

Nochar's Petrobond and Acidbond are a group of third generation polymers specifically polymerized to absorb organic compounds, sludges, acids, alkaline and aqueous radioactive waste into a solid matrix. Nochar polymer technology has been used with success in the immobilization of waste oil by a number of nuclear facilities. This technology also offers a solution as it reduces the reliance on incineration technology.

The Imbiber Beads® and Nochar® products consist of polymeric repeat units consisting of a polystyrene backbone. Nochar used as aqueous solution spill stabilizers originate from functionality modifying polypropylene and polyacrylates polymers whereas Petroset® and Aquaset® materials are modified aluminosilicate minerals (clays).

The Nochar polymer technology consists of a range of granulated polymer products which act to immobilise a variety of liquid waste streams via absorption and an inter-

molecular bonding process. This mechanism of immobilization is not encapsulation. The organic waste becomes part of the granular polymer via this process of inter-molecular bonding. Nochar has been shown to be able to immobilize liquid waste streams with a volumetric increase of typically 5% of that of the liquid waste stream. The absorption process is neither endothermic nor exothermic, therefore no heat is involved and no harmful chemical gases are formed. These polymeric resins are non-toxic, non-hazardous, non-biodegradable, produce no leaching of material, maintain long-term stability without degradation and is incinerable, which make them attractive for use in industry (Kelly, 2005). An example of gamma irradiation (Cobalt ^{60} source, at 30 Rad per second) that was applied to the solid waste form can be seen (Figure 2.12). Other advantages of this product are that it is a safe and simple mixing process delivering a final product for short, intermediate or final storage / burial. If incinerated it produces less than 0.02% ash. It also combines well with grout / cement and is stable against radiation. It was tested with Cobalt ^{60} gamma radiation under the following conditions: 270 million Rad on organic / acid waste, 90 million Rad on organic waste mixed with TBP and 75 million Rad on aqueous waste at pH 14.2.

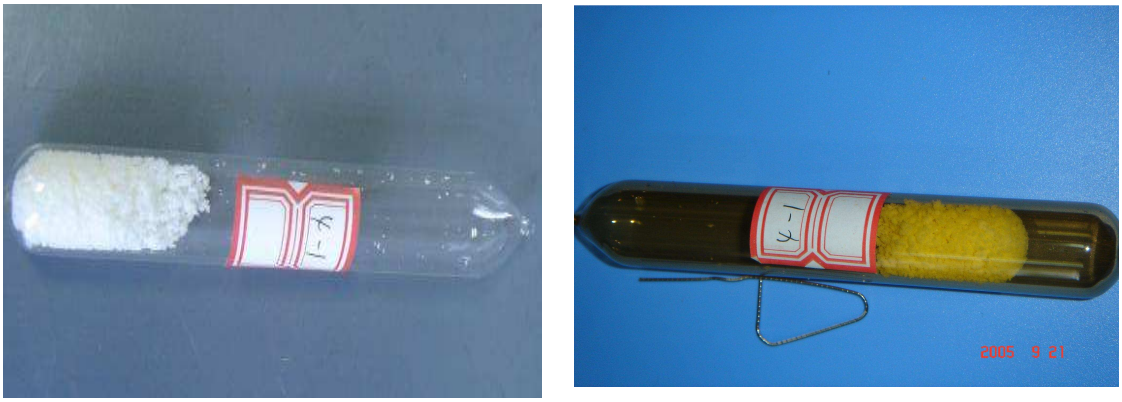

A - Before B - After

Figure 2.12 Influence of 70 Million Rad gamma radiation on Nochar encapsulated oil

The supplier of this resin recommends the testing of the waste prior to treatment with its resin for optimal absorption. With their different types of bonding polymers, the consultants would then formulate unique polymer combinations for every waste stream (waste drum) to absorb liquid waste. This can in certain aspects require chemical treatment to adjust the pH to an acceptable level for maximum absorption.

2.6.2 Direct immobilization with cement

Encapsulating organic waste directly in cement is not feasible without pretreatment with adsorbents (Sora et al., 2002). The biggest concerns are that the cement curing is compromised and that the organic constituents can leak out of the paste whilst mixing and or curing. Studies done on the leaching of 2-monochloroaniline (2MCA) from cement by Sora and co-workers found that up to 75% was released as shown in Figure 2.13. This negative aspect can be prevented by using adsorbents for the organic component before mixing it with cement. Adsorbents such as organophilic clays and polymeric resins are presently being researched. In this study polymeric resins discussed in section 2.6.1 were used in cement matrixes. PVA fibres that are widely used in the building industry for reinforcement of cement (Bezerra et al., 2004) have been studied as a binding agent for Nochar resin in order to improve Nochar resin's encapsulation into cement. Polyacrylonitrile (PAN) fibres are not used commonly as reinforcement in the cement industry but were considered as these fibres are used in bag filters used to clean particulates in gases originating from coal combustion.

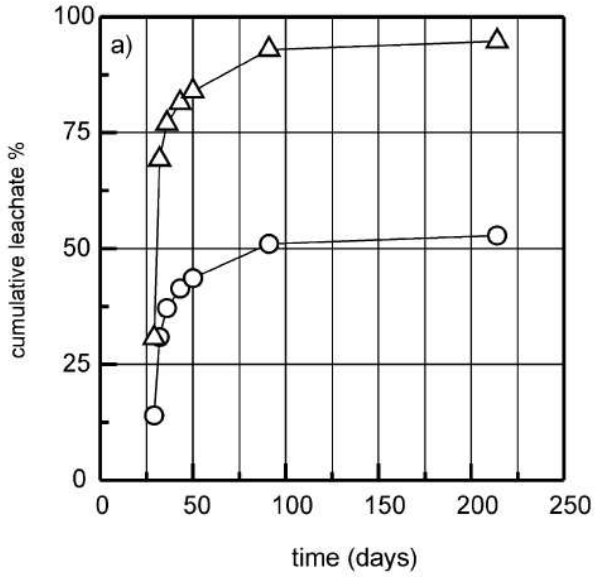

Figure 2.13 Cumulative amount of 2-chloroaniline released during the dynamic leach test.(○ = 40% organic solution loading and Δ = loading of 65%)

2.7 Conclusion

The criteria for disposal at Vaalputs clearly points in the direction of solidification and therefore generation of additional waste streams after treatment (for example with huge volumes of oxidants such as peroxides) are not acceptable. Ozone purging, UV radiation and or the combination should therefore be ideal for use in destructing organic components. Plasma thermal treatment could also be considered.

Solidification techniques, such as absorption into radiation stable absorbents are practical as these absorbents are capable of being encapsulated into cement.

2.8 Objectives of Research

The main objectives of this research are therefore to:

Develop a sampling procedure to acquire samples from the highly contaminated organic solutions without damaging the brittle containers.

Develop a process for treating radioactive organic waste streams with the objective to minimize secondary waste, and the safe encapsulation of organic waste into a suitable matrix for disposal.

Determine if the properties of the unique encapsulation matrix (with organic waste) satisfies the WAC of Vaalputs in terms of leachability, stability, durability, etc.

Chapter 3 METHODS AND TECHNIQUES USED

3.1 Sampling of Liquid Waste in Carboys

3.1.1 Safety requirements to collect samples from radioactive waste drums

During initial sampling safety clothing that includes safety shoes; a laboratory coat, hand gloves and a face shield were worn. All the work was performed in a well ventilated area. During this process the Radiation Protection Officer (RPO) was responsible for air sampling. After the sampling procedure, the plastic bag, used peristaltic tubing, paper wipes and rubber gloves were discarded into a non compressible red drum. Samples from the carboys were tightly closed after sampling and taken to a blue licensed National Nuclear Regulatory laboratory.

3.1.2 Sampling procedure

The carboy was placed inside a thick 40 L polyethylene bag (Figure 3.1) to ensure that if it perishes during sampling, that liquid radioactive waste would still be contained. The original lid of the carboy was gently removed to allow for gas release and replaced by the sampling lid which was screwed onto the container. This sampling lid was taken from an unused carboy in which two holes were drilled for the suction pipe and stirring rod. The rod attachment was slowly lowered into the carboy through the sampling lid and the top section was securely attached to a brushless motor (Figure 3.2). The stirring rod's bottom blades were positioned in such a manner as not to touch the sides and bottom of the container. The speed was increased in small steps.

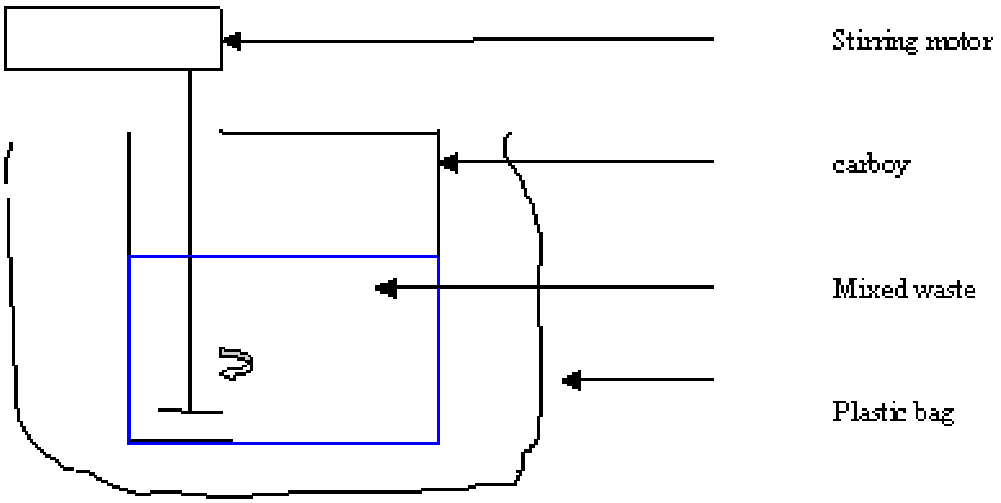

Figure 3.1 Schematic representation of the stirring of the liquid organic waste

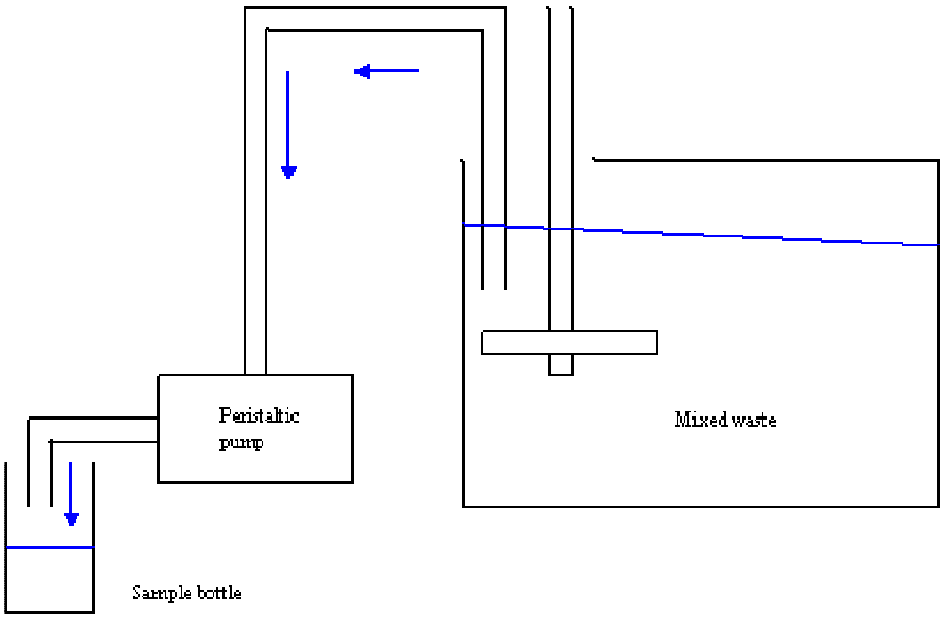

Figure 3.2 Schematic representation of the sampling setup for the liquid organic waste

To ensure that this technique is adequate it was demonstrated in a laboratory with the assumed contents of a carboy except that no activity was involved and clay / soil were used as particulate matter. This demonstration was inspected by the RPO and the facility managers to ensure that there are no risks for personnel in performing this task. After a successful demonstration, an approval was granted for this research and two samples of 500 ml each was taken from three carboys.

3.2 Experimental Procedure for Alkaline Hydrolysis of Organic Waste

A 12.5 M NaOH (100 ml) solution was prepared by dissolving 50 g analytical grade NaOH in 50 ml deionised water and diluting it further to 100 ml. As a reference a 30% TBP in kerosene mixture (50 ml) supplied by Nuclear Liquid Waste Management, was combined at a ratio of 1:1 with 50 ml 12.5 M NaOH. This organic-alkaline mixture was heated (Figure 3.3) under reflux for 4 hrs at 130 °C. The hydrolysed mixture was cooled and washed with additional 100 ml deionised water and poured into a 250 ml polyethylene bottle for analyses. The experiment was repeated with real waste organic solutions.

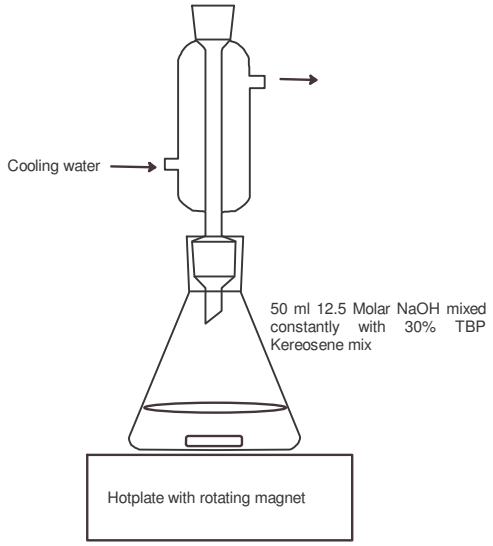

Figure 3.3 Experimental setup for the alkaline hydrolysis process

3.3 Experimental Procedure for Ozone Degradation

A 500 ml three neck flat bottom flask was filled with a 200 ml mixture consisting of deionised water and the organic component. The ozone was delivered to the organic aqueous mixture by an ozone generator (Fischer Ozon-Generator 500M) connected with HDPE tubing and by means of a glass tube with a frit at the end enabling it to form small bubbles in the mixture. A peristaltic pump with a flow rate of 20 $ml.min^{-1}$ transferred the organic mixture continuously to a quartz flow cell in the Carry UV Vis spectrophotometer (Figure 3.4). Evaporation of the organic aqueous mixture was prevented by using silicon seals and the flask was fitted with a reflux condenser (Figure 3.5). The oxygen gas supply was switched on and controlled at 140 kPa with a dual stage oxygen regulator. The ozone generator was switched on and the controlled set to maximum power. Ozone was bubbled into the deionised water through a pipette glass tube placed inside the water at a flow rate of 50 $ml.min^{-1}$. The amount of ozone delivered to the three neck flask was measured beforehand under same conditions and determined to be 470.6 mg O_3 h^{-1} (Appendix 5).

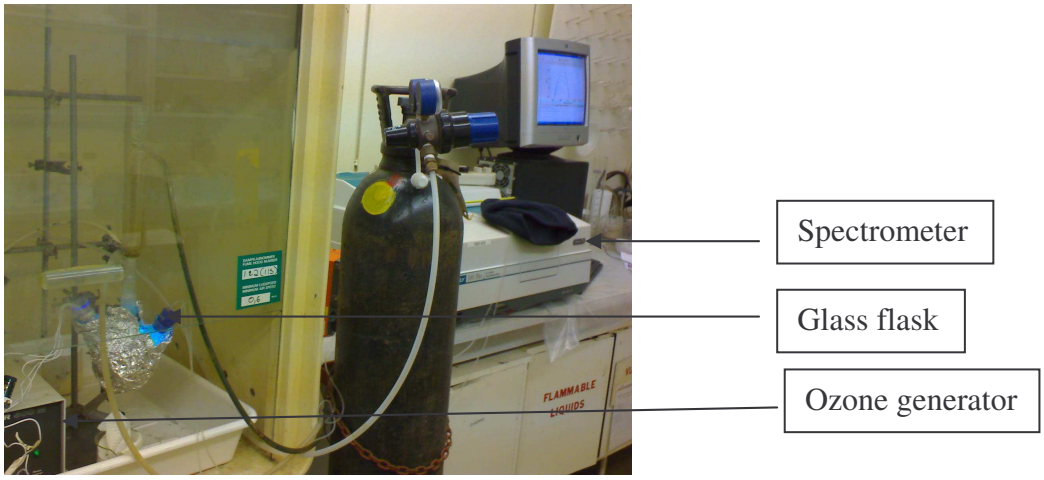

Figure 3.4 Ozone / UV degradation experimental setup

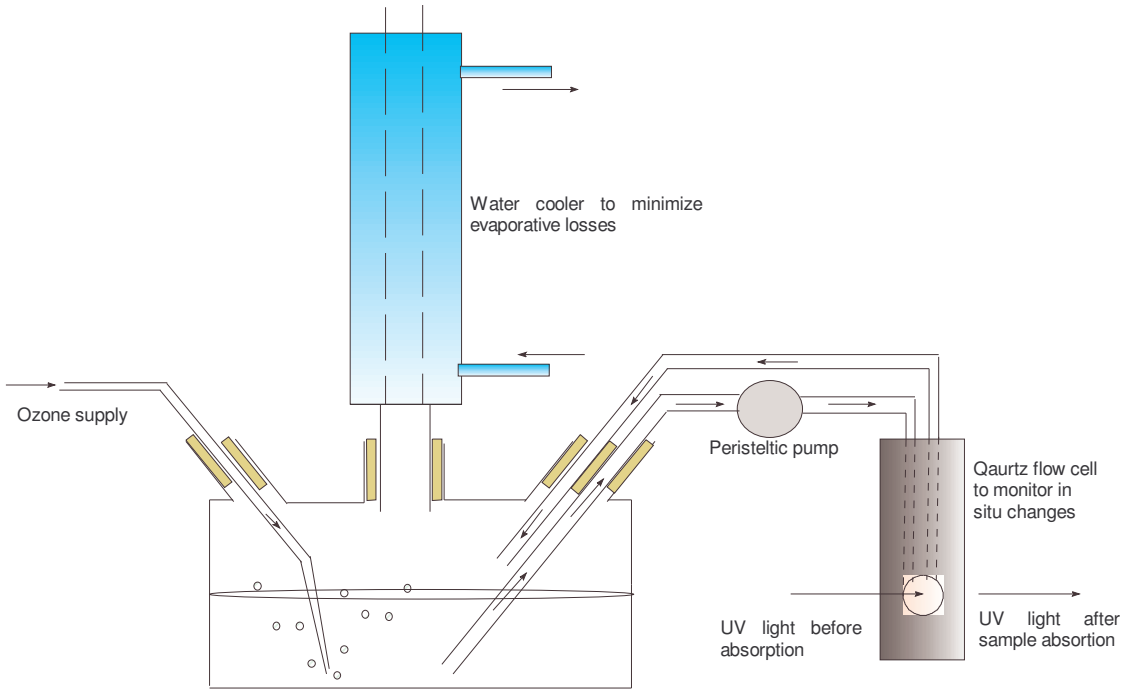

Figure 3.5 Schematic representation of the ozone degradation experimental.

3.4 Experimental Procedure for UV and Ozone Destruction

The same experimental setup as described in 3.3 (Figure 3.5) was used, except for a quartz tube with a UV lamp fitted inside which was lowered into the solution in order to be exposed constantly to UV light (Figure 3.6). Initially, a medium pressure UV lamp was used with a power consumption of 400 W, but the heat generated by the lamp inside the quartz tube proved to be the major factor in destroying the organic components and attempts to cool the lamp to prevent this was unsuccessful. A low pressure lamp emitting UV radiation between 180 nm and 200 nm were then installed in the experimental setup and no excess heat was generated. (See Appendix 3 for lamp power requirements and spectral output). The destruction of organic components was studied by using the UV lamp on its own, or with a combination of UV and ozone together.

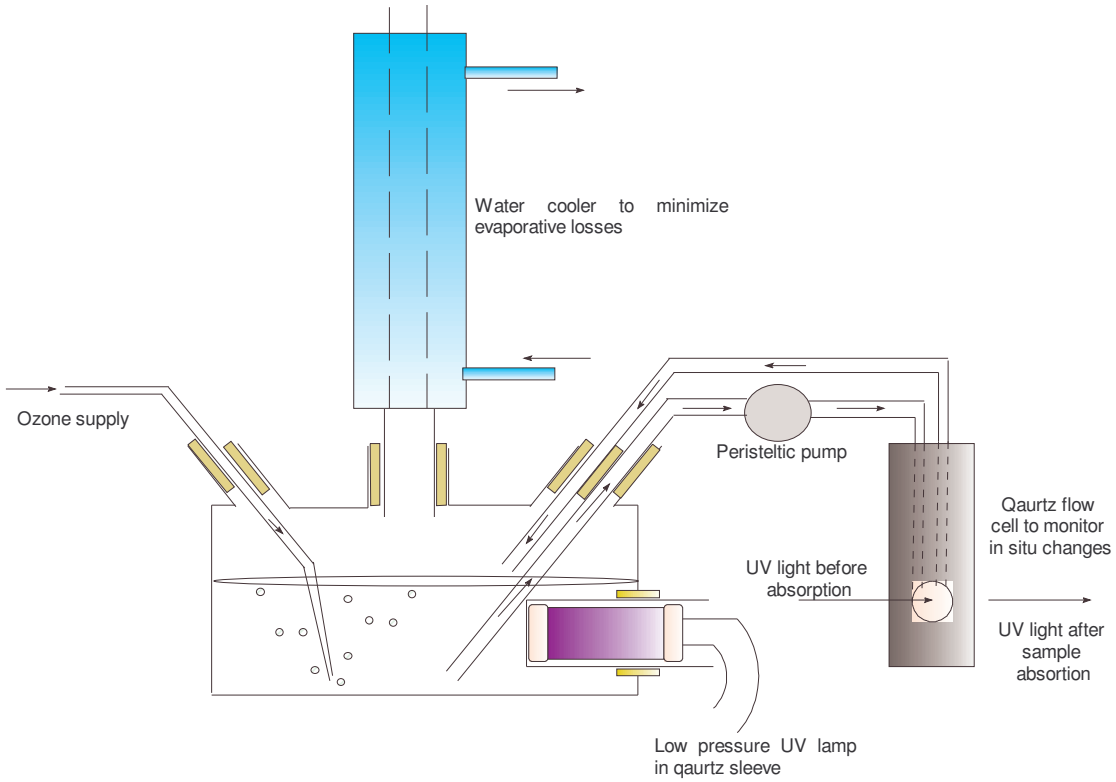

Figure 3.6 Schematic representation of the experimental setup of ozone combined with UV degradation

3.5 Plasma Destruction Technique

A 1000 ml non-radioactive organic test mixture consisting of 100 ml acetone, 100 ml ethanol, 100 ml scintillation liquid (Perklin Elmer Gold), 100 ml methanol, 100 ml chloroform, 200 ml 10% Contrad detergent, 90 ml TBP, and 210 ml kerosene were introduced into the non-transfered plasma flame by means of vacuum created by the cooling argon gas.

This argon gas prevents that high temperatures formed by the plasma, melts the torch.

The volumetric flask containing the organic mixture was stirred vigorously with a magnetic stirrer to keep the suspension homogeneous. The organic mixture was pumped into the plasma flame through a flexible high density polyethylene tube connected to a flow controller and stopper valve (Figure 3.7). Samples were taken at the exhaust of the plasma reactor with a sample loop submerged in liquid nitrogen and closed off at both ends by valves.

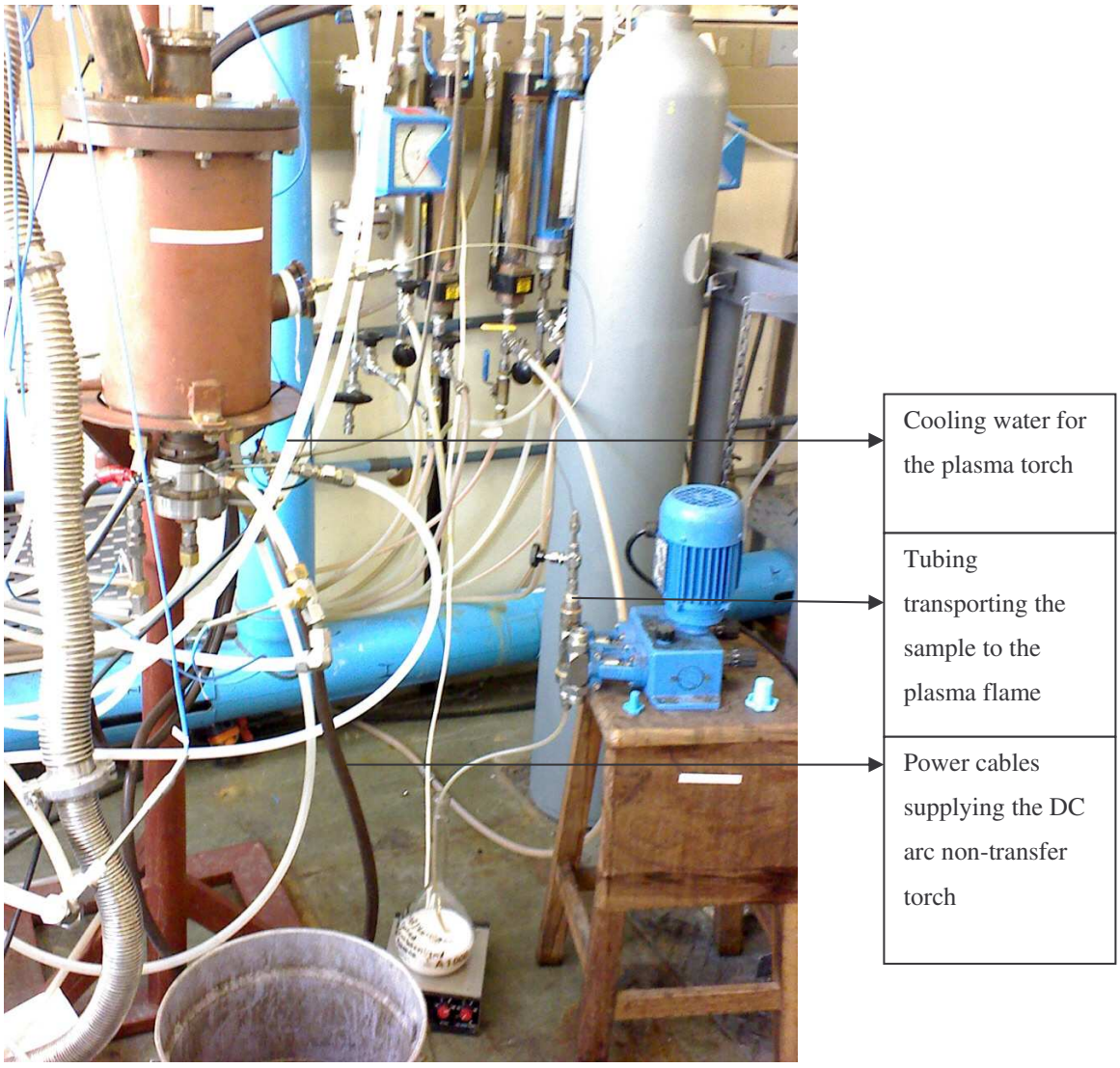

Figure 3.7 Plasma torch used for destruction of test mixture

The plasma flame was kept running for 10 min before the organic mixture was introduced into the flame. After 5 min of steady current and voltage conditions on the plasma flame, the valves directing the exhaust gases through the sample loop were open and ran for another 5 min before this sample loop was closed off, containing the exhaust gases from the plasma treated organic mixtures.

This sample loop was analysed with GC-MS. The GC column separated the organic gas into components and these separated components were in turn identified by the MS.

3.6 In Line Filter Sorption

The removal of TBP from an aqueous test solution was evaluated with the experimental setup illustrated in Figure 3.8. Solutions of TBP containing low level enriched uranium were pumped by means of a peristaltic pump through a filter that contained a known weighed amount of Nochar resin. Low enriched uranium was used as a tracer (as described in the PUREX process in chapter 2.2) to form a complex measurable with a Gamma detector. Nitric acid solutions were varied from 0.1 M to 3 M HNO_3 for samples A to F whereas with samples G to H 10% Contrad detergent solution were added (Table 3.1). The amount of tracer and TBP (0.5 ml) added to each sample were identical. The volume of each sample was 10 ml and this was in turn pumped for 10 min through the Nochar filter.

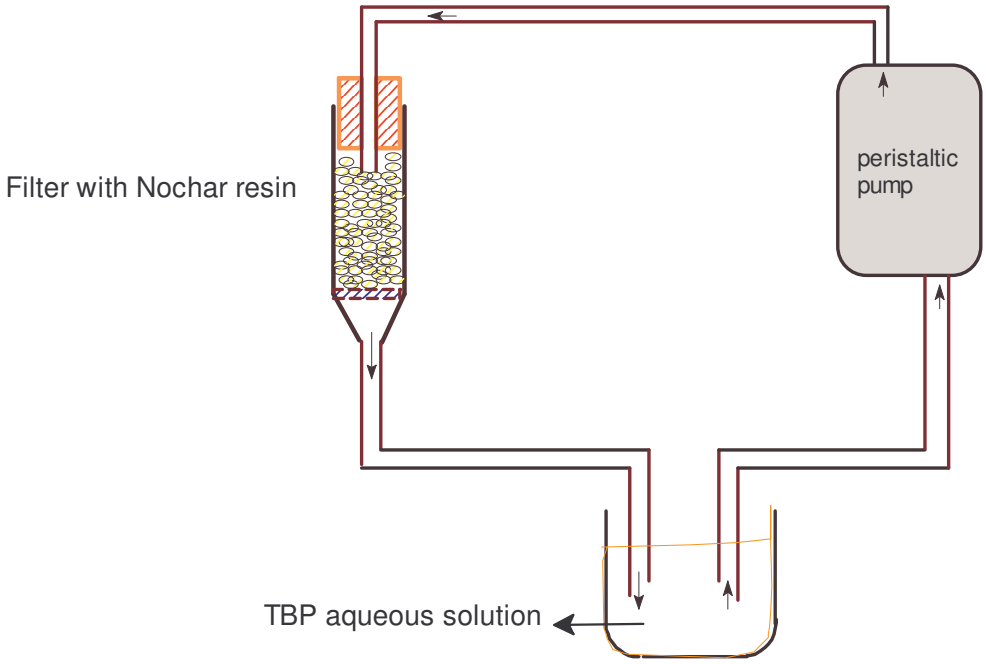

Figure 3.8 Resin absorption experimental set up

Table 3.1 Tracer samples prepared

sample	Nochar N 910 (g)	Solution with TBP
A	1.1909	0.1 M HNO_3
B	1.3030	0.1 M HNO_3
C	1.2705	3.0 M HNO_3
D	1.1681	3.0 M HNO_3
E	1.0198	3.0 M HNO_3
F	1.0656	0.1 M HNO_3
G	0.9927	10 % Contrad detergent
H	1.1689	10 % Contrad detergent
I	1.1365	10 % Contrad detergent

A sorption or distribution coefficient (K_d) is commonly used to establish the ratio of the adsorbed phase concentration to the solution phase concentration (Alley 1993). The solution to resin ratio is kept at 20 ml: 1 g.

$$K_d = \frac{Ci - Cf * Vs}{Cf * m} \quad (7)$$

K_d – distribution coefficient, Ci – initial counts / concentration; Cf – final counts / concentration, V_S – volume (ml), m – resin mass (g)

The K_d values for TBP dissolved in acetone were analysed with capillary GC. About 1 g of Nochar resin (see Table 3.2) was weighed in to a centrifuge tube. TBP, and acetone were added and the tube was sealed with its screw-on lid. These tubes were then rotated for 24 h before analyses with the GC were conducted. Contrad detergent solutions (samples 1 to 5 in Table 3.2) were also analysed added to Nochar resin, mixed for 24 h and analysed with UV VIS.

Table 3.2 Sorption tests of Contrad and acetone on N910

sample	Nochar (g)	adsorbed component	Analysis method
1	1.0509	10 % Contrad in H_2O	UV VIS
2	1.0061	12 % Contrad in H_2O	UV VIS
3	1.0783	15 % Contrad in H_2O	UV VIS
4	1.0575	18% Contrad in H_2O	UV VIS
5	1.0400	20% Contrad in H_2O	UV VIS
6	1.0277	0.5% TBP in acetone	GC
7	1.0572	1% TBP in acetone	GC
8	1.0333	1.5% TBP in acetone	GC
9	1.0297	2% TBP in acetone	GC
10	0.9931	2.5% TBP in acetone	GC

3.7 Encapsulation of the Nochar Resin into Cement

One of the acceptance criteria at Vaalputs, the waste site in South Africa, is that the waste can only be disposed if it is in a solidified form. Nochar resin forms a gel when TBP is absorbed into the polymer and needs further solidification. The cement that was used for Nochar encapsulation was PPC cement and the ratio of TBP - kerosene absorbed into the resin was kept as close to the ideal prescribed ratio of 2:1. (Kelly, 2005). Low enriched uranium was used as the radioactive tracer to determine the leaching rates in differently composed cement bricks. Different encapsulated samples were also prepared to test the incorporation of polyacrylonitrile and polyvinyl alcohol fibres for their reinforcing properties (Table 3.3).

In the laboratory Nochar resin was thoroughly mixed with TBP, kerosene and trace amounts of low enriched uranium with PPC cement. Two sets of samples, as describe in Tables 3.3 and 3.4 were prepared; one contained low level enriched uranium, while the second set contained a TBP-kerosene mixture. The non-radioactive cement samples were tested for porosity. All the radioactive samples were tested for leaching. The polymeric fibres used were polyvinyl alcohol fibres (PVA supplied by Everite) and homo polymeric polyacrylic fibres (PAN supplied by Beier Albany SA).

Table 3.3 Sample compositions without uranium

Sample	PPC (g)	Nochar (g)	PVA Fibre (g)	PAN Fibre (g)	TBP Kerosene mixture (g)
A	110.2110	9.9132	0	0.7800	19.8264
B	102.1423	9.8729	0	2.1134	19.7458
C	99.4280	13.3004	0	0	25.8905
D	101.2673	9.1700	0	0	19.2431
E	97.1905	14.8374	0.7082	0	38.2539
F	99.3430	14.6500	0.9396	0	34.8483
G	103.4188	11.6759	0.9965	0	20.2501
H	95.3782	13.7837	0.8790	0	27.9010

35 ml water were mixed with all above samples

Table 3.4 Composition of samples containing uranium

Sample	PPC weight in (g)	Nochar (g)	PVA Fibre (g)	PAN Fibre(g)
1	50.5729	4.9433	0	0
2	49.8667	5.3099	0	0
3	49.6471	5.1682	0	0
4	50.0756	5.1844	0.5438	0
5	49.4856	5.2914	0.7082	0
6	50.0409	4.9596	0.9396	0
7	50.1875	5.2536	0	0.3007
8	49.4469	5.0349	0	0.2696

20 ml water was added to each sample

To confirm whether the results from the gamma detector was correct, water samples were additionally subjected to the chemical method, Bromo – Padap method [2-(5-bromo-2-pyridylazo-)-5-diethylaminophenol]. This chemical method is a spectrometric technique suited to determine concentrations of uranium in the 0.2 ppm to 2 ppm range.

3.7.1 Analysing for sorptivity

Sorptivity is a measure of the water penetration rate by means of capillary action. The penetration is measured only through one edge of the specimen, by adding sealant around the vertical edge of the specimens (e.g. epoxy paint or vacuum grease). It is measured gravimetrically as a function of time. It is calculated using the following formula:

$$A = [(\Delta g / (Area \times t^{1/2}) \qquad (8)$$

The units are g m^{-2} $hour^{-1}$. The surface of contact as in the circular samples is calculated by πr^2 for a cylinder shape. The specimens were weighed and placed in a tray. Water was added to about 2 cm as seen in Figure 3.9. After the specified time interval, the specimens were removed and the excess water was wiped off. The specimens were weighed again and then placed back in the tray with water.



Figure 3.9 Sorptivity measurements with bottom side and top sides of samples not coated with vacuum grease

3.7.2 Leaching analysis

Leaching test studies were performed on the waste-forms in accordance with the procedure described in the American Nuclear Society's ANSI/ANS 16.1 (1986) standard. In this analysis the leachant used was demineralised water. The water volume used was ten times the total surface area of the test samples during the leaching interval, which is the ratio of the leachant volume to the specimen external geometric surface area was maintained within fixed bounds of 10 ± 0.2. In this test, leachant solutions were changed periodically (at time intervals 24, 48, 72 and 96 h) to simulate dynamic leaching conditions. The leachant was kept at room temperature (17.5 °C to 27.5 °C) for the duration of the test. The mass transport equation under these conditions permits the calculation of effective diffusivity. If less than 20% of the leachable species have been removed by the time $t = \Sigma(\Delta t)_n$, the effective diffusivity can be calculated by the formula.

$$D = \pi \left[\frac{a_n / A_0}{(\Delta t_n)} \right]^2 \left[\frac{V}{S} \right]^2 T \qquad (9)$$

Where:

D = effective diffusivity, $cm^2.s^{-1}$

a_n = activity of a nuclide released from the specimen during leaching interval n

A_o = total activity of a given radionuclide in the specimen at the beginning of the first leaching interval (i.e., after the initial 30 s rinse)

$\Delta t_n = t_n - t_{n-1}$, duration of the nth leaching interval, s

V = volume of the specimen, cm^3

S = geometric surface area of the specimen as calculated from measured dimensions, cm^2

T = leaching time in seconds

Samples of this demineralised water (Figure 3.10) were taken at set intervals and measured to determine whether the tracer that was initially added, leached.



Samples containing activity | Submerged in demineralised water

Figure 3.10 Leaching tests on samples containing radioactive nuclides (LEU)

3.8 Instruments Used in Study

3.8.1 Gas chromatography analysis method

Gas chromatography is a separation technique (Figure 3.11) in which the mobile phase is a gas and the stationary phase either a solid (gas –solid chromatography) or a liquid dispersed on a solid (gas-liquid chromatography). The technique is similar to fractional distillation because the separation of the components in the sample is based on boiling point differences, but also on the interaction between the stationary phase and plug of vapour being carried by the inert carrier gas. The column used for the analyses of the organic components was an open tubular column known as a capillary column with a thin layer of stationary phase coated on the inner walls (Figure 3.12), trade name SLB^{tm}-5 MS. This is a fused silica capillary column, having a length of 30 m, inner diameter of 250 µm and with a coating thickness of 0.25 µm (5% phenyl groups in a methyl polysiloxane polymer backbone).

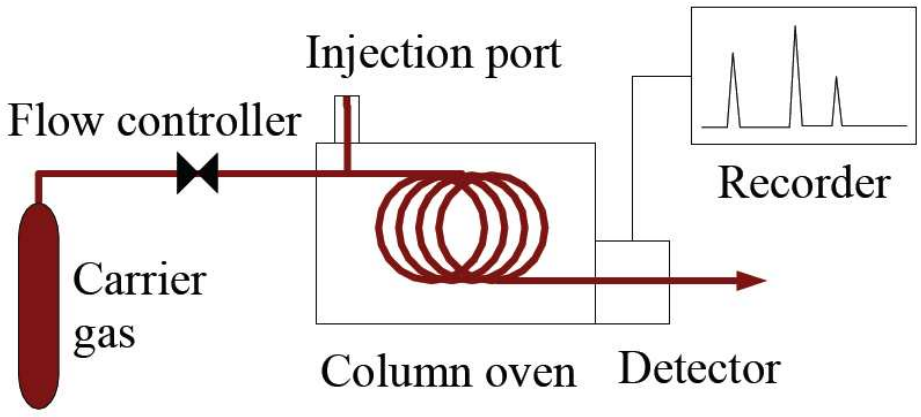

Figure 3.11 Gas chromatography schematically represented

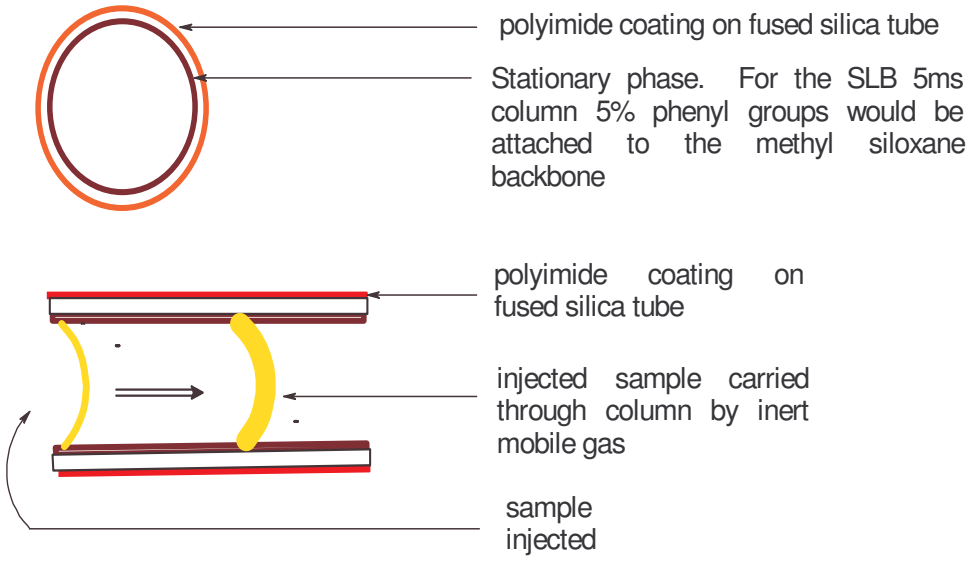

Figure 3.12 Open tubular capillary tubing

The Perkin Elmer Clarus 400 GC was set up with user friendly TotalChrom software to control the instrument parameters. Column temperature started at 50 °C, held constant for 5 min, and thereafter increased at a rate of 15 °C to 300 °C. The carrier gas was helium used at a flow rate of 0.85 ml .min^{-1} (Pressure in carrier gas system electronically maintained at 75 kPa). The injector, with glass insert, was set at 340 °C with the injection split (1 µL of sample was injected at a time) in such a way that the sample was split 1 to 60.

The flame ionization detector temperature was set at 350 °C. The method was calibrated (Appendix 6) with three known standard solutions with concentrations of 2, 5 and 10% respectively of each component in the mixture. The components in the mixture were analytical grade methanol, ethanol, acetone, butanol and tributyl phosphate diluted to the required concentration. 1-Cedene was used as internal standard. The components were dissolved in analytical grade heptane. The integrated area for each peak was used for concentration calculation purposes. Figure 3.13 is an example of a gas chromatogram analysis.

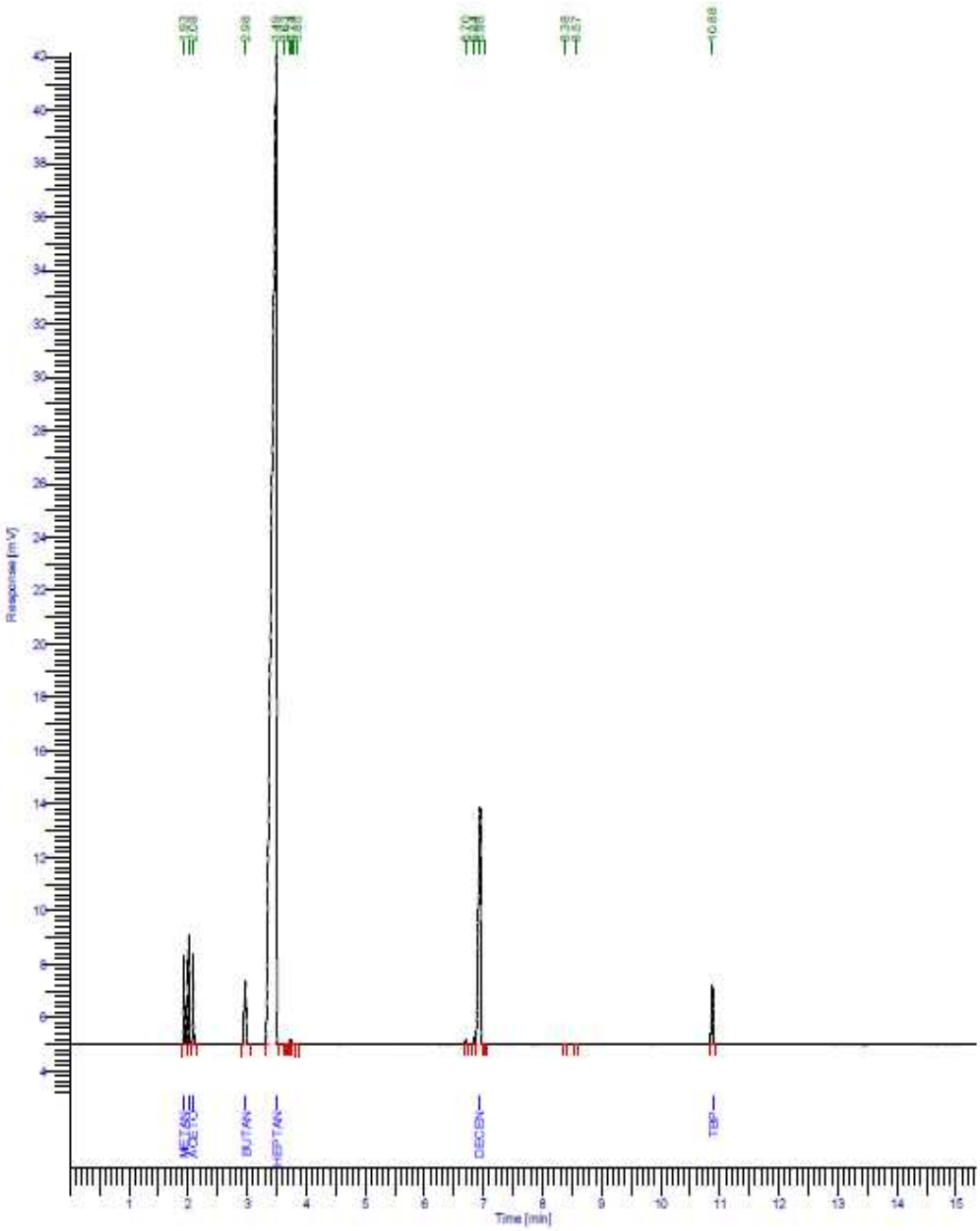

Figure 3.13 GC chromatogram of a standard solution of organic substances dissolved in heptane

3.8.2 Gas chromatogram mass spectrometry (GC-MS)

In Figure 3.14, the quadrupole MS analyzer (used for the gas analysis after plasma destruction of the organic components) consists of the gas chromatogram / mass spectrometer interface, ionizer, lenses, quadrupole filter and detector. An ion formed in the ionizer will be accelerated through the filters and undergo transverse motion (because of the quadrupole field formed by the parallel electrically conducting rods), along the longitudinal axis of its movement. The lighter the ion mass, the smaller the number of cycles it undergoes before it is collected by the detector electrodes. The heavier charged particles will gradually drift through the quadrupole field towards the detector.

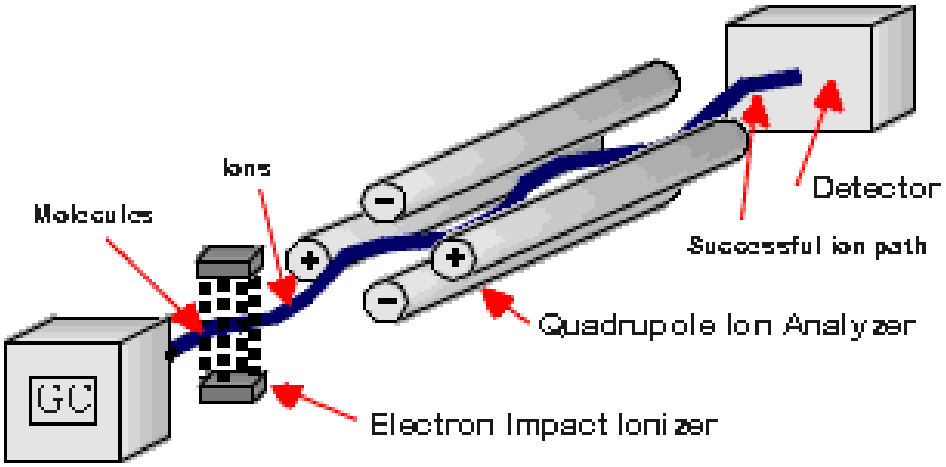

Figure 3.14 GC Mass spectrometry

A 0.2 µL aliquot of the sample was injected into the injection port of an Agilent 7890A GC using a 7683B Auto Injector. Data collection and instrument control was performed with E.02.00.493 Molecular Spectroscopy Chem Station software. The injection port was set to 25 °C and split injection was performed, with a split ratio of 10:1. Separation was achieved with a DB-1 capillary column, J&W Scientific

(30 m X 0.25 mm and 1.0 µm film thickness) at a helium flow rate of 1.4 ml.min^{-1}. An initial oven temperature of 50 °C was held for 5 min and subsequently raised at a rate of 20 ˚C per minute to 280 °C and then held for 10 min at this temperature. The solvent delay was set at 7 min. The column outlet was inserted directly into the source of an Agilent 5975C Mass Selective Detector. The Mass spectrometer was operated with a filament current of 300 µA and electron energy of 70 eV in the EI (electron ionization) mode. The mass range scanned was 10-550 atomic mass units (amu). The transfer line was set to 280 °C and the quadrupole and source temperatures were 150 and 230 ˚C respectively.

Organic layers: An aliquot of the sample was diluted 5 times with dichloromethane and injected. The instrument was internally tuned as shown in Appendix 7.

Water layers: 500 µL of the sample was extracted with 2 x 500 µL of dichloromethane, dried over magnesium sulphate and filtered.

Plasma gas samples: approximately 20 kPa of the gas contained in a sampling tube was loaded and injected via a 6 port valve fitted with a 250 µL sample loop into the injection port of a Varian 3800 GC. The injection port was set to 200 °C and a splitless injection was performed. Separation was achieved with a Varian Pora-bond Q capillary column, (30 m X 0.25 mm and 0.25 µm film thickness) at a helium flow rate of 1.5 ml.min^{-1}. An initial oven temperature of 30 °C was held for minutes and subsequently raised at a rate of 20 °C per minute up to 200 °C and then held for 5 min at that temperature.

3.8.3 Ultra violet visible spectrophotometry method

Modern UV VIS instruments are double beam recording spectrophotometers in which the light beam is split into two equal parallel beams (Brain et al., 1998). These

beams pass through the sample and reference cells respectively before it ends at the detector. A deuterium discharge tube is used as a light source for the region 200 – 300 nm and a tungsten filament light used as a source for the 325 – 750 nm regions. Molecules absorb ultraviolet or visible light when exposed to light of a certain frequency (f) or wave number (λ), causing electron transitions from lower to higher energy levels with a difference given by the expression as $\Delta E = hf = hc / \lambda$ where h is Planc's constant and c is equal to the speed of light. The Cary 100 in Figure 3.15 is a double beam spectrophotometer with a chopper (moving slot) to direct the reference and sample beam respectively to the detector.

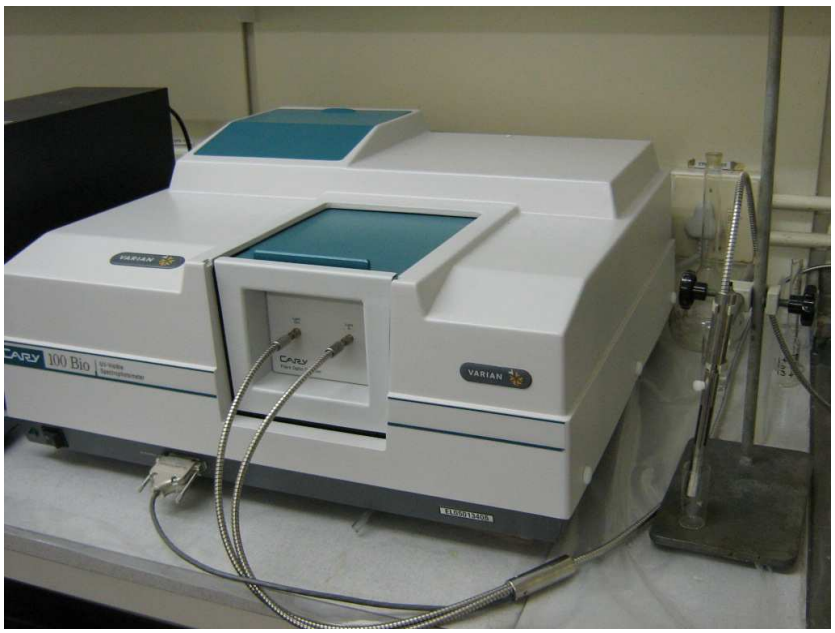

Figure 3.15 Cary 100 UV-visible spectrophotometer

The resultant spectrum produced from the light passing through the sample (I) compared to the blank (I_0) is a graph of light absorbance versus wavelength. The ratio I / I_0 is called the transmittance (T) expressed as $\%T$. The absorbance A is based

on the transmittance where A = -log*($\%T$) and by using the Beer Lambert law, $A = \varepsilon.c.L$, the concentrations of the absorbing species can be determined. For each of the absorbing species c is the concentration, L is the path length through the sample and ε is a constant known as the molar absorptivity. This molar absorptivity is a fundamental property for molecules at a certain temperature and pressure in a specific solvent. The instrument is evaluated with an internal performance test as shown in Appendix 8.

Varian Cary WinUV software was used and samples scanned from 200 nm to 800 nm. The spectral bandwidth was selected at 2 nm with the beam mode chosen at double. The switch over from visible light to UV light was set at 350 nm. Baseline correction was done. An example of a spectrum of 5% acetone solution can be seen in Figure 3.16.

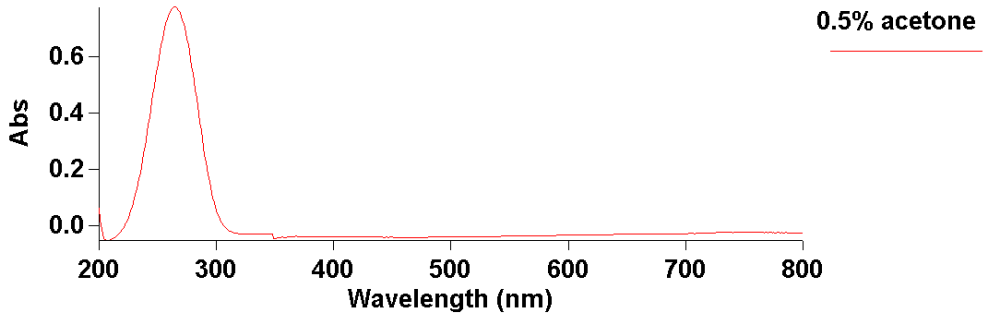

Figure 3.16 UV-visible absorbance spectra of 0.5% acetone in deionised water

The analysis was started by first getting a baseline scan with the deionised water in the reactor, adding the sample to be treated whilst mixing thoroughly. A sample is then pump at a set rate (20 ml.min^{-1}) through the flow cell and at specific time intervals the sample is analysed in situ as the reaction proceeds with the scanning kinetic software (Figure 3.17and Figure 3.18).

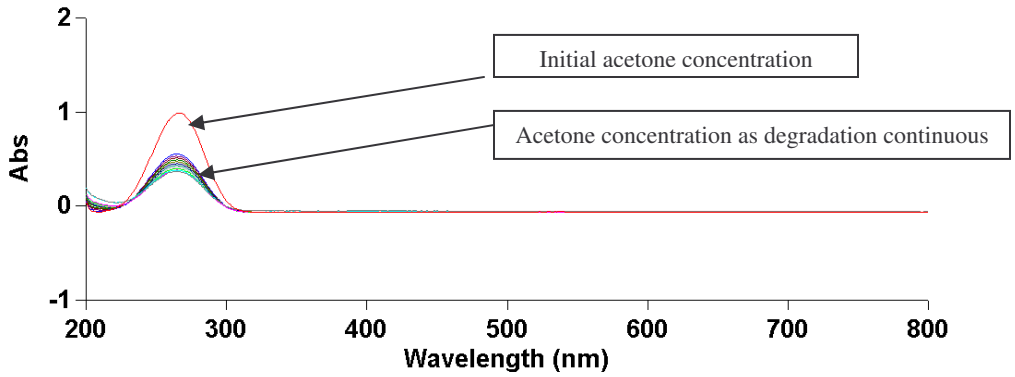

Figure 3.17 Scanning kinetics (acetone degradation) detected by UV-visible instrument

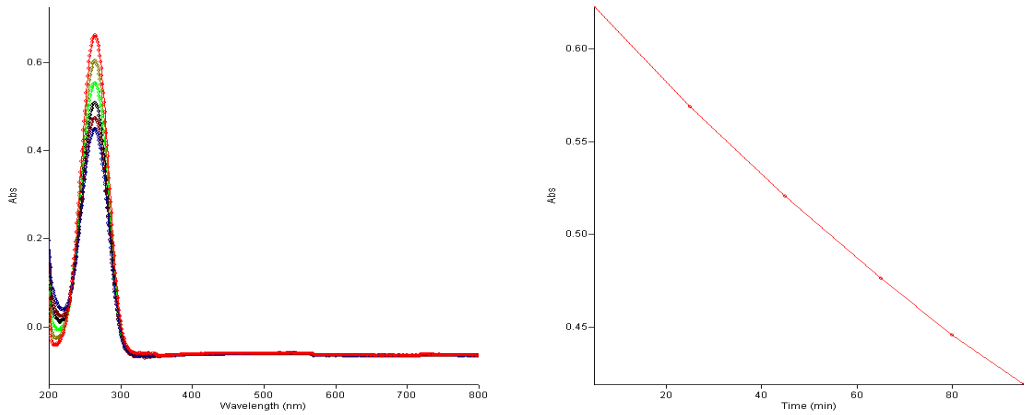

Figure 3.18 Scanning kinetics from UV-visible spectra at 270 nm

3.8.4 Infrared spectrophotometer analyses

Infrared spectroscopy is a measure of the interaction between light and vibrational motion of the covalent chemical bonds in molecules and in the covalent bonds in lattice ionic crystals. The system consist of an infrared source (Appendix 10), a device to decode the radiation into frequency and intensity information, a pathway for this encoded radiation to interact with the sample and a detector-recorder. A plot

of measured infrared light versus wavenumber provides a unique infrared spectrum as shown in Figure 3.20 for a specific infrared active compound that follows Beer's law as mentioned previously ($A = \varepsilon.c.L$). The type of infrared instrument that the samples were analyzed with uses attenuated total reflectance (Figure 3.19) providing quick and rapid analyses for liquids and solids. The disadvantage of utilizing FTIR analyses for the waste streams is the presence of water that strongly absorbs. Although the water spectrum can be deducted from the sample spectrum to cancel the water influence, the sensitivity of the technique ranges from 0.1% to 1%.

The Varian resolutions 4 software is opened and with a calibrated instrument (Appendix 10.1), the scan menu is selected and the following conditions were chosen:

Background: 100 scans at resolution 4 and display type in transmission. Sample scans can range from 50 to 100 at resolution 4 and spectral range from 600 to 4000 wavenumber (cm^{-1}) as shown in Figure 3.19. The sample is placed onto the ZnSe crystal with a glass pipette, the sample compartment closed and scan initiated.

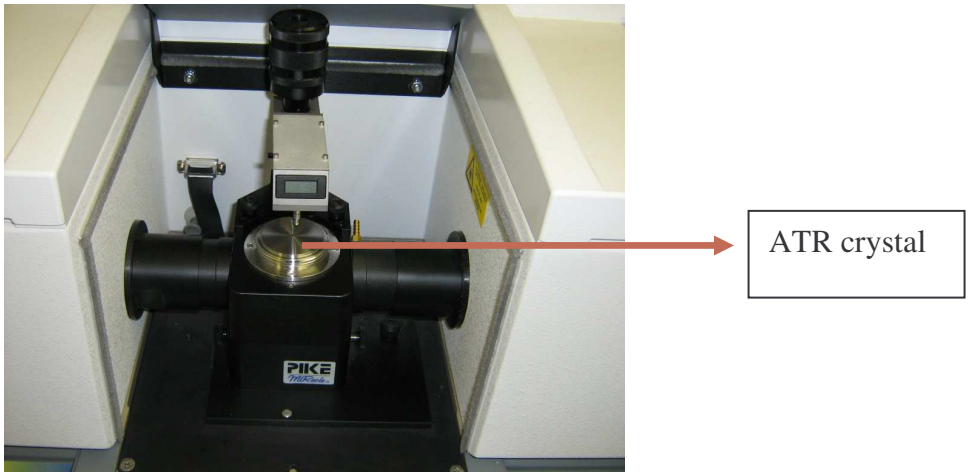

Figure 3.19 FTIR instrument with ATR diamond crystal for quick and rapid sample analyses

The wavenumers between 2845 cm^{-1} and 2970 cm^{-1} are contributed by the methyl C-H and methylene (CH_2) stretching whereas the peaks around 1466 vibrations due to the methyl and methylene bending vibrations. The huge peaks between wavenumbers 990 cm^{-1} and 1050 cm^{-1} are due to P-O-C stretch from the phosphate in the TBP structure. The organic phosphate stretching is visible at 1264 cm^{-1}confirming the TBP structure (Coates, 2000)

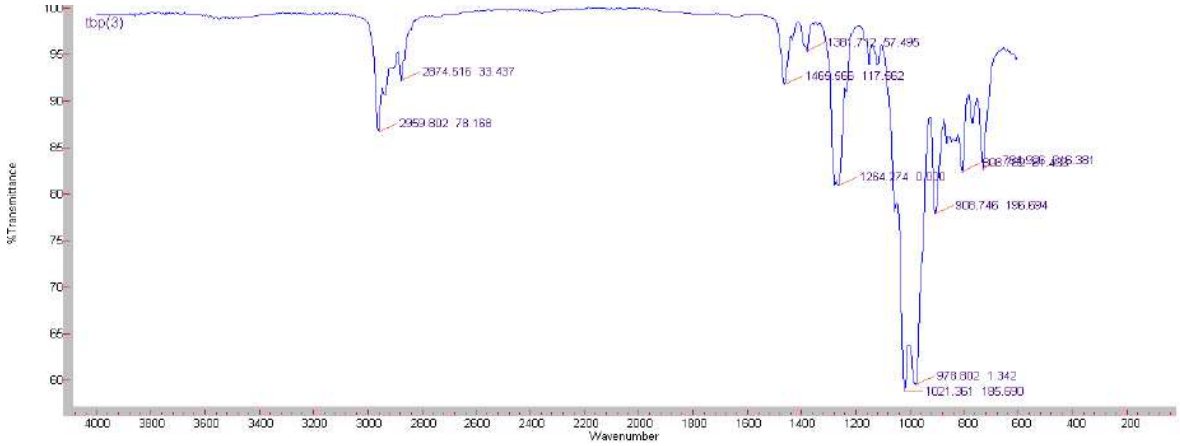

Figure 3.20 FTIR transmissions scan of TBP

3.8.5 Gamma spectrophotometry

An unstable atom with too many particles in its nucleus or too much energy will disintegrate to a more stable state releasing radiation. One of several forms of radiations is gamma radiation. It is emitted by many radionuclides such as Cobalt, iodine, Cesium, etc. and gamma spectroscopy can be used to detect the presence of these gamma emitting radionuclides.

Quantitative assessment of gamma emitting radionuclides in solid, liquid and gaseous samples can be determined with high accuracy and sensitivity by a number of solid state detectors, such as Germanium and Sodium iodide detectors that are used to identify and quantify gamma-emitting radionuclides in effluent and

environmental samples in and around a wide variety of facilities handling radioactive waste.

The detector used for measurements at Necsa was a Sodium Iodide detector which consists of a (NaI) crystal, optically mounted to a photo multiplier tube. Incident radiation interacting in the NaI crystal will result in the production of a light. The light is transmitted into a photo multiplier tube and produces electrons. The number of electrons produced is amplified in this phototube. The signal out of this phototube is transformed into an electrical pulse that signifies the incidence of a photon. Pulse is recorded by various means and easily interpreted by user friendly software.

Instrumental parameters:

The instrument is set up and calibrated (Appendix 11) in accordance with the instrumental operating procedure, AC-BPMS-WIN-09010 (Necsa internal document Radiochemistry)

Chapter 4 RESULTS AND DISCUSSIONS

4.1 Extraction of a Representative Sample

Three samples were collected from the carboys over a two week period under required supervision. As allowed daily radiation dose of 100 μ Sievert was exceeded during the collection of the samples in the first three hours of sampling, this process was extended over a two week period. The sampling was done as described in Section 3.1.2 and the sampling equipment can be seen in Figure 4.1.



Figure 4.1 Sampling equipment

Samples were drawn after 15 min of thorough mixing. This minimum period to acquire a representative sample from the carboy was determined beforehand in a laboratory simulation as indicated in Figure 4.2.

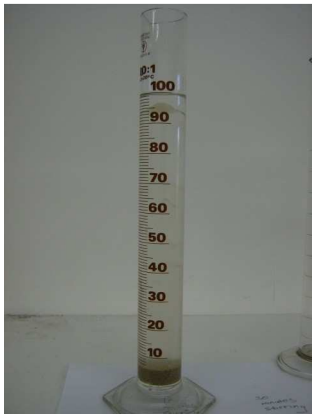

After 100 ml sampling



Top with hydrocarbon top visible



Bottom with clay visible

Figure 4.2 Sampling 100 ml of waste solution demonstrating that all components in the test mixture can be sampled

The three waste samples (H014, RARW167, and RARW140) were analysed by GC-MS qualitatively in order to determine the organic components present in the carboys. The GC-MS analyses (Table 4) identified a mixture of organic constituents that possibly originated from radiolysis reactions. To separate these constituents, vacuum distillation was used but unfortunately it was impossible to isolate components from these waste solutions. The organic components in these solutions (excluding TBP) can therefore be considered minimal, thus only trace quantities.

Table 4.1 GC-MS analyses results of samples taken from carboys

HO14	RARW140	RARW167
Hydrochloric acid	Hydrochloric acid	Isopropenyl acetone
Nitric acid –methyl ester	Formic acid	Isobutenyl methyl ketone
3-Hexene -2-one	Vinegar acid	Diacetone alcohol
Diacetone alcohol	Nitric acid –methyl ester	Butyl diglycol
1,2-dimethyl -4 – tert	Isobutenyl methyl ketone	$C_6H_{10}O$
butyl -6-	Diacetone alcohol	$C_8H_{18}O_3$
cyclopentylbenzene	Chloroacetic acid	
$C_{24}H_{44}$	Butyl glycol	
$C_{15}H_{26}$	Diglycol	
	Pentachloroacetone	
	Butyl diglycol	
	$C_{17}H_{26}$	
	$C_8H_4O_3$	
	$C_{10}H_{10}O_2$	
	C_9H_9NO	

The test waste samples were also analysed with UV-visible spectrophotometry to determine the UV-visible organic active transitions. The results in Figure 4.3 indicate that all the sampled containers have an electronic transition at 280 nm. As this transition is nearly the same as a Contrad transition, calibration curves with

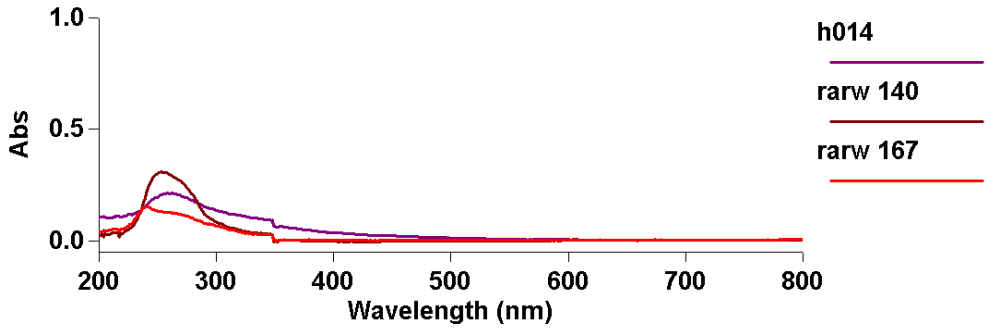

Figure 4.3 UV-visible spectra of waste samples (H014 RARW140 and RARW167)

Three different Contrad standards (0.1 to 0.6%) were determined. The spectrum of 0.6% Contrad is shown in Figure 4.4.

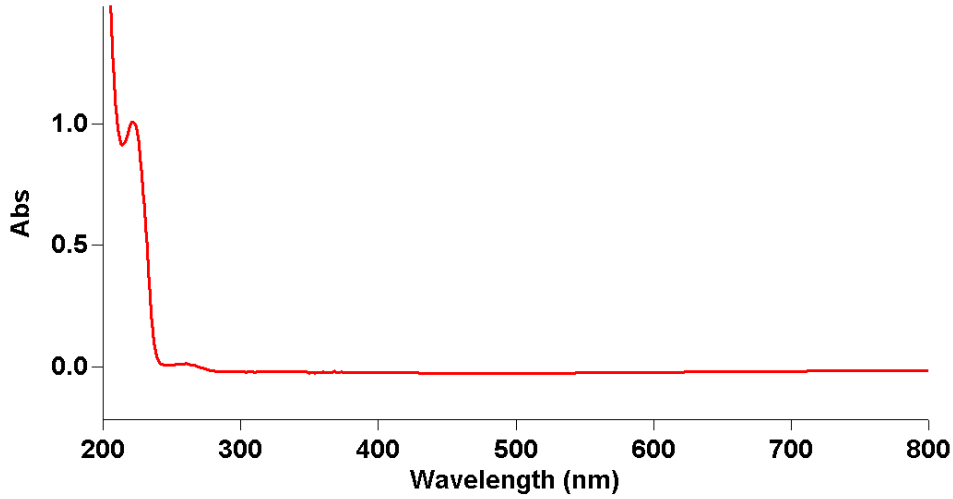

Figure 4.4 UV-visible spectrum of 0.6% Contrad standard

From the electronic data a calibration curve was constructed as shown in Figure 4.5.

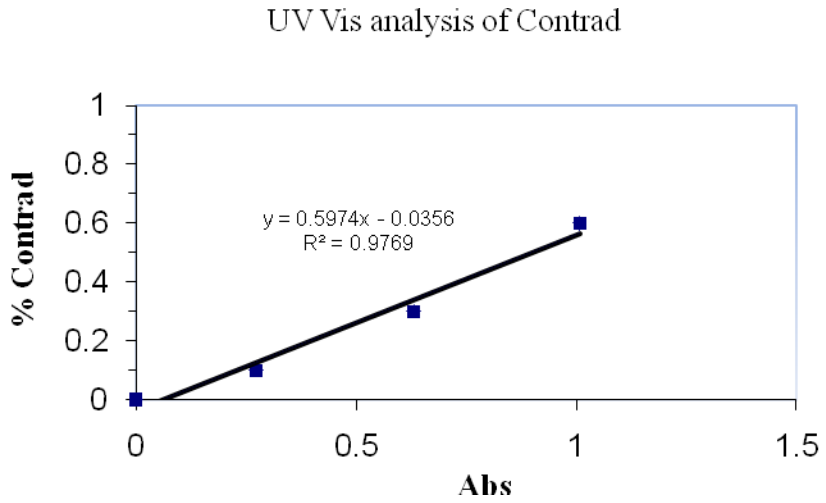

Figure 4.5 Calibration curve for Contrad standards

Based on the calibration curve of the Contrad solutions, the possible amount of Contrad detergent in these waste solutions could be around 0.3%.

The IR analyses of the three sampled waste solutions displayed a typical OH peak broadening around 3500 cm^{-1} with similar peaks around 1640 cm^{-1} and 1400 cm^{-1} (Figure 4.6). The hydroxyl groups responsible for this typical peak broadening due to intra- and intermolecular hydrogen bonding lowered and obscured the CH_3 and CH_2 peaks at 3000 cm^{-1}. The peaks observed at 1400 cm^{-1} indicates the presence of long aliphatic chains (Coates, 2000).

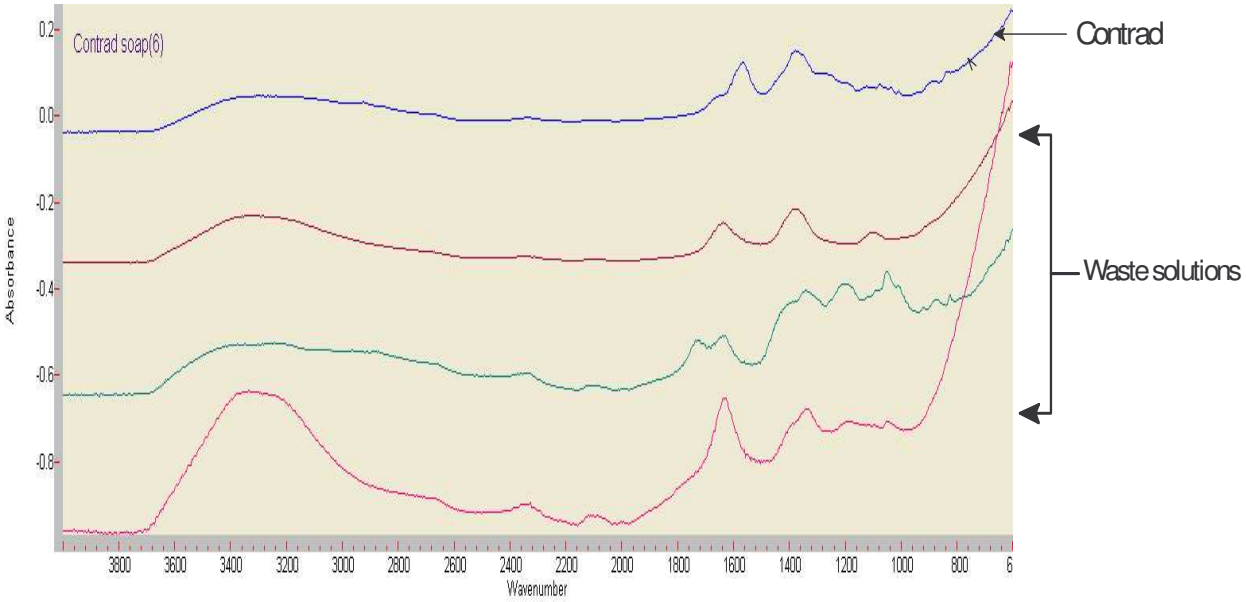

Figure 4.6 Infrared analyses (absorption) of the sampled waste solutions compared to Contrad detergent

When comparing the FTIR spectra of Contrad with the waste solutions (Figure 4.6) the corresponding vibrational frequencies indicate the possibility of Contrad in these waste solutions, thus confirming the UV-visible spectroscopy results. The very low quantities of organic solvents such as acetone, butanol, kerosene and other organic degradation products present in the GS-MS results (Appendix 6) could not be observed in the FTIR analyses.

As the composition of the carboys could differ dramatically, it was decided to formulate a test solution for this study. The organic test solution was based on a historical inventory of organics used at Necsa.

The composition of the organic test solution ($1dm^3$) was as follows:

- 100 ml acetone
- 100 ml ethanol
- 100 ml scintillation liquid (Perklin Elmer Gold)
- 100 ml methanol
- 100 ml chloroform
- 200 ml 10% Contrad detergent
- 90 ml TBP
- 210 ml kerosene

4.2 Alkaline Hydrolysis Treatment Method on the Test Mix Components

The alkaline hydrolysis treatment technique was specifically developed for the destruction of organic liquids such as TBP (Pente et al., 2008). The effectiveness of the hydrolysis treatment technique was studied with the method described in Section 3.2 on the following mixtures to determine the applicability for Necsa's waste solutions. Each of the mixtures was reacted with12.5 M NaOH in a 1:1 ratio.

(i) Analytical grade (30%) TBP mixture in (70%)
(ii) The same test mixture as (i) with the addition of Contrad detergent
(iii)The organic test solution described in section 4.1also reacted
(iv)The organic test solution with a 10% Contrad solution added

The FTIR spectra (Figure 4.7) of the alkaline hydrolysis of solution (i) containing only TBP and kerosene showed a decrease of the P-O-C stretch vibration at wavenumber 1000 cm^{-1}, which indicated a decrease in TBP concentration. This is in correlation with alkaline hydrolyses of TBP to form DBP and butanol.

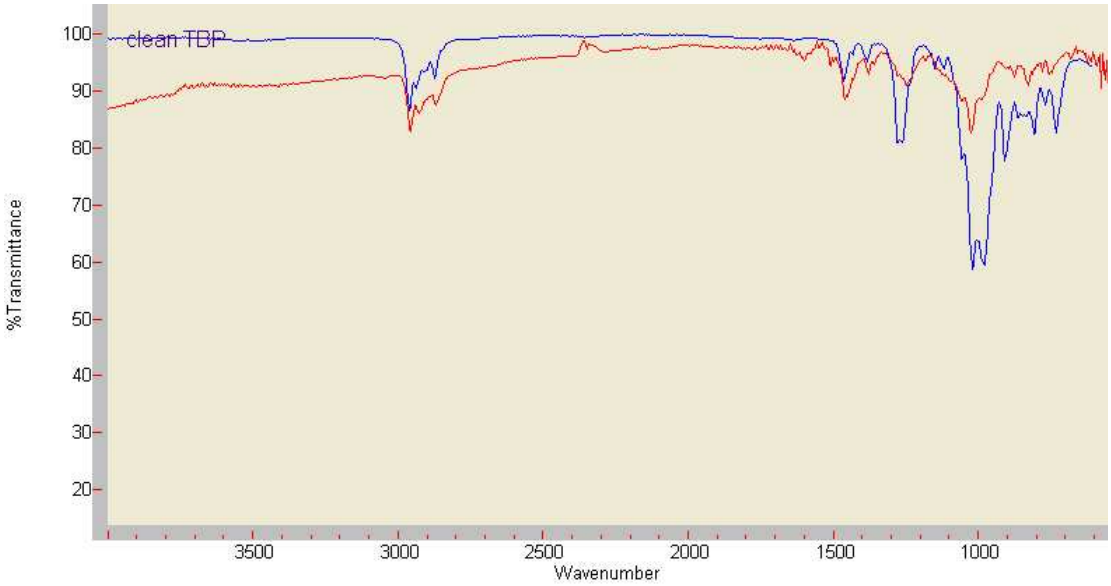

Figure 4.7 FTIR spectra of analytical grade TBP (blue) and TBP that underwent alkaline hydrolysis (red)

As described in chapter 2.4.1 the two main products that form during the alkaline hydrolysis of TBP are butyl alcohol and sodium dibutyl phosphate according to the following reaction (2)

$(C_4H_9O)_3PO + NaOH \rightarrow (C_4H_9O)_2POONa + C_4H_9OH$

The butyl alcohol remains in the top organic phase whilst the inorganic sodium dibutyl phosphate dissolves into the water phase.

To confirm the FTIR results, the resulting organic phase was analysed by GC-MS. The GC-MS indicated in Figure 4.8 the presence of butanol which is a by-product of TBP hydrolysis.

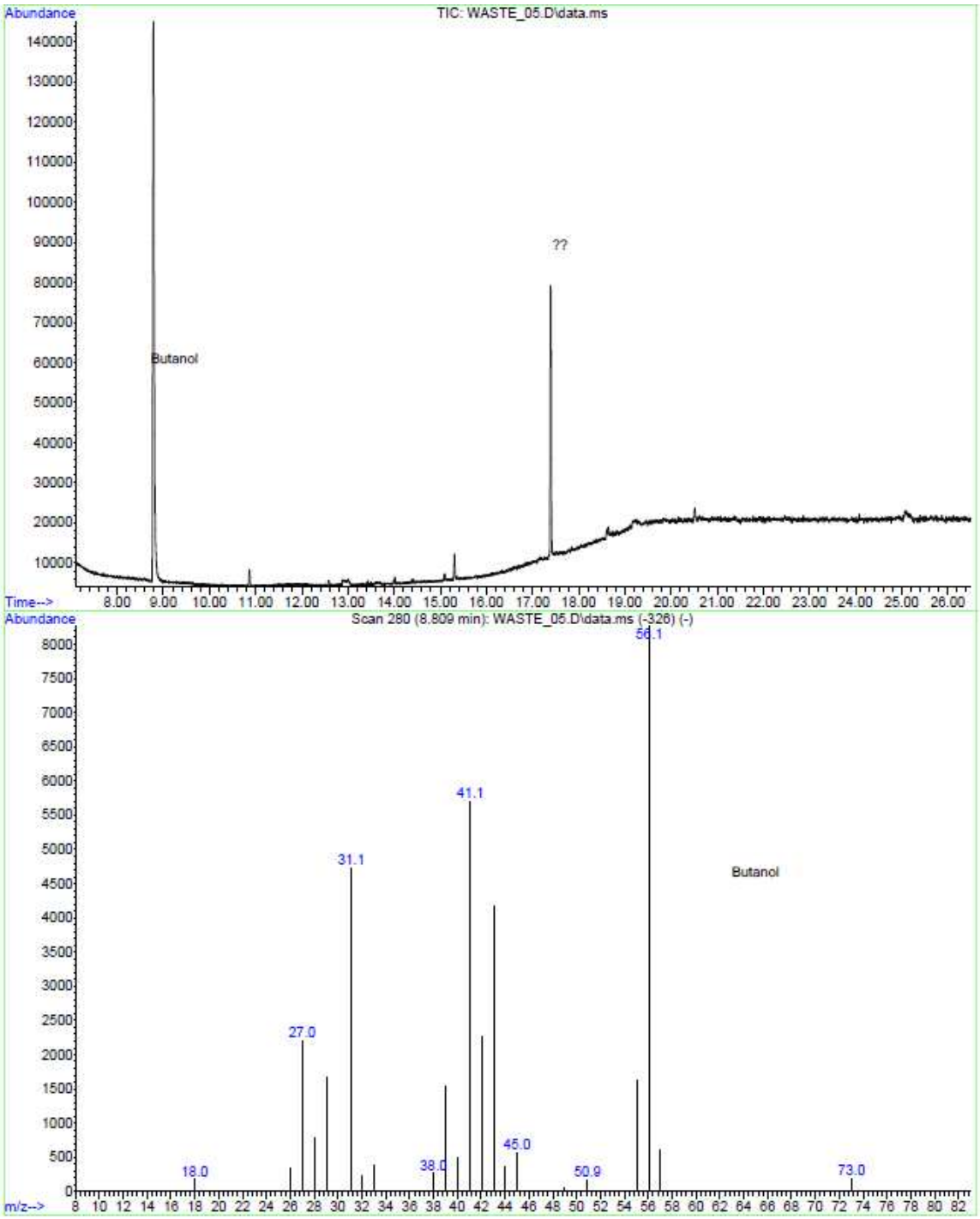

Figure 4.8 GC-MS analysis of an alkaline hydrolysed 30% TBP-kerosene solution

The TBP / kerosene / Contrad test solution before and after hydrolyses show similar IR spectra with only a slightly higher hydroxyl associated peak around 3500 cm^{-1} (Figure 4.9).

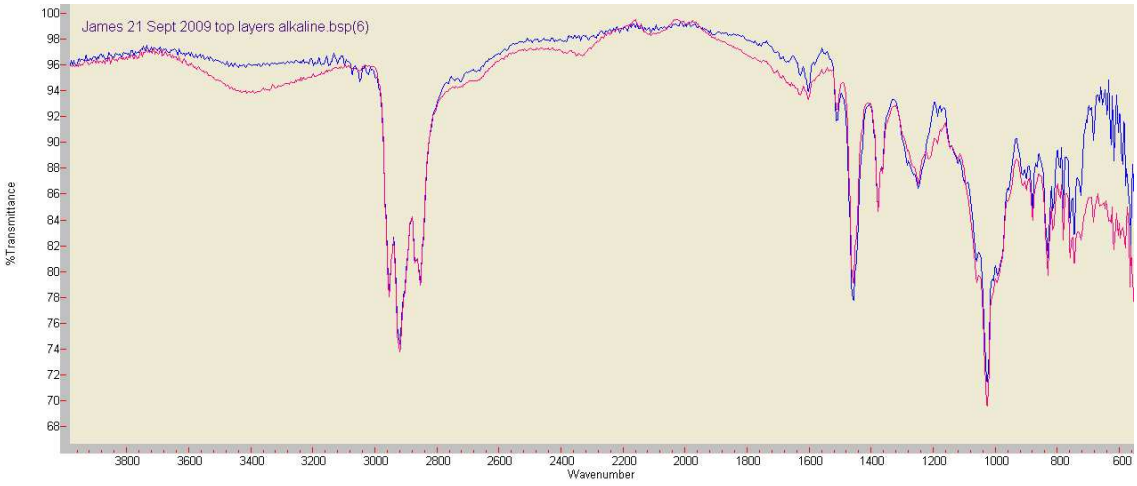

Figure 4.9 FTIR spectra of TBP with 5% Contrad detergent before (blue) and after alkaline hydrolyses (red)

This result indicate that the presence of Contrad inhibit the destruction of TBP. As the possibility exists that Contrad is present in the carboys, this technique would therefore not be suitable for Necsa waste. Results for a standard TBP / kerosene mixture and scintillation liquid are obtained in Figure 4.10 and Figure 4.11 repectively showing the different carbon structures for kerosene and elution time for TBP.

The organic test, with and without Contrad, was hydrolised and analysed with the GC-MS to investigate what structures were formed in the organic phase of the alkaline hydrolysed solutions. Results are shown in Figure 4.12 and Figure 4.13.

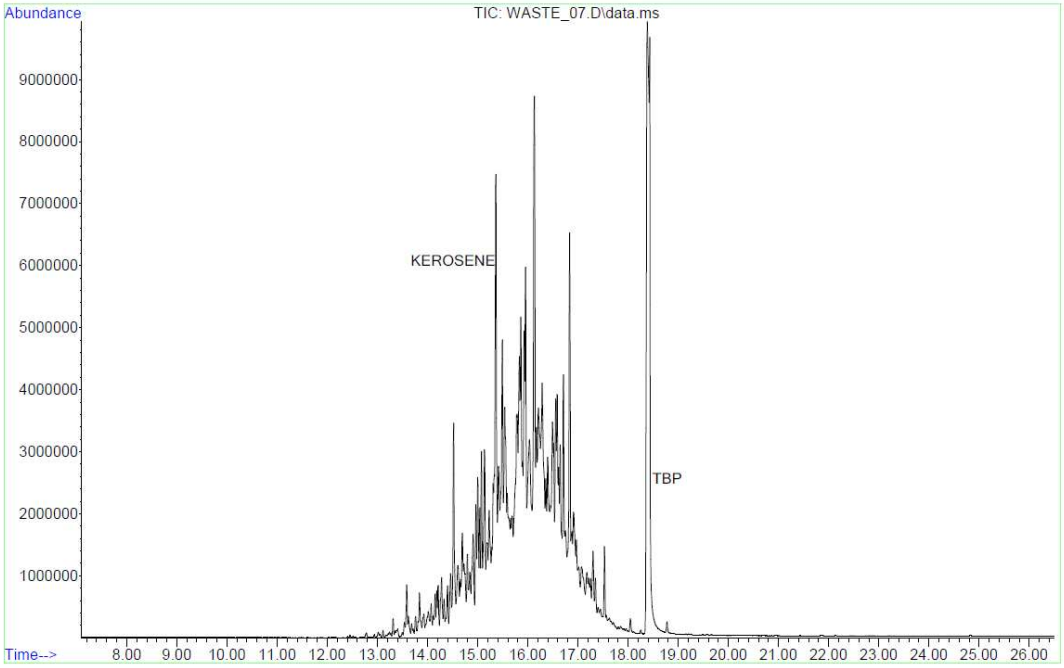

Figure 4.10 TBP Kerosene (30/70%) standard mixture

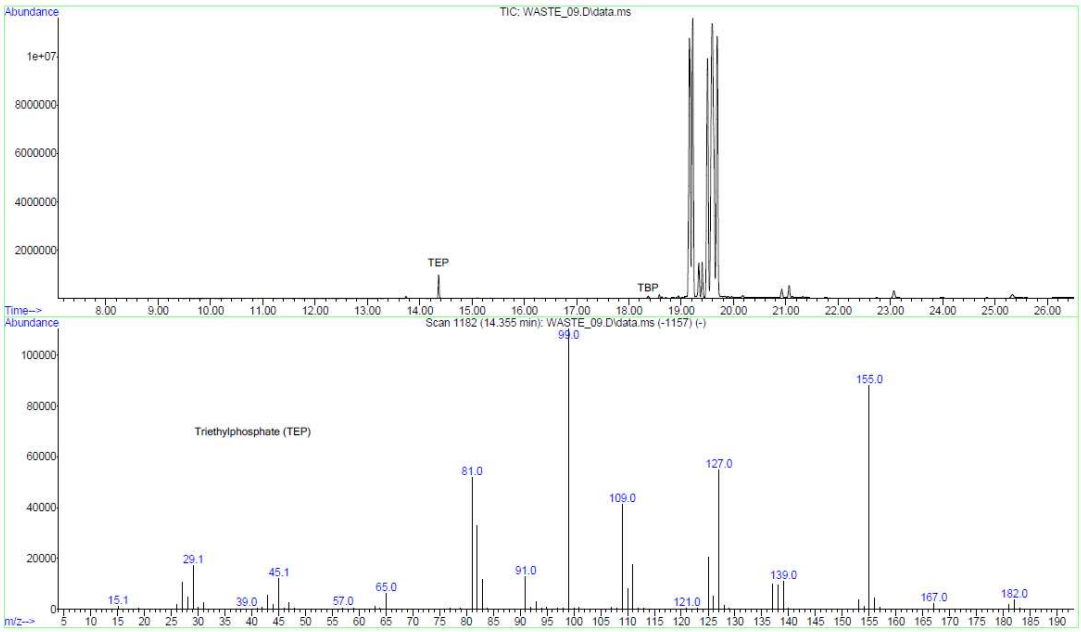

Figure 4.11 Scintillation liquid

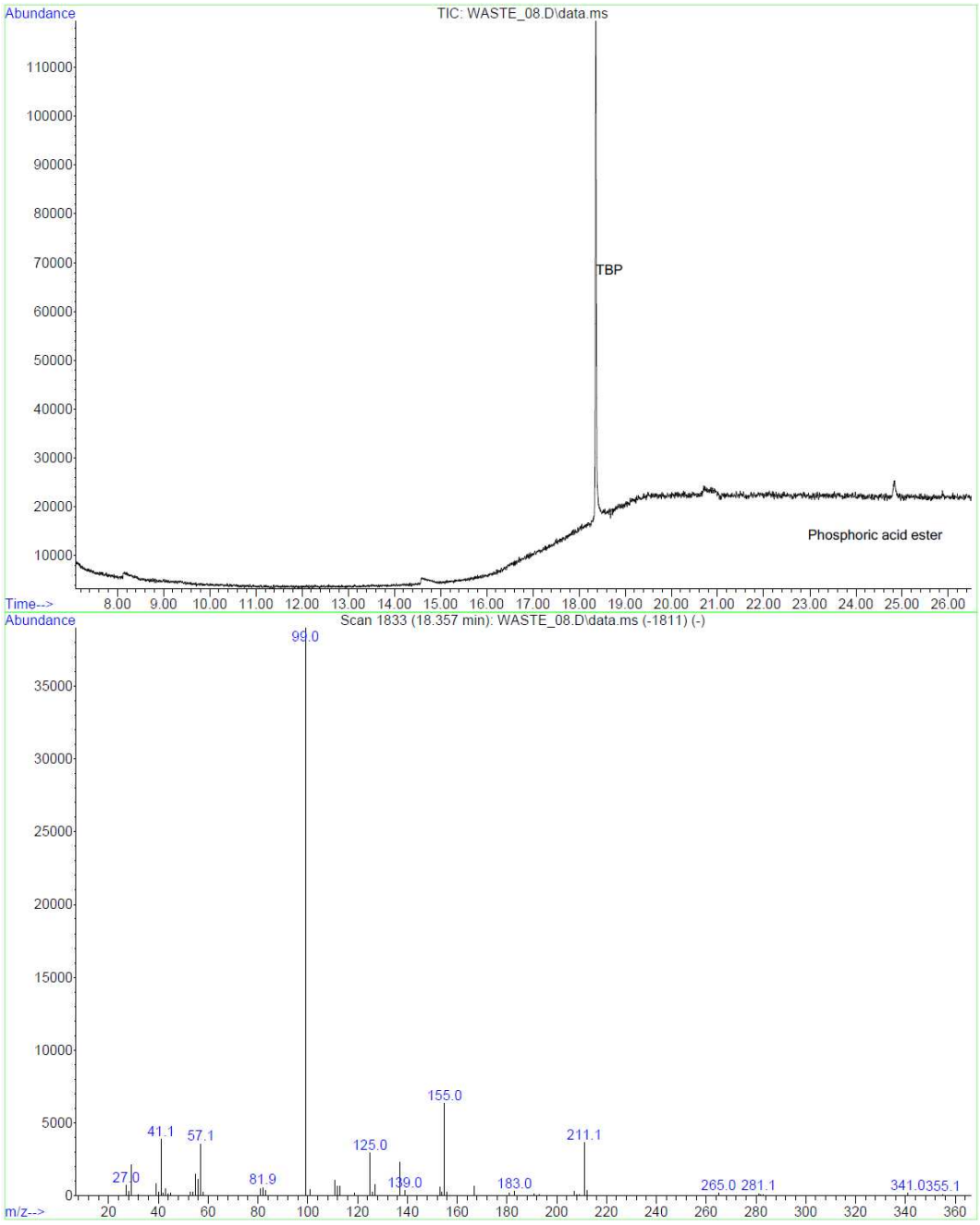

Figure 4.12 GC-MS analysis of an alkaline hydrolysed organic test mixture without 10% Contrad detergent

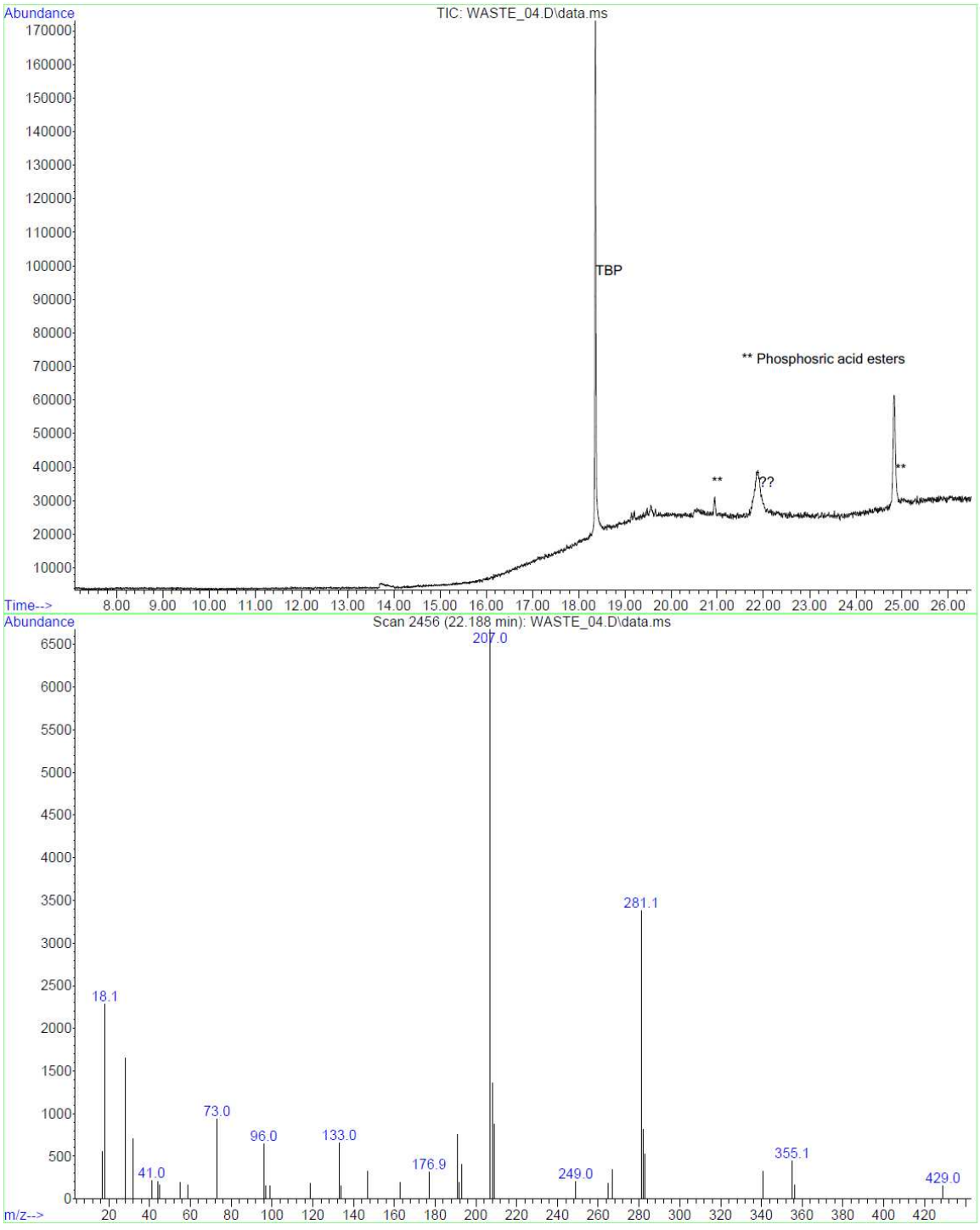

Figure 4.13 GC-MS analysis of the organic test mixture with additional 10% Contrad in the water

Results in this section indicates that the alkaline hydrolyses method can be used to destroy TBP with the formation of butanol and DBP. However, when a TBP / kerosene solution contains other organic constituents and / or detergent such as Contrad, the hydrolysis reactions are not effective. As the possibility exist that Contrad detergent could be present in the carboys, this technique cannot be considered for Necsa.

4.3 Non Thermal Treatment of the Components of the Test Mixture

4.3.1 Ozone and UV Treatment

As indicated in Section 2.4.4 ozone can be used to destroy organic molecules. In order to study the influence of ozone on the organic components, 470.6 mg O_3 h^{-1} were purged (as calculated in Appendix 5) through a deionised water solution containing the organic components These tests were done on scintillation liquid, Contrad detergent and acetone, with and without UV radiation. The rates of destruction of these components were calculated as 1st order rates.

4.3.2 Stability and UV Lamp Tests

Stability tests (Figure 4.14 and Figure 4.15) were performed to eliminate possible artefacts in the experimental setup that could be misinterpreted for the destruction of scintillation liquid. The experimental setup has no influence as shown in Figure 4.15. The emissions of the UV lamp (Figure 4.16) was analysed to determine if these corresponds with the electronic transition of scintillation liquid demonstrated in Figure 4.14. The emission result in Figure 4.16 corresponds with the electronic transition of scintillation liquid and therefore the possibility for destruction exists.

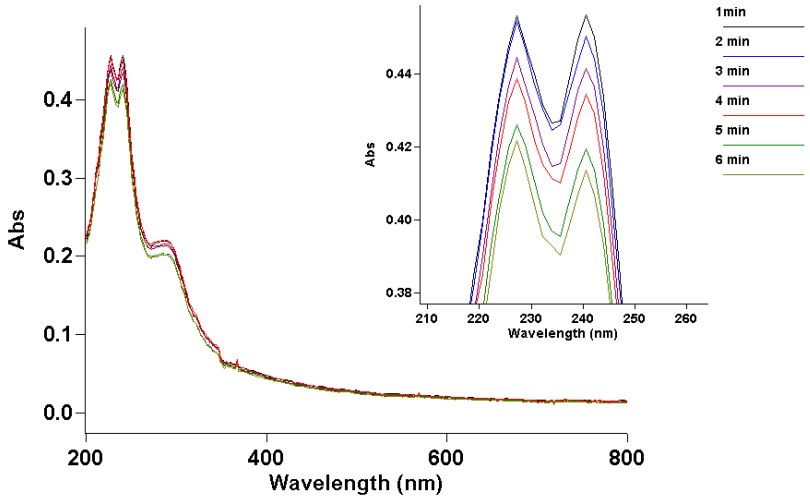

Figure 4.14 Stability test for scintillation liquid (20 ppm)

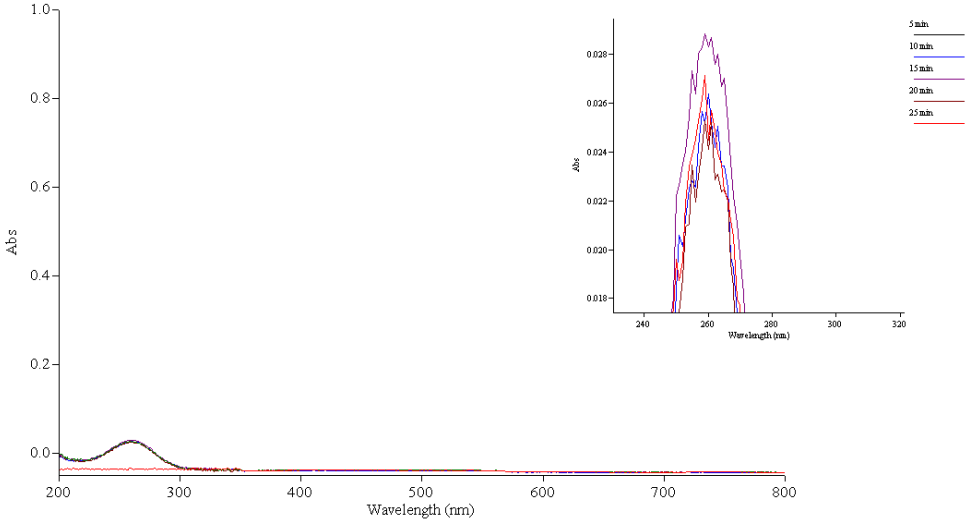

Figure 4.15 Stability tests on deionised water when purged with ozone to evluate the influence on the baseline

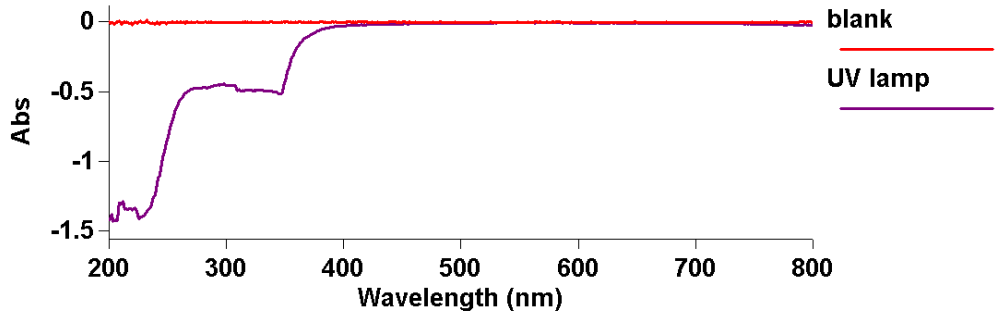

Figure 4.16 Determination of the emissions of the UV lamp

4.3.3 Scintillation Liquid

4.3.3.1 Destruction with ozone

Initial results of 10 ppm scintillation liquid diluted in deionised water subjected to ozone are indicated in Figure 4.17. The results clearly show the destruction process as the absorbance decrease with time. The rate of destruction is presented in Figure 4.18.

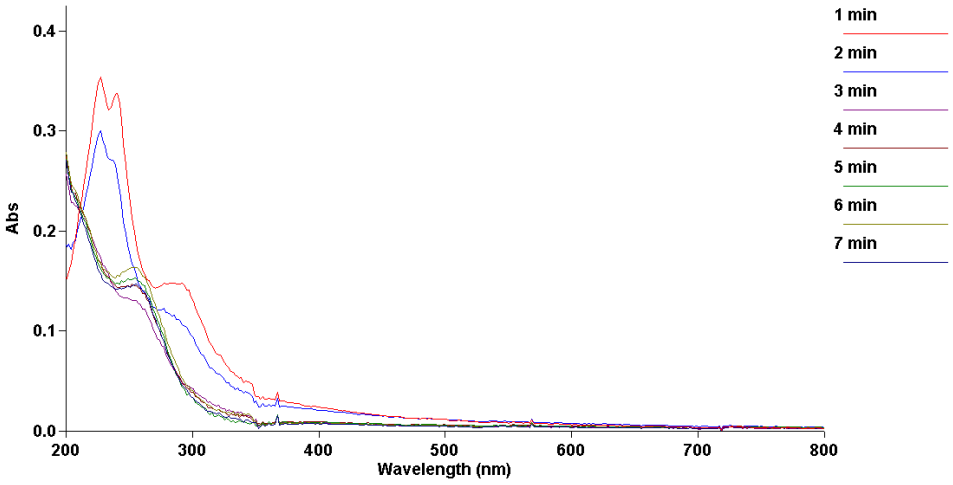

Figure 4.17 Scintillation liquid, 10 ppm, purged with ozone

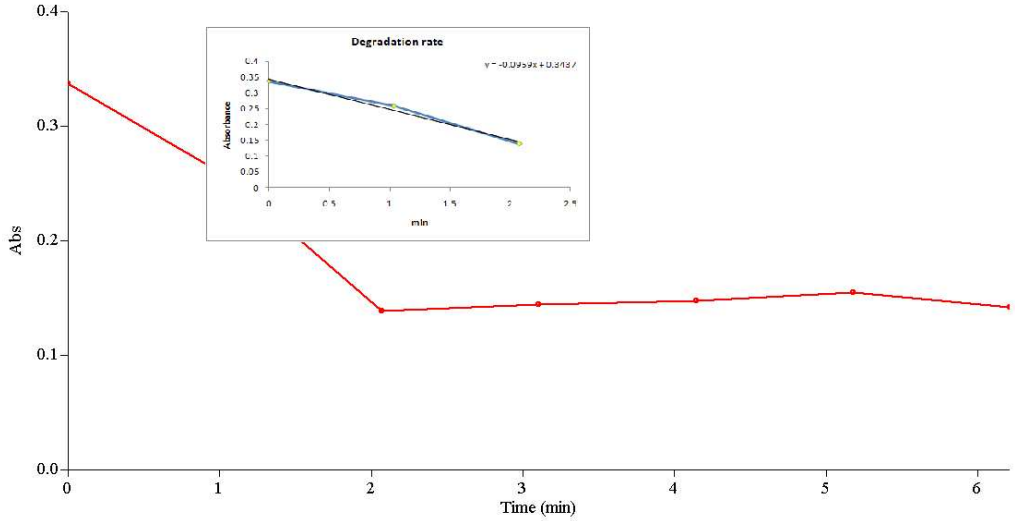

Figure 4.18 Degradation rates for 10 ppm scintillation liquid

4.3.3.2 Destruction with UV

The results of scintillation liquid in deionised water subjected to UV radiation are indicated in Figure 4.19. The results clearly indicate the destruction of scintillation liquid as the absorbance decrease with time. By schematically presenting the decrease of absorbance with time, the results in Figure 4.20 indicate a first order reaction.

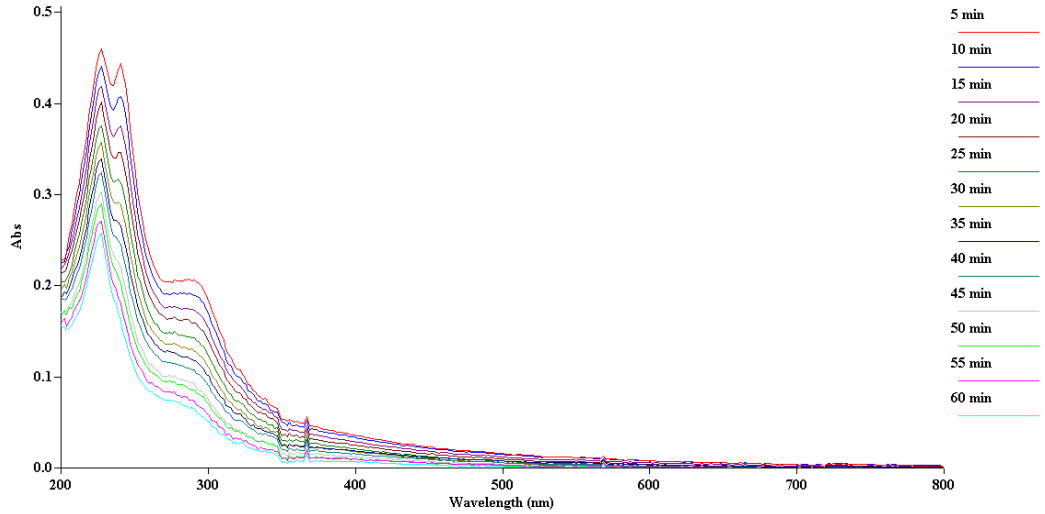

Figure 4.19 Degradation with UV radiation of scintillation liquid (20 ppm)

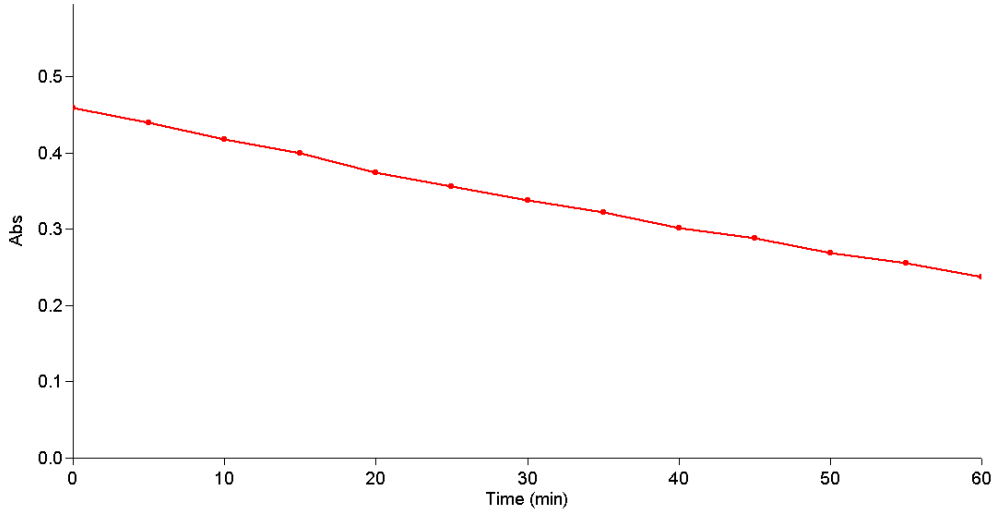

Figure 4.20 Degradation rate of UV radiation on scintillation liquid

4.3.3.3 Destruction of scintillation liquid with a combination of ozone and UV radiation

In order to catalyse the degradation reaction of scintillation liquid additionally, the

experiment was repeated bubbling ozone through the solution whilst radiating it with UV radiation. The concentration of the scintillation liquid was increased to 40 ppm to acquire better results. The purpose of UV radiation as describe in Section 2.3.7 is to increase the formation of hydroxyl radicals and possibly causing the direct breaking of bonds by absorption of the required energy.

Results in Figure 4.21 show the degradation of scintillation liquid and while the destruction rates from these reactions are illustrated in Figure 4.22. Two reaction rates (as 1st order reactions) are observed in Figure 4.22 when scintillation liquid is degraded by a combination of UV radiation and ozone purging. A possible explanation for this is that scintillation liquid composition consisting of detergent organic components and organic solvents. The solvents are generally more resistant against degradation and degrade slower as can be seen with acetone destruction in Section 4.3.3.

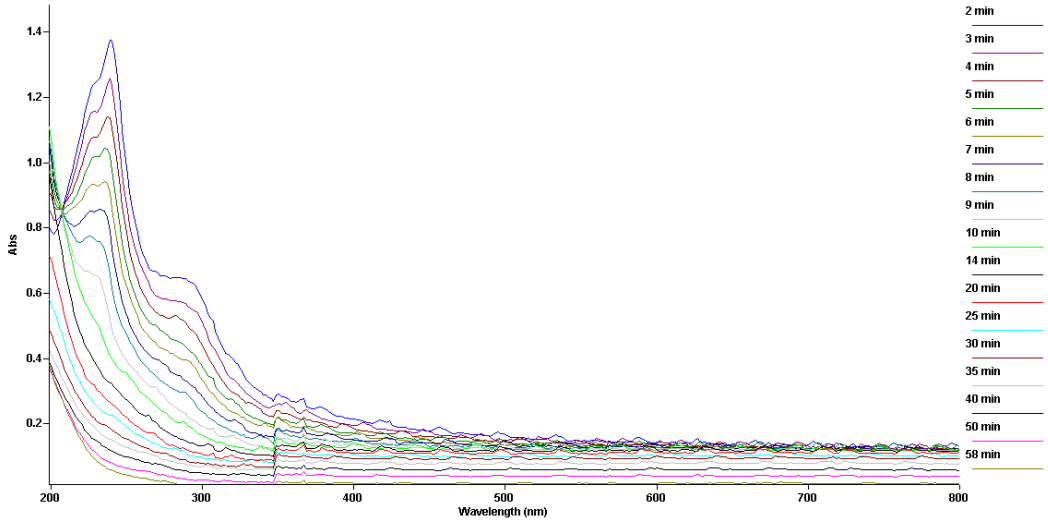

Figure 4.21 Influence of ozone purging combined with UV radiation on scintillation liquid (40 ppm)

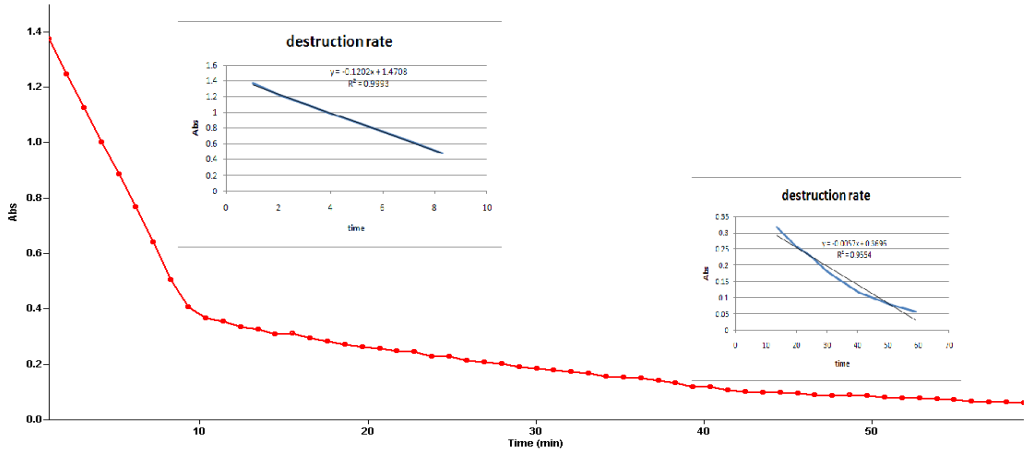

Figure 4.22 Degradation rates of scintillation liquid at 240 nm for UV and ozone

The results confirm that UV-ozone rapidly degrades scintillation liquid and could be applied to treat organic waste containing scintillation liquid. By comparing the different rates as indicated in Figure 4.23, it is clear that the presence of ozone can be used to destroy Necsa waste.

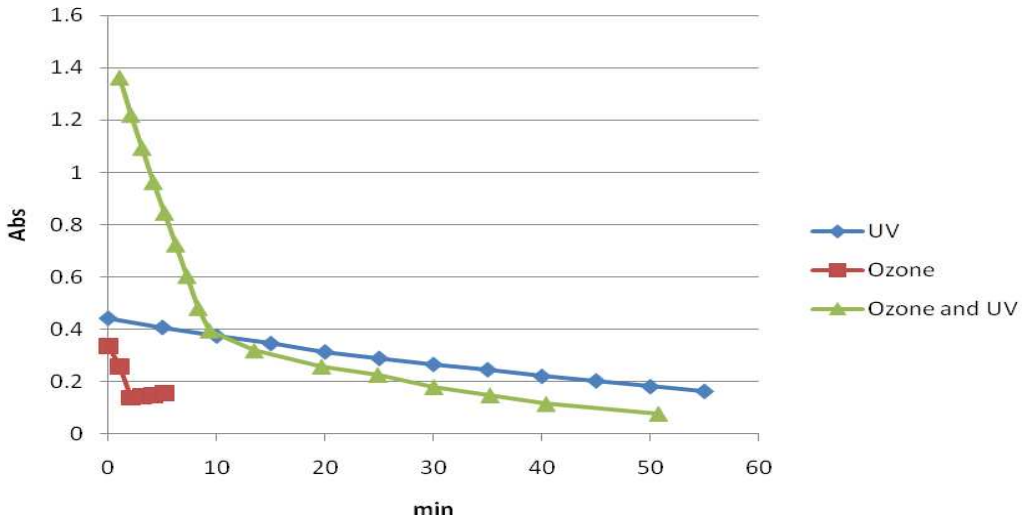

Figure 4.23 UV and ozone degradation rates of scintillation liquid

4.3.4 Contrad

4.3.4.1 Stability tests with Contrad solution

Stability results (Figure 4.24) indicated that the experimental setup will create no artefacts that could be misinterpreted during the destruction tests on Contrad solutions. Contrad is an amine containing EDTA detergent used for decontamination.

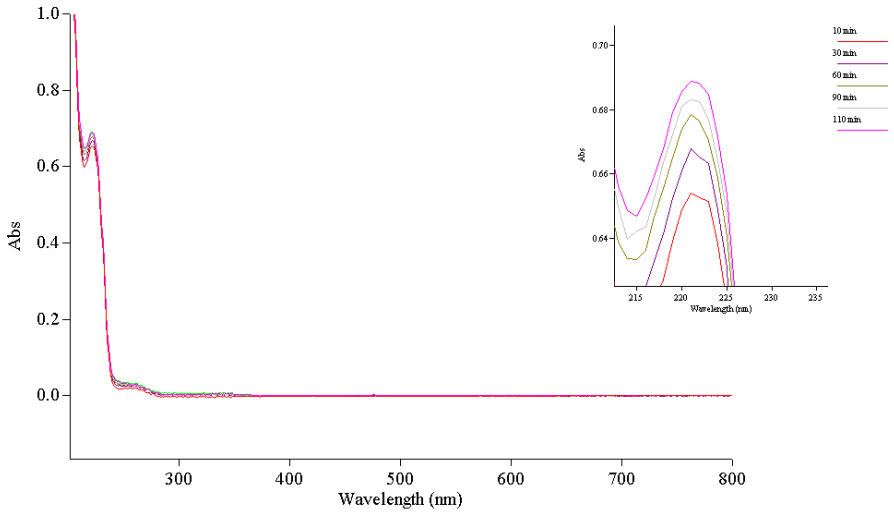

Figure 4.24 Stability tests for experimental setup with a 0.2% Contrad solution

The emission from the UV lamp determined in Figure 4.16 corresponds with the electronic transition of Contrad detergent in Figure 4.25 and therefore the possibility exists that excitation can destruct the Contrad detergent. Dilute solutions of Contrad in deionised water were subjected to ozone, UV and a combination of the UV-ozone.

4.3.4.2 Destruction with ozone

Experiments were performed as described in Section 3.3. Results of a 0.2% solution

of Contrad are presented in Figure 4.25. The results indicate that ozone can be use to destroy Contrad detergent.

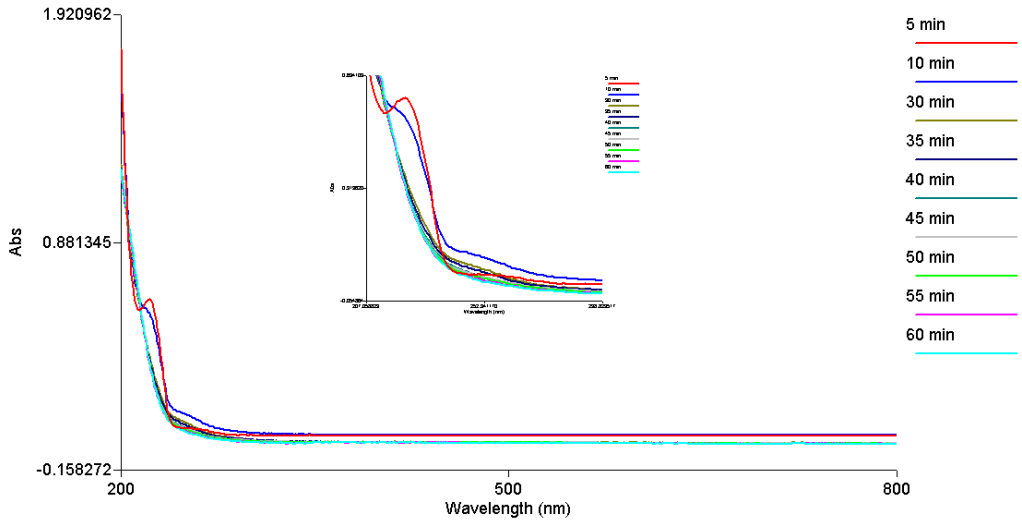

Figure 4.25 Ozone degradation of Contrad soap (0.2%)

By schematically plotting the absorbance at 220 nm versus time, a destruction rate of 0.045 min^{-1}, were obtained (Figure 4.26).

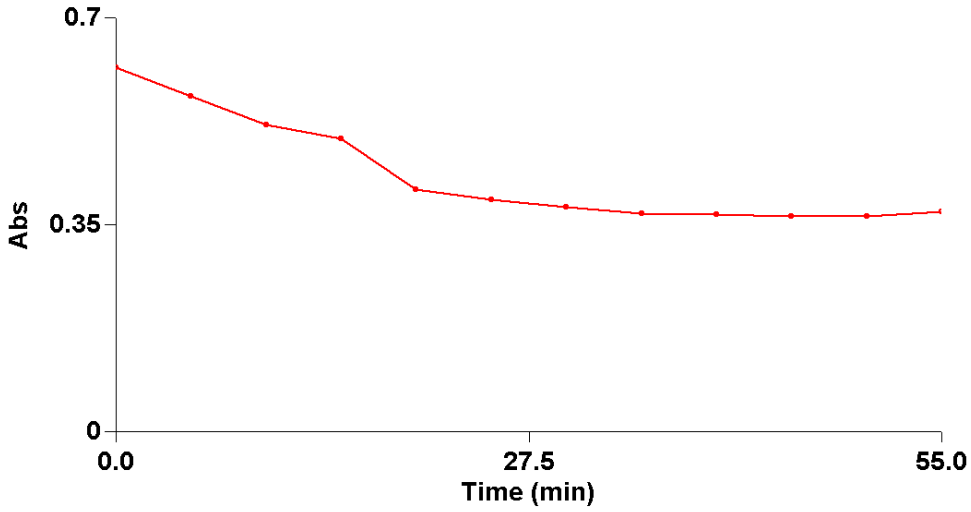

Figure 4.26 Ozone degradation rate of Contrad soap (0.2%) at 220 nm

4.3.4.3 Destruction of Contrad solution with UV radiation

The results of Contrad detergent subjected to UV radiation are presented in

Figure **4.27**. The results clearly indicate that UV can be used to destroy Contrad detergent (decrease in absorbance). This confirms the assumption that the electronic transitions of the Contrad detergent correspond to the energy bandwidth regions emitted by the UV lamp.

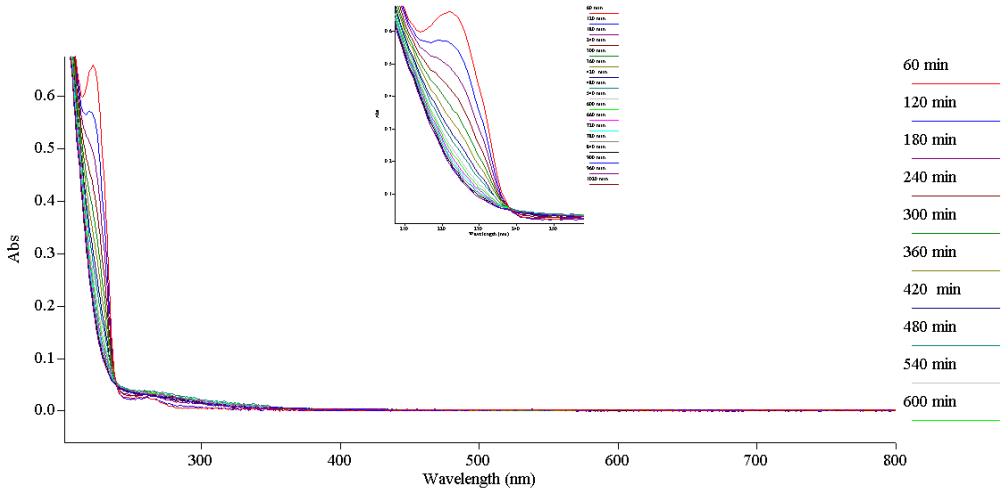

Figure 4.27 UV degradation of Contrad (0.2%)

The graph in Figure 4.28 indicated that the rate of Contrad destruction with UV radiation is 0.0035 min^{-1} as measured from the absorbance at 220 nm. The rate is much slower (>10) when compared to ozone destruction.

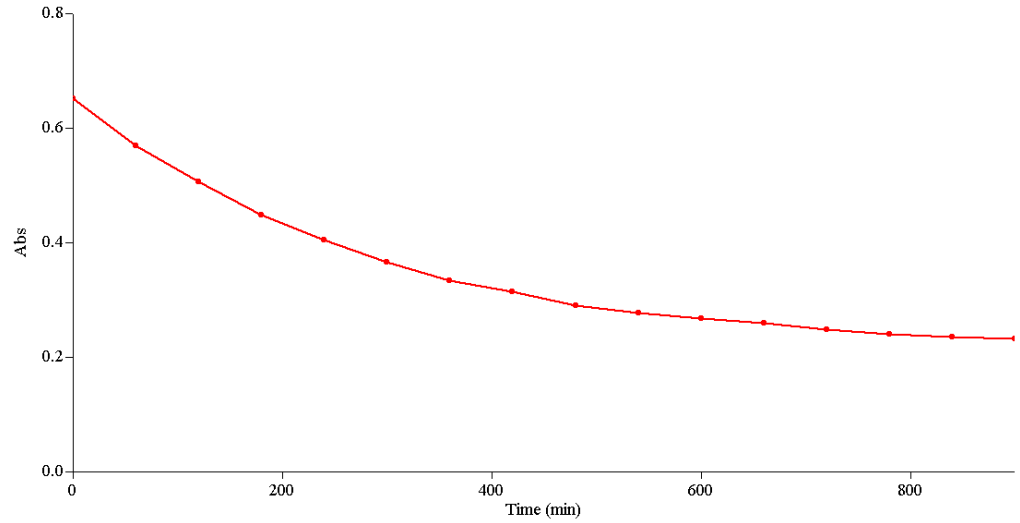

Figure 4.28 Degradation rate of Contrad (UV radiation)

4.3.4.4 Destruction of Contrad solution with UV radiation and ozone

In order to determine if the combination of UV radiation and ozone purging have an accelerated destruction of Contrad detergent, experiments were performed as described in section 3.4. The results of the destruction of Contrad detergent by UV / ozone combination are indicated in Figure 4.29. The combined effects are schematically presented by the rate graph in Figure 4.30.

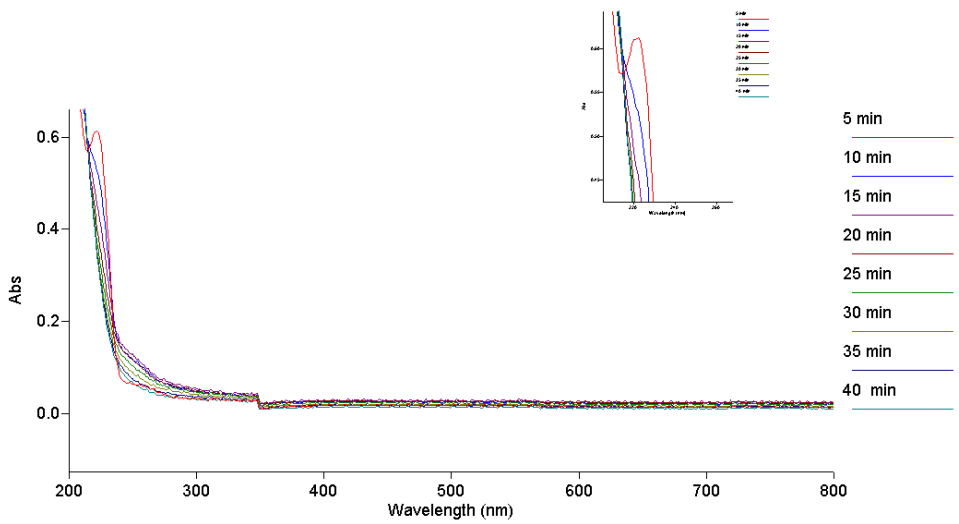

Figure 4.29 Contrad degraded by UV radiation and ozone purging

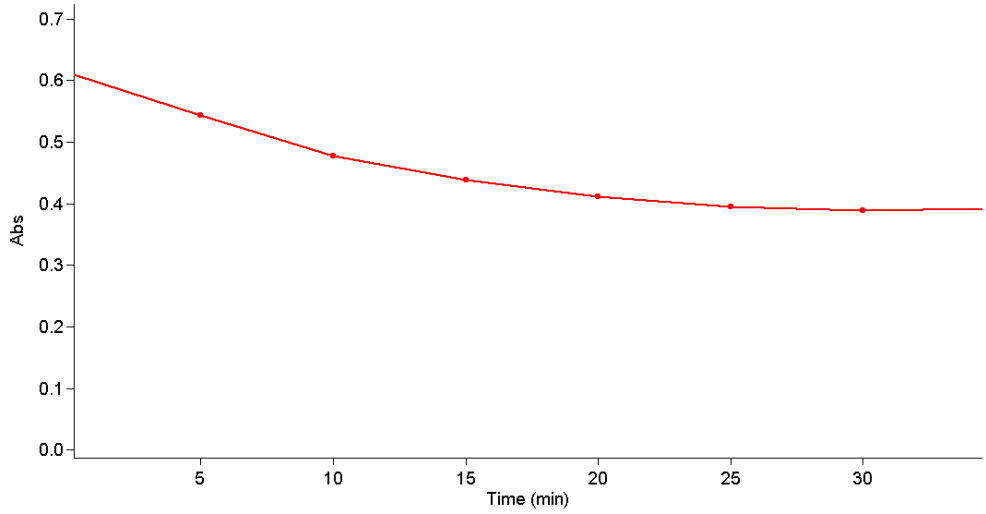

Figure 4.30 Degradation rate of Contrad because of UV radiation and ozone purging

When comparing the destruction rates of UV, ozone, and combined UV / ozone in Figure 4.31, it is clear that the rates of ozone purging alone and when combined with UV radiation are the same and faster than UV alone. Results show that UV and

ozone can be used to destroy Contrad, however ozone alone can destruct Contrad as effective as the combination of ozone and UV.

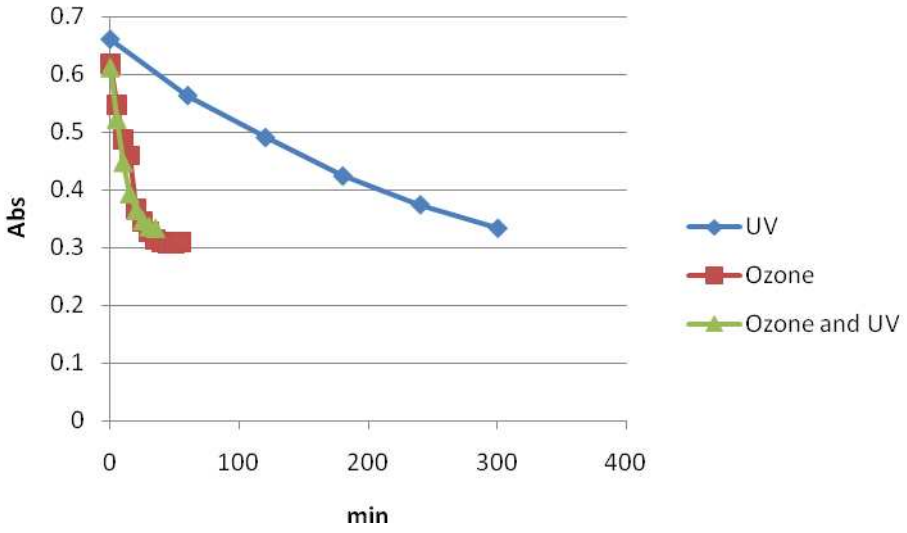

Figure 4.31 Comparison of degradation rates of Contrad detergent

4.3.5 Acetone

4.3.5.1 Stability test

Acetone is used in the nuclear industry to remove organic compounds from glassware surfaces before and after experimentation. Acetone will therefore be present in organic waste and the destruction must be investigated. In order to ensure that the experimental setup had no influence on the analysis / destruction of acetone, stability tests were performed. The stability results in Figure 4.32 indicate that the experimental setup is acceptable.

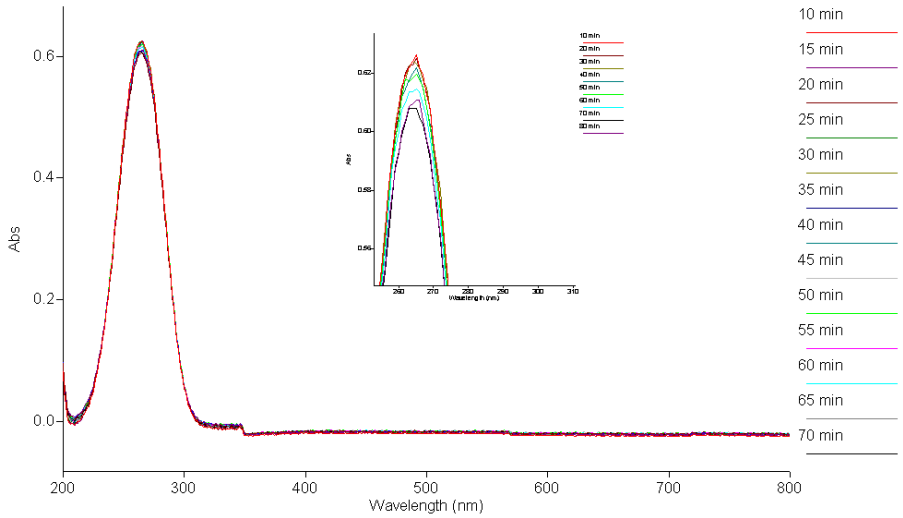

Figure 4.32 Acetone Stability tests

4.3.5.2 Ozone destruction of acetone

Results of the destruction of acetone with ozone are presented in Figure 4.33. The results indicate that ozone can destroy acetone, although at a slow rate (as1st order 0.007 min^{-1}) shown in Figure 4.34.

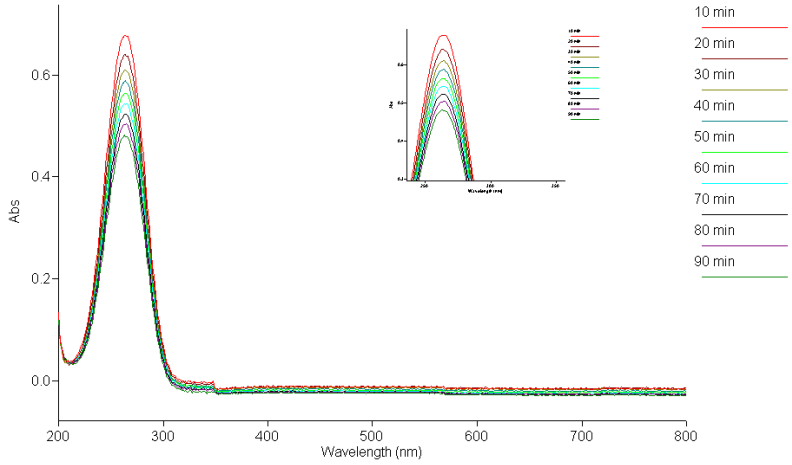

Figure 4.33 UV spectra of ozone degradation of acetone

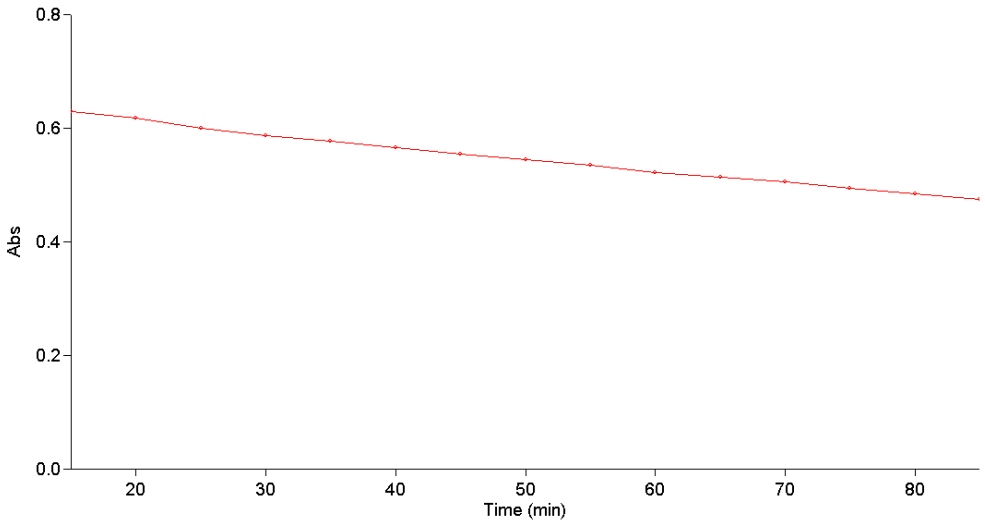

Figure 4.34 Degradation rate of ozone destruction of (0.6%) acetone

4.3.5.3 UV radiation destruction of acetone

The results of acetone subjected to UV radiation are shown in Figure 4.35. Also clearly indicated is the destruction of acetone. This confirms that UV can be use to destroy acetone. Schematically the decrease in absorbance against time can be presented in Figure 4.36 as a 1st order reaction (0.0005 min^{-1})

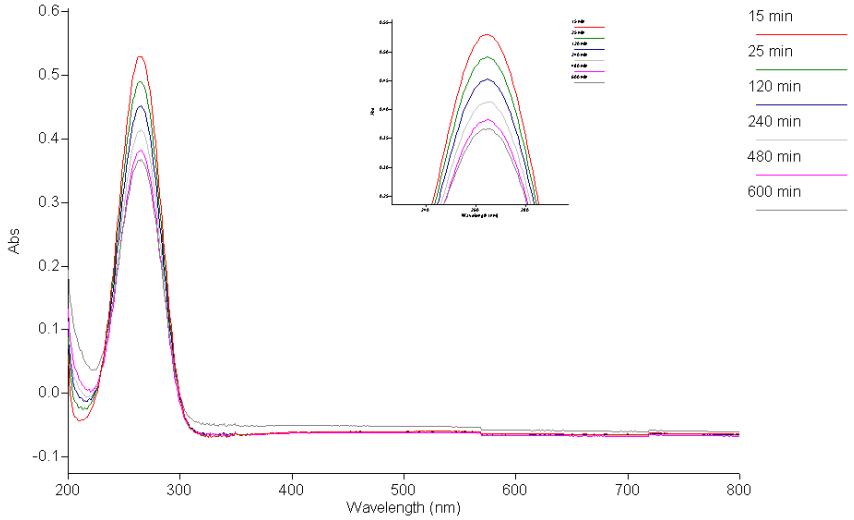

Figure 4.35 UV spectra of acetone radiated with UV light

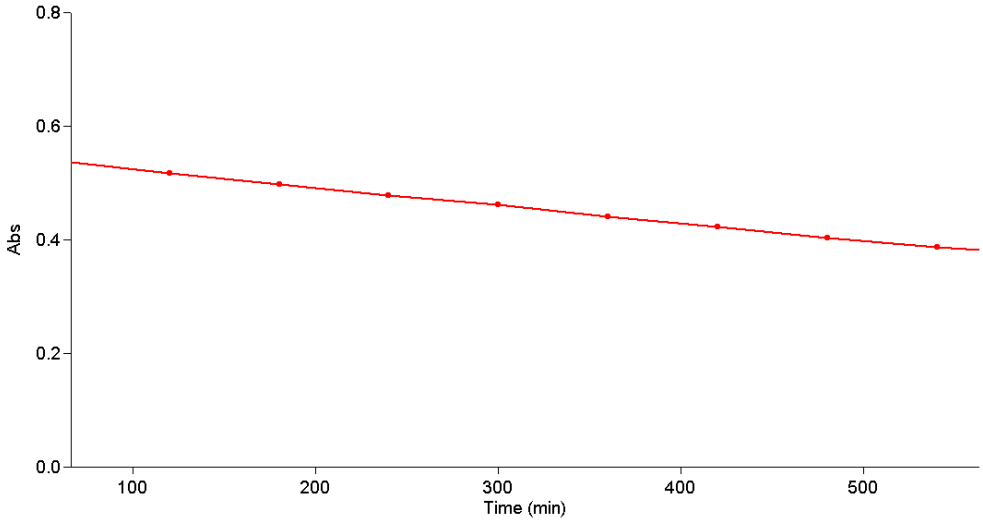

Figure 4.36 Degradation rates of acetone with UV light

4.3.5.4 Ozone and UV radiation destruction of acetone

In order to determine whether the combined effect of acetone and UV has an accelerated influence on the degradation of acetone, experiments were performed and the results presented in Figure 4.37 and Figure 4.38.

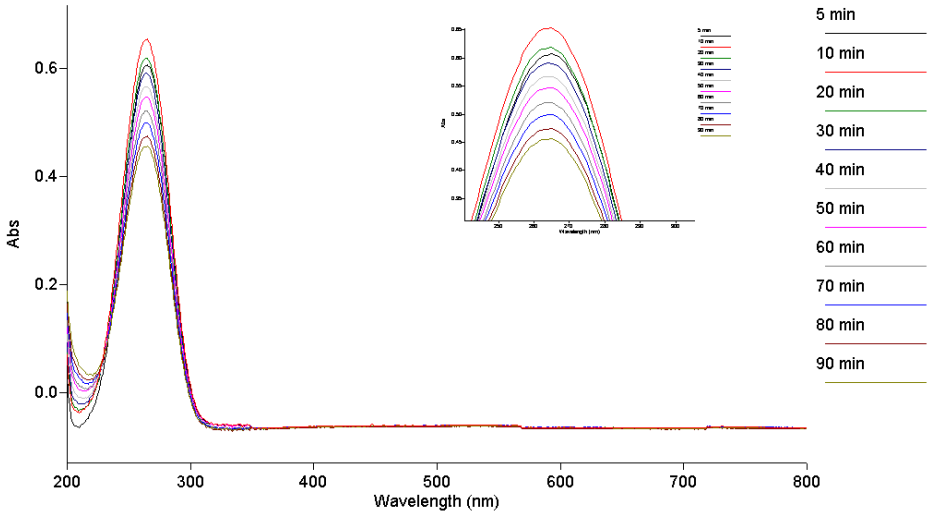

Figure 4.37 UV spectra of degradation of acetone by UV radiation and ozone purging

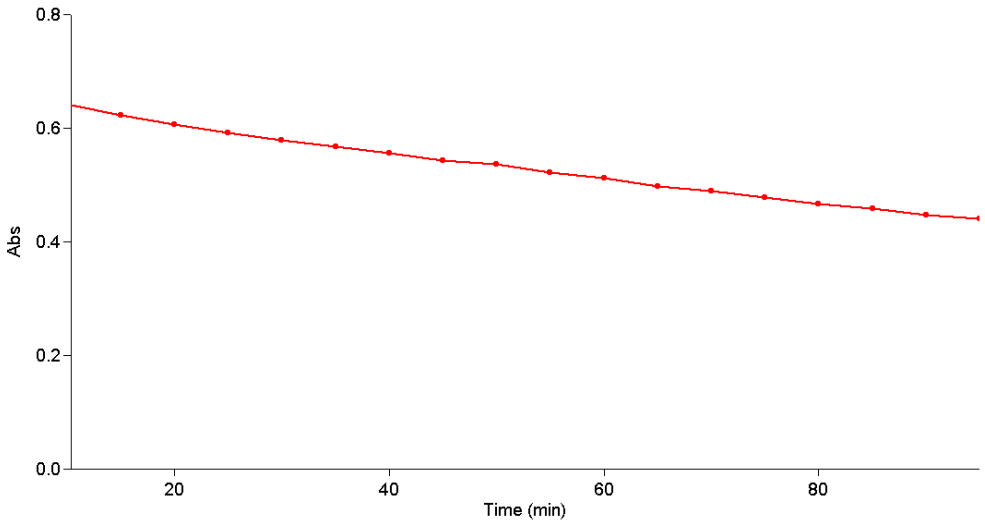

Figure 4.38 Degradation rate of acetone with UV radiation and ozone purging

A comparison of the rates of degradation with time as shown in Figure 4.39 indicate that degradation of acetone is faster with ozone than UV alone. UV does destruct acetone, but slower (0.0005 min^{-1})

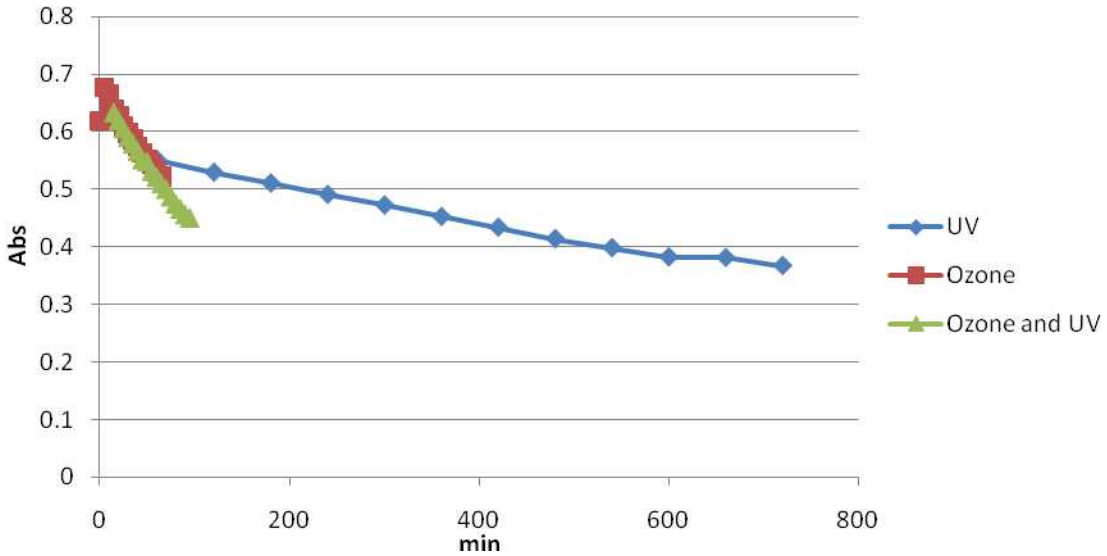

Figure 4.39 Comparison of degradation rates of acetone

The results confirm that UV and ozone treatment degrades acetone and could be applied to treat organic waste containing acetone.

4.4 Treatment of the Organic Test Mixture with the Non Transfer DC Thermal Plasma

The organic test solution was subjected to a plasma process in order to destroy the organic components by high temperature as described in Section 3.5. Gaseous reaction products were analysed using a GC MS and the results are presented in Figure 4.40 and Figure 4.41. Results indicate that at high temperatures, TBP and kerosene are split into smaller molecules such as ethane, ethylene, ethyne and other short chain carbon isomers.

Although the results confirmed that the organic mixtures can be pyrolysed with plasma techniques, these gases would require further treatment prior to release to the environment. As Necsa does not have a license to operate this technology, it will not be further researched.

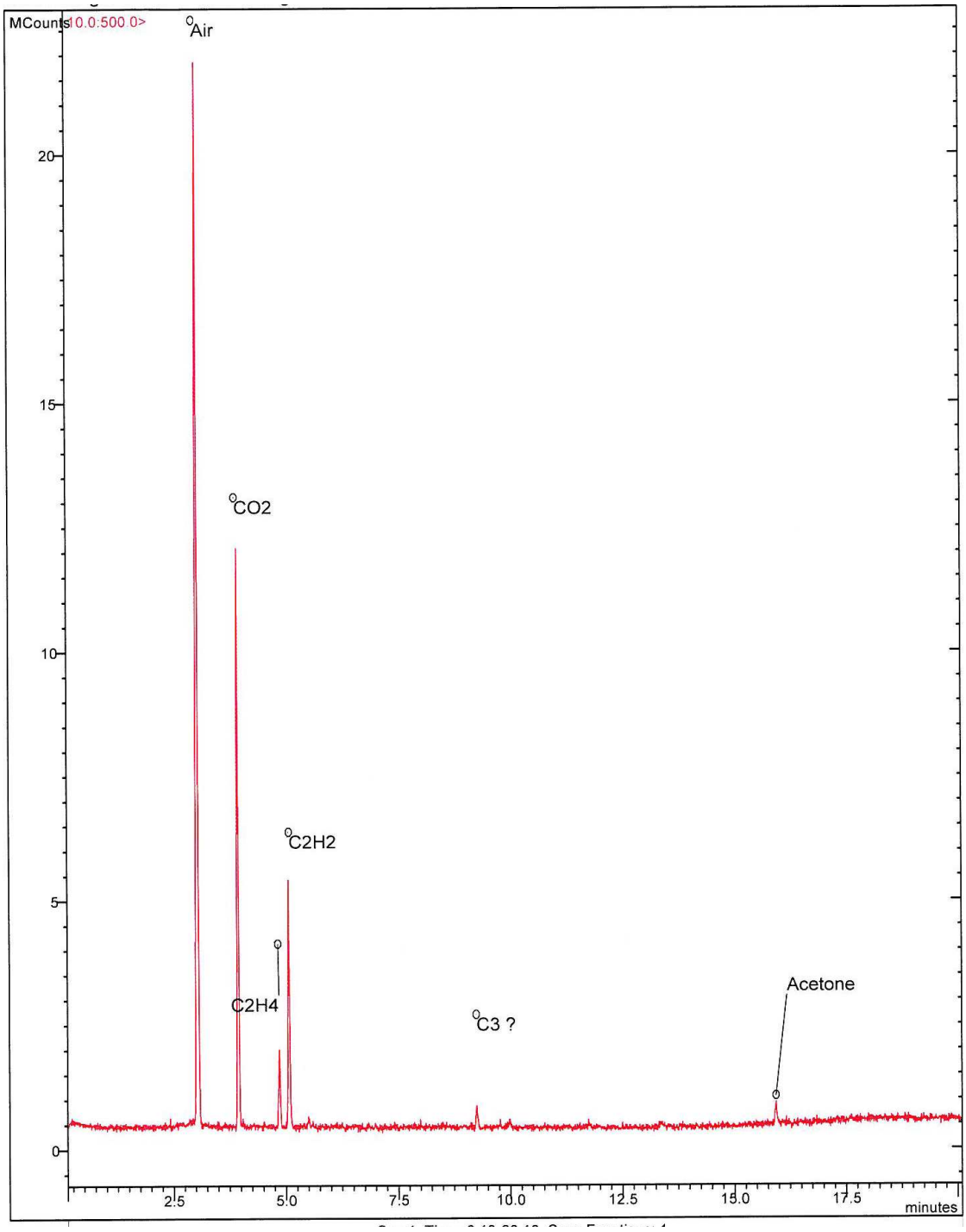

Figure 4.40 GC results of gaseous sample from plasma experiment on the test mixture 1st run

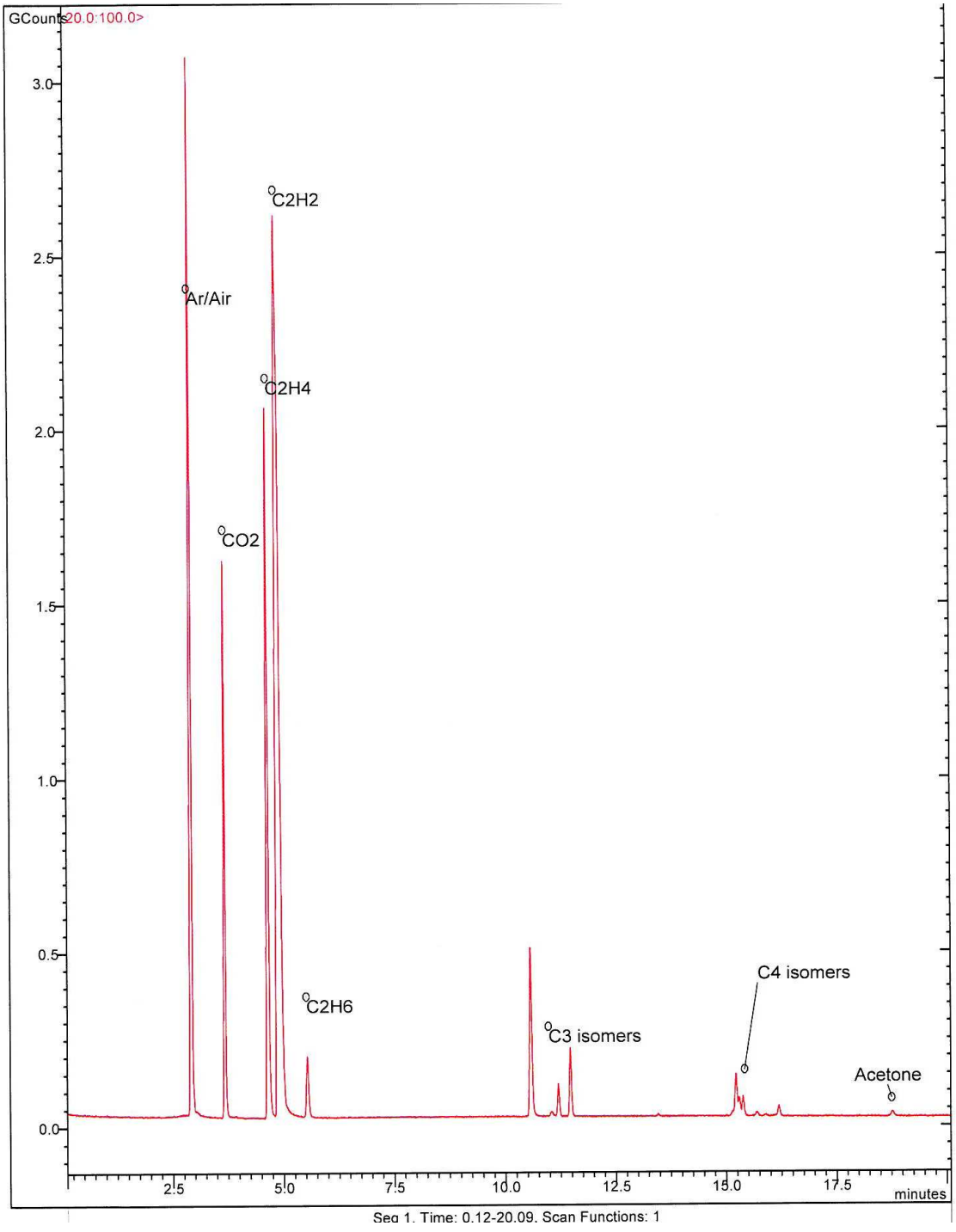

Figure 4.41 GC results of gaseous sample from plasma experiment on the test mixture 2nd run

4.5 Absorption of Organic Components onto Nochar N910, Polymeric Resins.

4.5.1 Absorbance of Contrad detergent on Nochar resin

Literature previously discussed in Section 2.6.1 describes that different polymeric resins exist that can be used to adsorb most organic liquids. Contrad solutions were evaluated for absorption onto Nochar resin and were mixed for 24 h in test tubes with Nochar resin as described in Section 3.6, Table 3.2. Analyses of the absorption with UV-visible spectroscopy presented in Figure 4.42, Figure 4.43 and Figure 4.44 clearly shows that Contrad detergent is not absorbed by Nochar resin

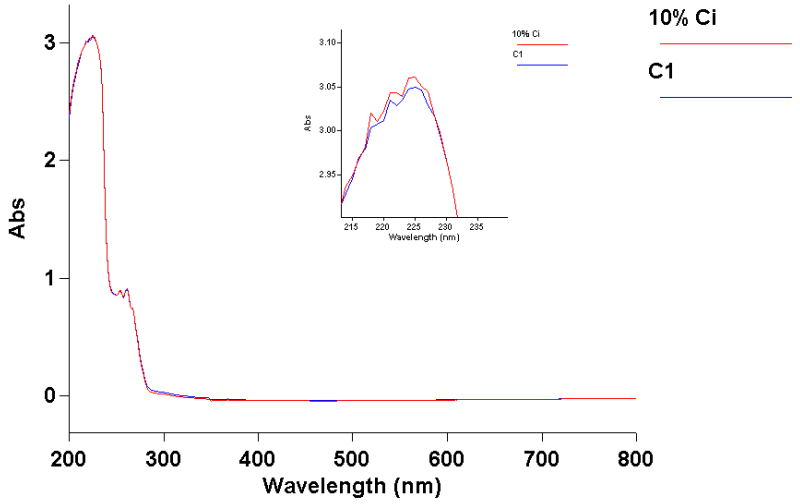

Figure 4.42 UV-visible spectrum of Contrad 10% (initial solution)

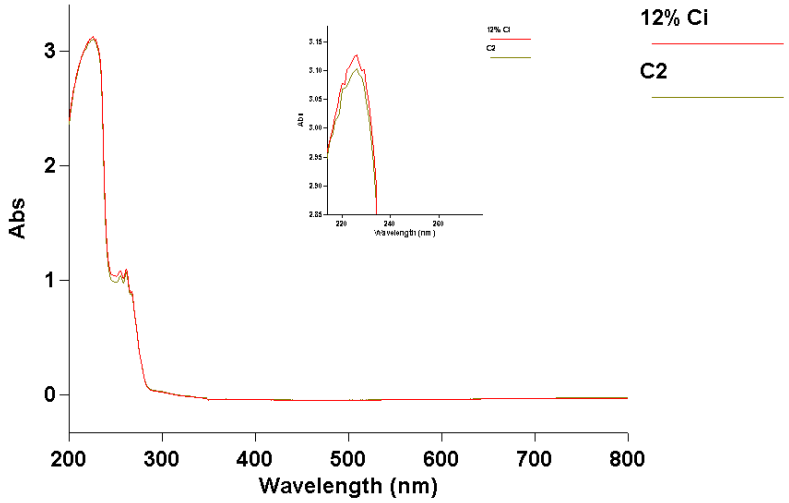

Figure 4.43 UV-visible spectrum of Contrad 12% (initial solution C2 after K_D tests)

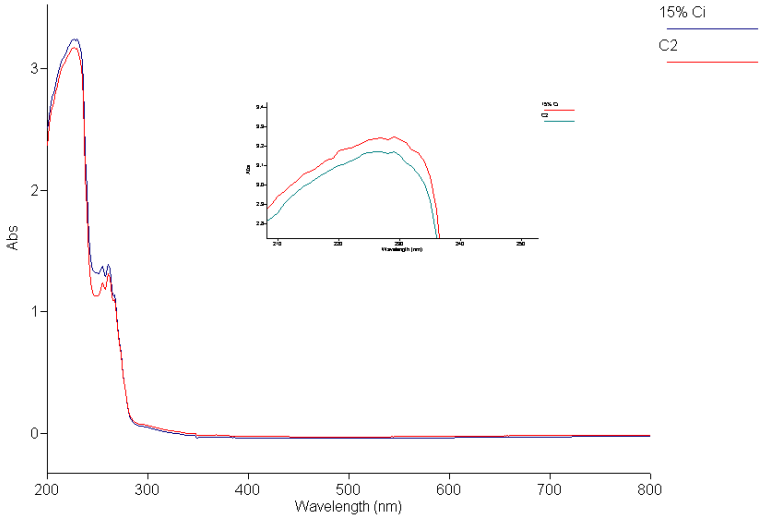

Figure 4.44 UV-visible spectrum of Contrad 15% (initial solution C3 after K_D tests)

The results indicate that Nochar resin cannot be used to remove Contrad from the organic waste streams.

4.5.2 Absorbance of scintillation liquid on Nochar resin

Scintillation liquid was also tested as described in Section 3.6 for its absorption onto Nochar with an in line filter constructed with Nochar resin. Scintillation liquid with a concentration of 10 ppm was analysed with a UV-visible spectrophotometer before circulation through the filter and after it has circulated for 3 h. Results are presented in Figure 4.45 and clearly show that only certain components of the scintillation liquid are removed with this technique.

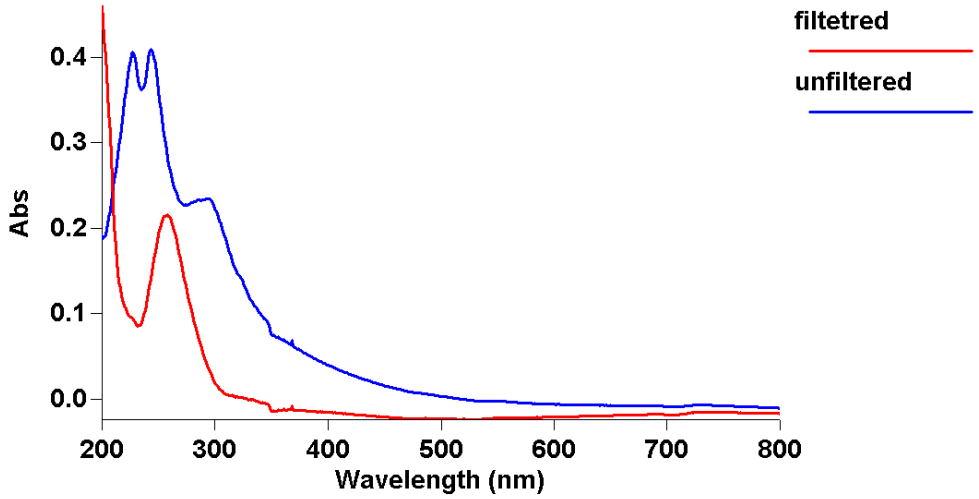

Figure 4.45 UV-visible spectraof scintilation liquid (10 ppm) before and after it has been filtered through a Nochar filter

4.5.3 Absorbance of acetone on Nochar resin

For this experiment a 1% acetone solution in deionised water was circulated through a Nochar filter as described in Section 3.6. By detecting the decrease in acetone with UV-visible spectroscopy, the spectra (Figure 4.46) clearly indicate that acetone can be removed by Nochar resin and it can therefore be considered to remove acetone from Necsa's waste solutions.

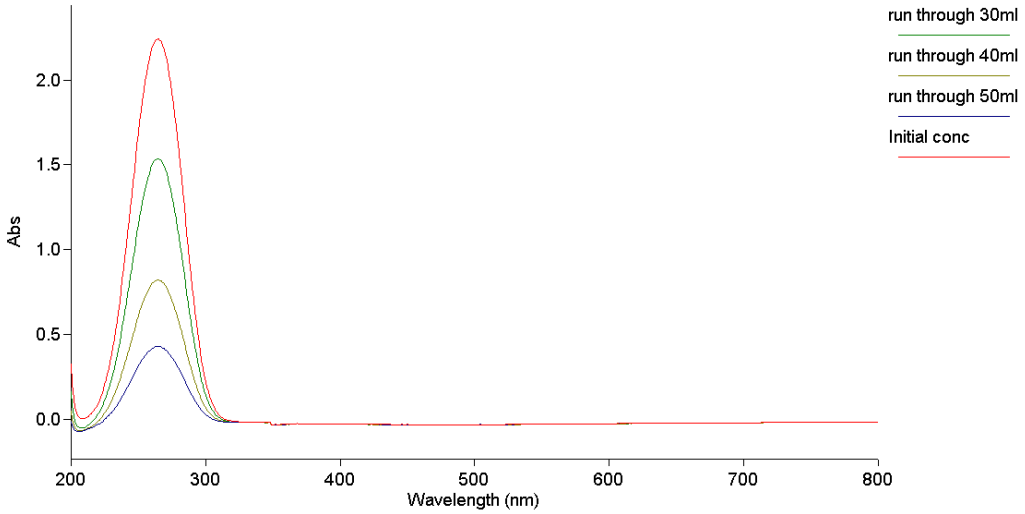

Figure 4.46 UV-visible spectrum showing the absorption of acetone on Nochar 910 resin

4.5.4 Absorption of TBP Diluted in Acetone onto Nochar

Although acetone is absorbed by Nochar resin, the resin still absorbs small amounts of TBP dissolved in acetone. Experiments were done according to Section 3.6, Table 3.2 and GC results show this trend clearly in Figure 4.47. UV visible analysis was not used for TBP analysis due to the fact that no electronic transition exists for TBP between 200 and 600 nm.

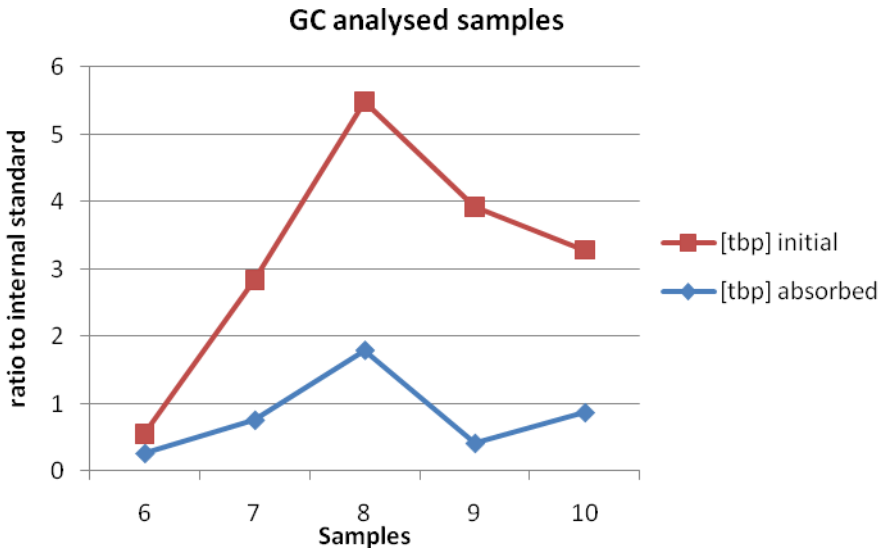

Figure 4.47 GC analysis of TBP in acetone absorbed onto Nochar resin

4.5.4 Stability of the TBP-Nochar complex

4.5.4.1 Influence of Redox conditions

TBP as a waste product in the carboys should not contain huge amounts of uranium because most of the uranium would have been stripped with HNO_3. The uranium originates from the liquid extraction processes at Necsa where the uranium is removed from the aqueous nitric acid phase with TBP. However the possibility exist that the Nochar when bonded with TBP, could now act as a stationary phase with the absorbed TBP and could therefore have the added advantage of uranium recovery from waste streams under suitable redox conditions. To confirm this possibility, two experiments were designed to study the possible absorption and release of uranium from the absorbed TBP. The results in Table 4.2 indicate that when 0.1 M solutions spiked with uranium is circulated through a TBP-Nochar complex, minimal absorption take place. However when changing the molarity of the solution to 3 M,

then a 50% reduction in the amount of uranium in the liquid phase occurs as shown in Table 4.3. This corresponds to the increase in uranium content in the filter as shown in Table 4.2 (C,D & E).The PUREX process also use 3 M HNO_3 to absorb the uranium onto the TBP and 0.1 M HNO_3 to release it from the TBP.

Table 4.2 Nochar in line filter activity counts

Filter	Weight of N910 resin in g	Molarity HNO_3	Activity
A	1.1909	0.1 M	1402
B	1.3030	0.1 M	1821
F	1.0656	0.1 M	1198
D	1.1681	3.0 M	8163
E	1.019	3.0 M	5423
C	1.2705	3.0 M	7342

Table 4.3 Uranium activity in liquid after 5 minutes

Circulating liquids used with Filters	Molarity HNO_3	Activity
Aqueous A	0.1 M	9412
Aqueous B	0.1 M	9830
Aqueous F	0.1 M	9693
Aqueous D	3.0 M	5261
Aqueous E	3.0 M	5386
Aqueous C	3.0 M	5651

In Necsa waste solutions TBP as well as Contrad are present. As both of these

uranium complexing agents could be present in liquid organic waste, the ability to use the TBP-Nochar in the presence of Contrad as an extraction matrix must be investigated. The results in Table 4.4 indicate that with Contrad solution present, the amount of uranium absorbed onto the TBP Nochar complex declined and are similar to 0.1 M HNO_3 results. Upon acidifying the solution an increase of uranium absorption onto TBP-Nochar complex is onbserved. This increase is probably due to destruction of the uranium – EDTA complex, thus releasing uranium to bind onto the TBP.

Table 4.4 Uranium activity when Contrad detergent is present

Sample	Nochar g	pH	Contrad	Acivity on Filter	Activity in solution
G	0.9927	> 7	with	1280	9400
G	0.9927	< 7	without	2556	8475
I	1.1365	> 7	with	1079	9696
I	1.1365	< 7	without	1777	8227

4.6 Encapsulation of the TBP / Kerosene Mixture by PPC Cement in Combination with Poly Acrylonitrile Fibres and Polyvinyl Alcohol Fibres

A very limited cement encapsulation test program was conducted to prove the compatibility of the solidified TBP polymer with cementitious grout. Polymeric fibres were added as reinforcement with the aim to anchor the Nochar resin into the cement. The polymeric fibres were polyvinyl alcohol and homo polyacrylic fibres. These fibres are widely used in the building industry for cement reinforcement and may serve as a binding agent for Nochar, improving Nochar resin's encapsulation (See also Appendix 15).

Sorptivity is a measurement of the penetration of water into the cured cements samples driven by capillary forces. The lower this value, the more resistant the cement is perceived to be (Bentz et al, 2001. The samples were prepared and evaluated for sorptivity according to Section 3.7.1. Results indicate that matrix A, containing PAN fibres was not as compact as the matrixes which all produced similar curves for the water absorbed. The sorption coefficients in Table 4.5 ($kg.m^{-2}.s^{-1/2}$) were determined from the slope of the line of best fit by linear regression analysis from Figure 4.48 as follows:

Sorptivity coefficients (A) = (gradient)

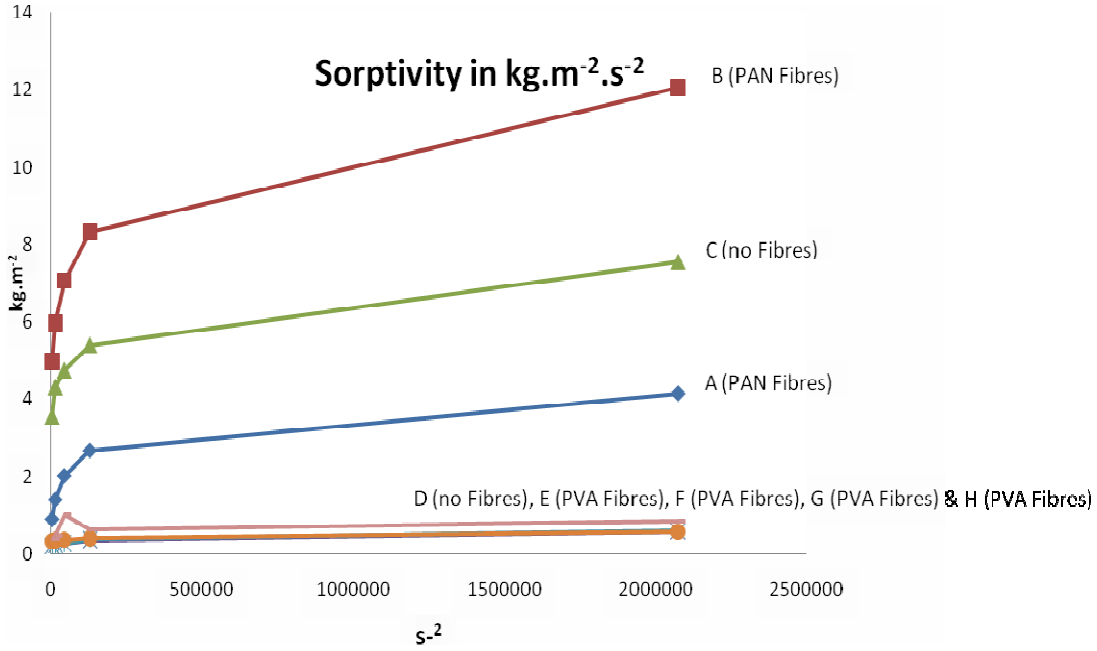

Figure 4.48 Sorptivity results

The sorption coefficients values as indicated in Table 4.5 are lower than the value of 3 $kg.m^{-2}.s^{-1/2}$ that are currently suggested for the WAC of Vaalputs (based on current disposed concrete waste containers) and are therefore acceptable for disposal at Vaalputs. The photos of the matrixes are shown in Figure 4.49.

Table 4.5 Sorption coefficients for the different matrixes

Matrix	Fibre added	Sorption coefficient *A*
A	PAN	0.5
B	PAN	1.1
C	0	0.6
D	0	0.1
E	PVA	0.1
F	PVA	0.1
G	PVA	0.1
H	PVA	0.1

To determine the possibility of leaching of uranium from the matrixes, TBP – kerosene mixture were spiked with low level enriched uranium, absorbed into Nochar 910 and encapsulated in PPC cement as shown in Table 3.4. The leaching tests were performed according to Section 3.7.2. Background activity for deionised water was similar to activity measurements for the samples after 14 days, as seen in Appendix 14. In order to confirm these gamma results, the water was also chemically analysed with the GC-MS and UV-visible spectroscopy. The Bromo – Padap [2-(5-bromo-2-pyridylazo-)-5diethylaminophenol] method performed on the UV-visible spectroscopy instrument gave results of 0 ppm of uranium (Appendix 13) for three water solutions. This confirms the gamma detection results that no uranium leached out of the samples.

The low sorptivity values and leaching rates can be contributed to the high density matrixes that are formed by the addition of fibres.

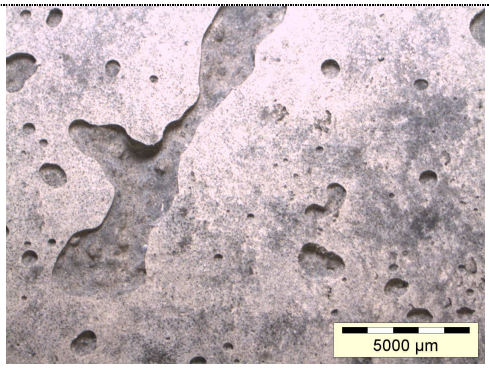

No fibres present in C

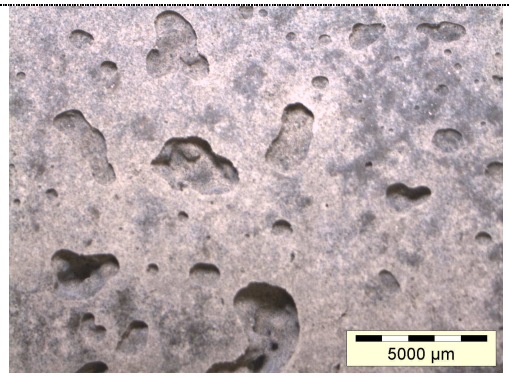

No fibres present in D

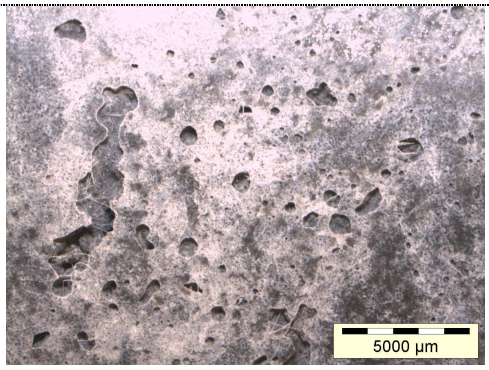

PVA fibres in Sample F

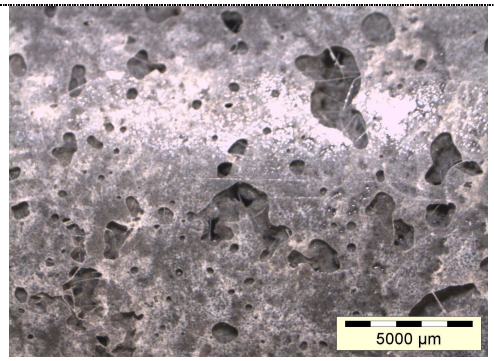

PVA fibres in Sample H

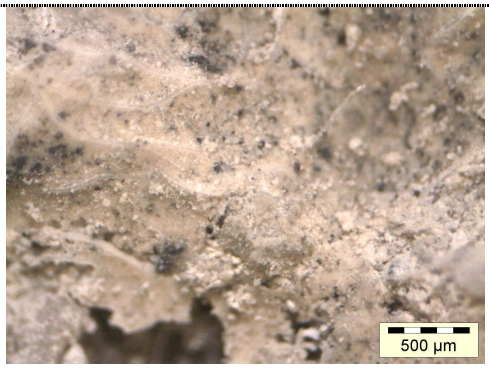

PAN fibres in A

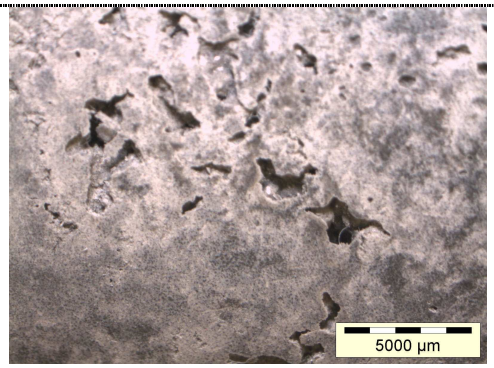

PAN fibres in B

Figure 4.49 Photos of the Fibre reinforced oil – N 910 encapsulated bricks.

Different homogeneous samples prepared with the specified amount of polymeric resin and TBP - kerosene mixture and were heated on filter paper to 50 °C in an oven as (shown in Figure 4.50) for 24 h to determine the possibility of TBP leaching from the matrix. This temperature represents the maximum temperature of the waste trenches experienced at Vaalputs. No TBP was observed on the filter paper, implying that the TBP is irreversibly absorbed into the structure of the polymer, for these conditions and no leaching occurred.

The results indicate that environmental circumstances such as temperature and standing water temperature did not have adverse effects on the leaching and sorption performances of the matrixes tested.



Figure 4.50 Temperature stability of TBP absorbed onto Nochar

Chapter 5 SUMMARY OF RESULTS

Treatment of Necsa Organic Waste

Mixed liquid waste at Necsa consists of different organic compounds that cannot be treated utilising a single treatment technique as studied in this project. The radionuclide content that contribute to radiolysis of the organic waste at Necsa can add to the formation of degradation products. The higher the uranium enrichment factor, the higher the possibility of dibutyl phosphate (DBP) degradation. IN Necsa β-emitters such as ^{14}C in the waste can be associated with scintillation liquid used for the analysis, while γ emitters such as ^{137}Cs, ^{60}Co, and ^{110}Ag can be associated with decontamination detergents, such as Contrad, used for decontamination of surfaces.

The results of this study regarding the treatment of organic waste can be summarized as follows:

Alkaline Hydrolysis

This technique worked excellent for the destruction of a pure organic solution containing 30% TBP diluted in kerosene as shown in literature (Manohar et al., 1999). However, GC-MS results indicate that when other organic constituents and / or detergents are present within the TBP – kerosene mixture, effectiveness of the hydrolysis technique declined dramatically.

UV destruction of organic components

The non-thermal oxidative techniques such as UV treatment showed slow degradation of detergents, especially for Contrad and acetone. UV treatment of scintillation showed good degradation.

Plasma destruction of organic components

The organic test mixture was degraded with plasma into smaller and shorter carbon structures which are volatile. Under the current test conditions this technique will generate gaseous secondary waste that must be treated. Necsa was not able to obtain a nuclear licence for operating such a facility and therefore the technique cannot be considered.

Ozone destruction of organic components

The successful treatment of ozone on scintillation liquid and Contrad detergent with ozone is an indication that it would also degrade other organic components in Necsa's waste. Destruction rate values between $4x10^{-3}$ s^{-1} to $4x10^{-4}$ s^{-1} for organic constituents were found in other laboratories (Klasson, 2002) and are in line with degradation rates of 1.5×10^{-3} s^{-1} to 1.5×10^{-4} s^{-1} found for scintillation liquid and acetone respectively. Results can be dramatically improved by increasing the concentration of supplied ozone, although handling such a system could be difficult.

Ozone combined with UV light showed an improvement only for the destruction of scintillation liquid. The destruction rates for acetone and Contrad detergent were similar for ozone on its own or when combined with UV radiation. It must also be noted that ozone degraded the organics miscible in the aqueous phase.

Sorptivity and leaching

Results indicate that environmental factors at Vaalputs will have no detrimental effects on the matrixes tested.

Chapter 6 RECOMMENDATIONS

The results from this study indicate that no single treatment process can be used for the treatment of organic waste stored at Necsa. Based on the results from this research, a combination of treatment processes schematically presented in Figure 6.1 is proposed.

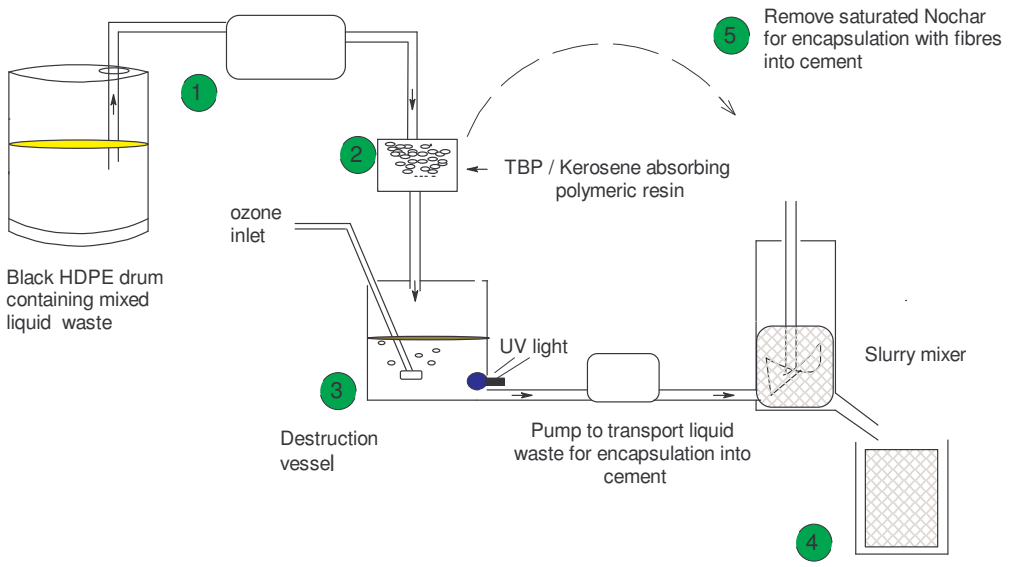

Figure 6.1 Schematic diagram for the proposed treatment of mixed liquid waste

The process can be described as follows:

1. Transfer of radioactive waste from a HDPE drum using a specified pump system into a holding tank(s) has been demonstrated.

2. The holding tank consists of Nochar absorbent and with a slurry mixer, the TBP, kerosene and other long chain organic molecules can be absorbed into the absorbent. After absorption the liquid can be drained into the destruction vessel.

3. In the destruction vessel the non-absorbed organic waste are subjected to ozone combined with UV radiation. The destruction process halts after confirmation with UV-visible analyses that the organic compounds are destroyed. The solution is then neutralised by addition of NaOH to an alkaline pH, suitable for encapsulation into cement. This solution is then pumped to the encapsulation tank.

4. At the encapsulation site the destroyed organic compounds in an aqueous phase can be encapsulated in a mixture of cement and vermiculite (standard procedure at Necsa). This solution will satisfy the WAC of Vaalputs.

5. When the capacity limit of the Nochar resin has been reached, the resin can be encapsulated into cement using fibres.

APPENDIXES

APPENDIX 1

Reprocessing – PUREX cycle schematically presented for recovering of uranium and plutonium from high level waste.

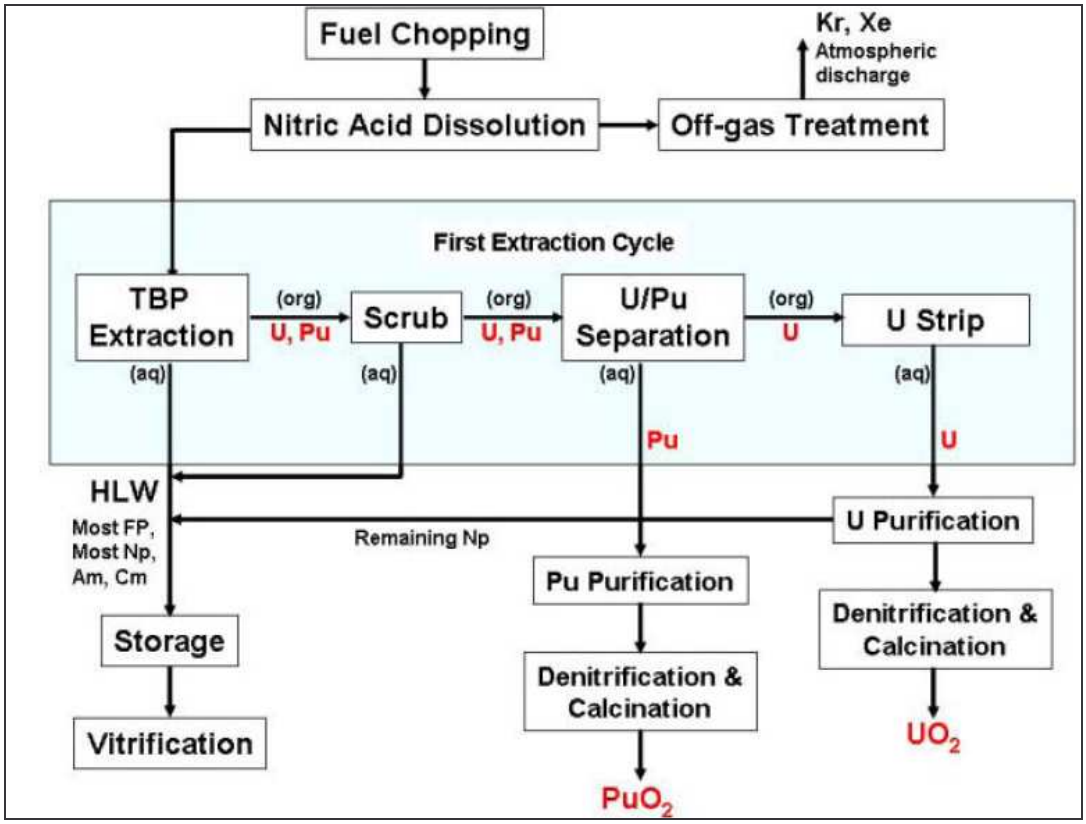

(European Nuclear Society, 2010)

APPENDIX 2

Evaporator schematically displayed used to decrease waste volumes in the nuclear industry.

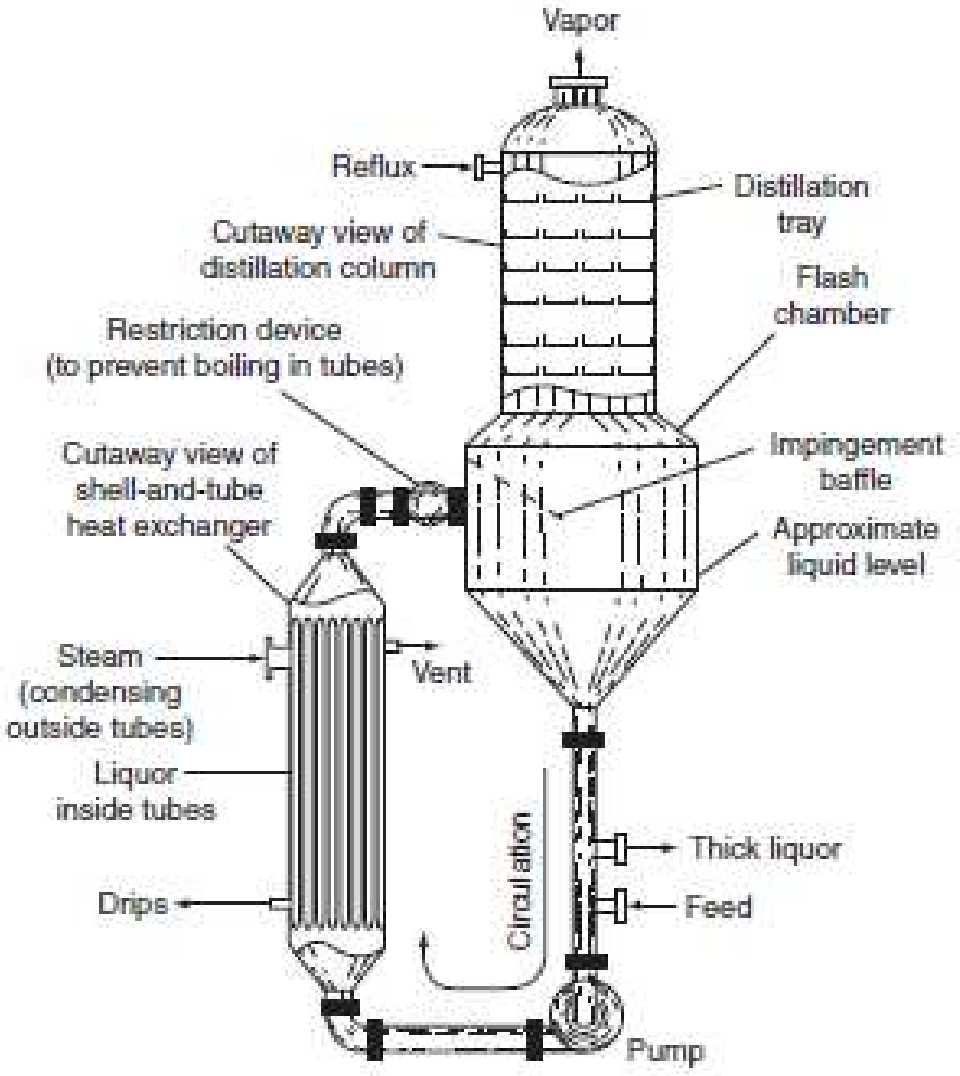

(IAEA, 2004)

APPENDIX 3

Low pressure lamp information

Spectral output between 185nm and 353.7 nm for arc input power 8W for a low pressure UV lamp

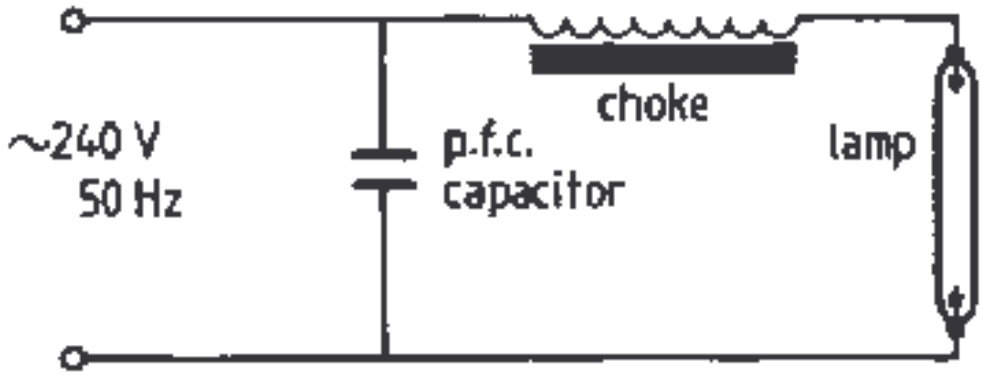

Figure 7.1 Circuit diagram of lamp setup (Phillips, 1983).

The lamp is constructed of vitreous silica with low thermal expansion ($5 \times 10^{-7} \cdot K^{-1}$). Low pressure mercury lamps are the most efficient converters of electrical energy into UV radiation between 200 nm and 280 nm. The lamps switch on immediately and operate at low temperatures not thermally influencing the material it radiates. They are extensively use for curing of coatings and polymers.

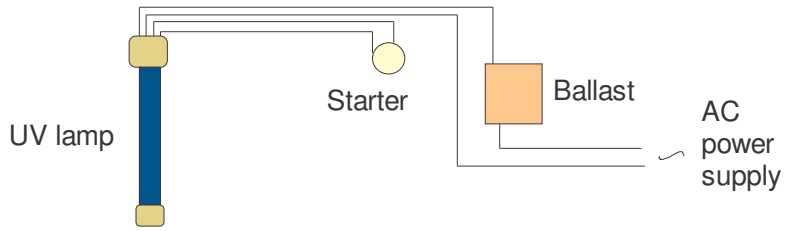

Figure 7.2 The 8 W low pressure UV lamp used and electrical connections.

APPENDIX 4

Ozone setup used for radioactive waste treatment is schematically presented below.

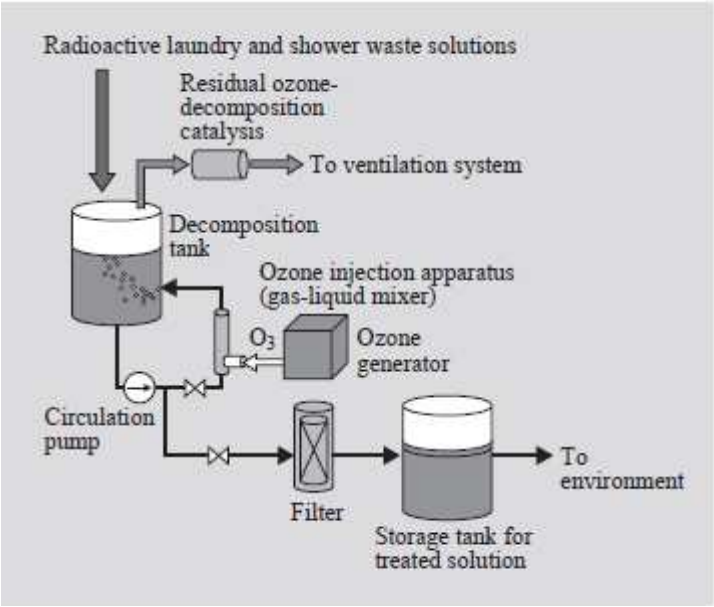



A pilot plant using ozone to destruct organic waste in Japan. (Fukasawa, et al., 2001)

APPENDIX 5

Determining the Concentration of ozone being generated

Potassium iodide (20 g) is dissolved in 210 ml distilled water wherein the ozone was bubbled (140 kPa regulator pressure) through for 5 min, Sulphuric acid (25%, 10 ml) is added to this and back titrated with 0.1 M sodium thiosulfate.

The iodine liberated in the reaction reacts with the sodium thiosulfate which is used to calculate the ozone concentration according to the following reactions:

$$O_3 + 2I^- + 2H_3O^+ \rightarrow O_2 + I_2 + 3H_2O$$

$$I_2 + 2S_2O_3^{2-} \rightarrow 2I^- + S_4O_6^{2-}$$

Therefore 1 mol ozone produce 1 mol iodine, consuming 2 moles thiosulfate.
The 1 ml 0.1 molar thiosulfate would therefore give (0.1 x 0.001x48) /2 g ozone
1 ml 0.1 ml thiosulfate = 2.4 mg ozone. The average reading for the volume thiosulfate consumed for 5 min were 16.34 ml.

The ozone generated is then 38.5 mg for 5 min and equal to 461mg h^{-1}.

Experimental run	0 0.1 M sodium thiosulfate titrated
1	16.9
2	17.2
3	15.0
Averaged	**16.34 (for 5min bubbling)**

APPENDIX 6

GC Calibration.

Mixtures of analytical grade reagents were injected and an internal standard was used to compensate for injector errors.

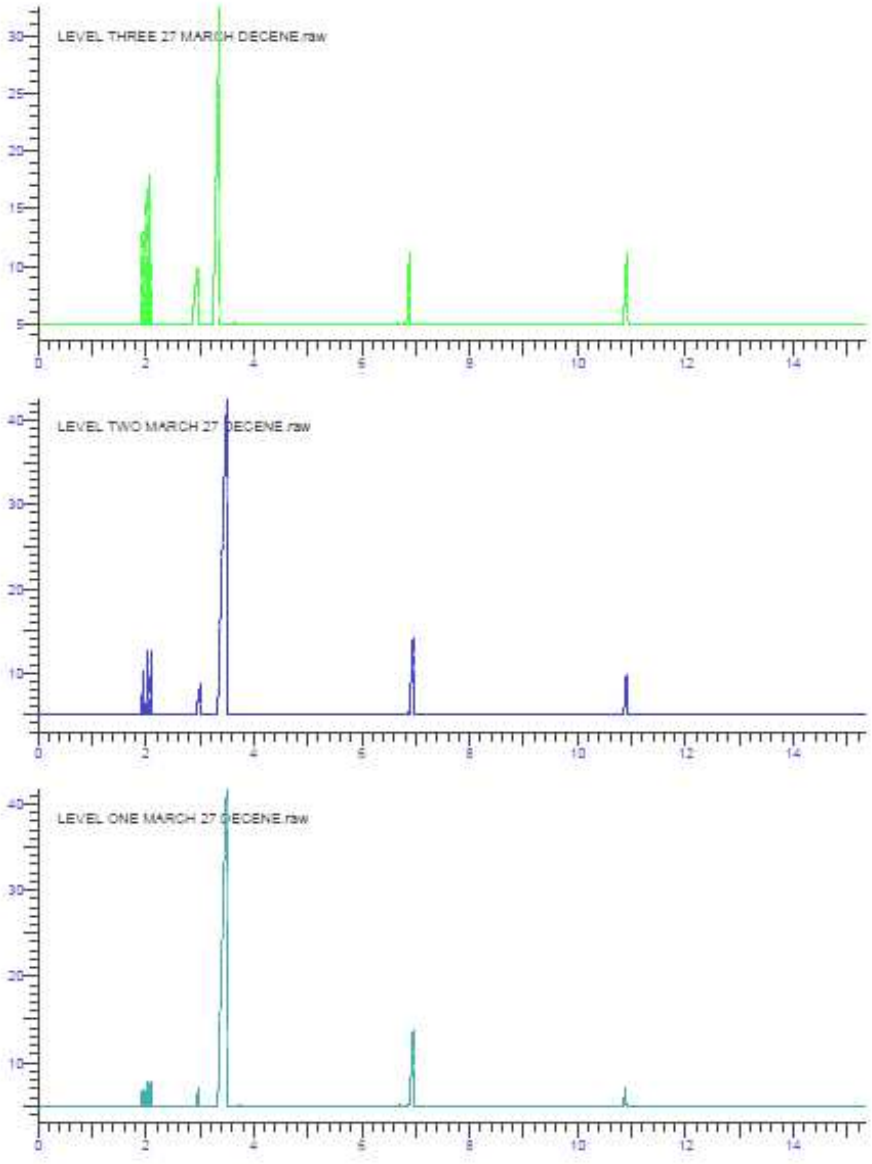

APPENDIX 7

GC MS Internal auto tuning was performed to evaluate whether the detector is performing satisfactorily prior to analysing samples.

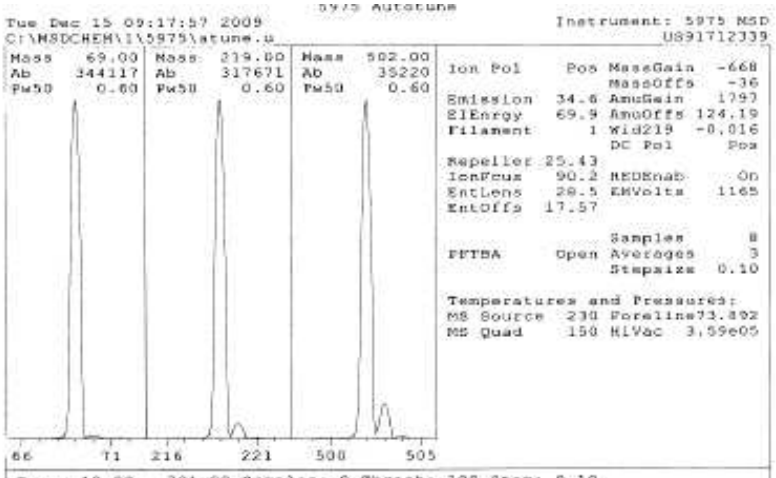

APPENDIX 8

Cary UV-visible spectrophotometer performance test results indicate that the UV-visible spectrometer is detecting the wavelengths correctly and can be use for analyses.

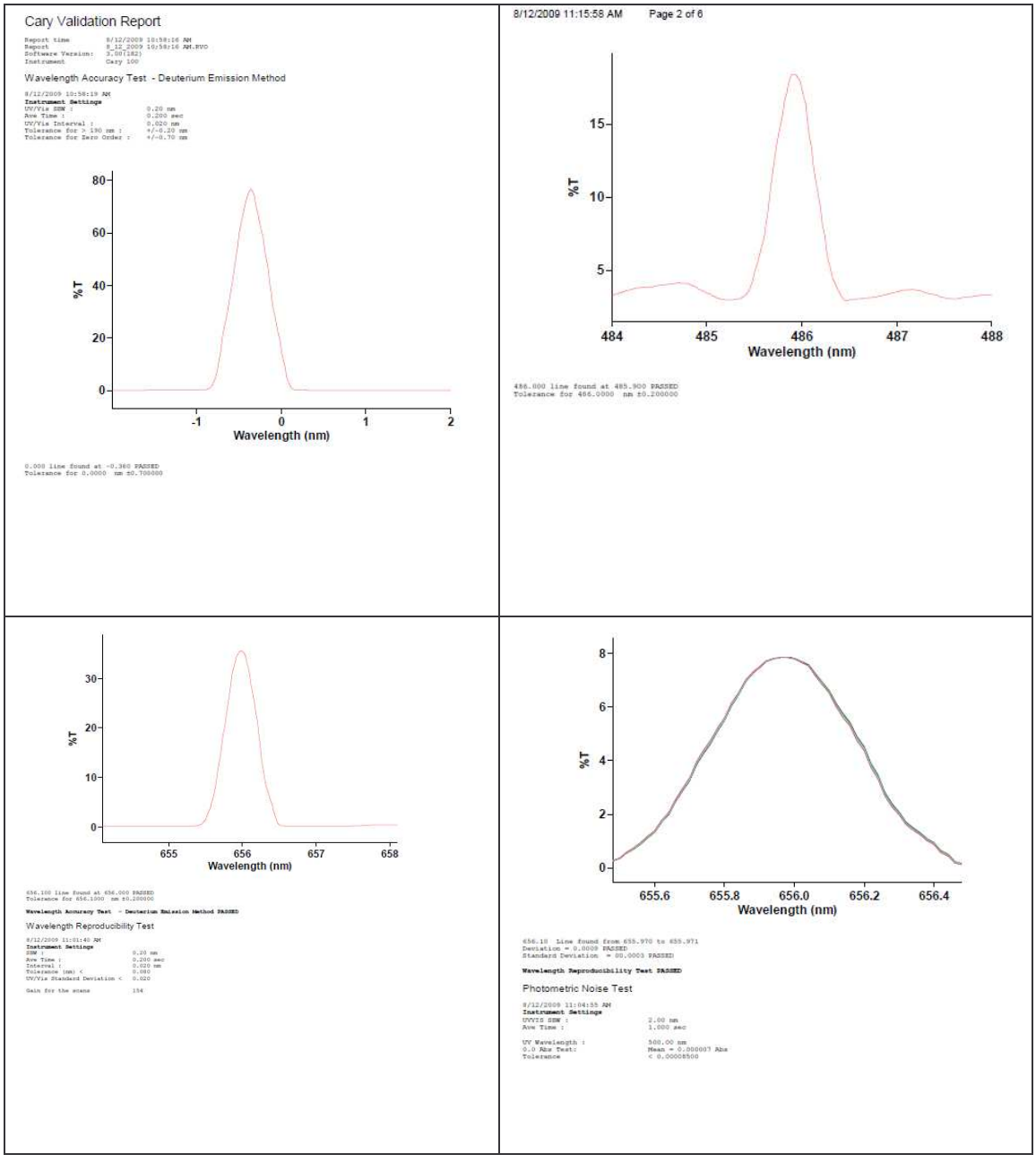

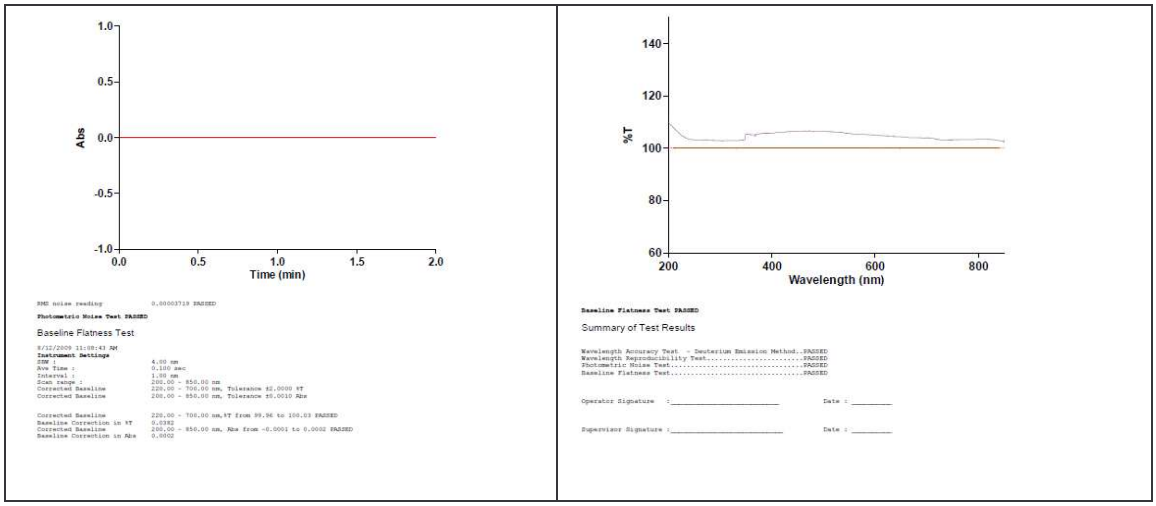
1.0
0.5
0.0
-0.5
-1.0
Abs
0.0
0.5
1.0
1.5
2.0
Time (min)
RMS noise reading 0.00003719 PASSED
Photometric Noise Test PASSED
Baseline Flatness Test
8/12/2009 11:08:43 AM
Instrument Settings
SBW : 4.00 nm
Ave Time : 0.100 sec
Interval : 1.00 nm
Scan range : 200.00 - 850.00 nm
Corrected Baseline 220.00 - 700.00 nm, Tolerance ±2.0000 %T
Corrected Baseline 200.00 - 850.00 nm, Tolerance ±0.0010 Abs
Corrected Baseline 220.00 - 700.00 nm,%T from 99.96 to 100.03 PASSED
Baseline Correction in %T 0.0382
Corrected Baseline 200.00 - 850.00 nm, Abs from -0.0001 to 0.0002 PASSED
Baseline Correction in Abs 0.0002
140
120
100
80
60
%T
200
400
600
800
Wavelength (nm)
Baseline Flatness Test PASSED
Summary of Test Results
Wavelength Accuracy Test - Deuterium Emission Method..PASSED
Wavelength Reproducibility Test.....PASSED
Photometric Noise Test.....PASSED
Baseline Flatness Test.....PASSED
Operator Signature :_____ Date : _____
Supervisor Signature :_____ Date : _____

=

APPENDIX 9

The FTIR were tested for correct energy intensities, noise levels and a calibration evaluation with polystyrene was performed to ensure that the instrument gave correct results.

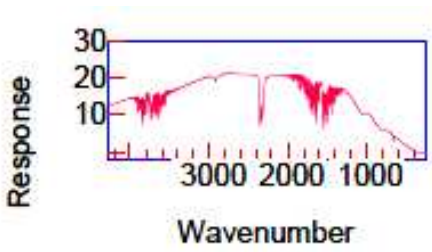

Energy

Average of 2400-2600, 2000-2100: 20.730

Value at 4000 / Value at 2000: 0.709

Value at 2000 / Value at 1000: 1.972

Value at 150 / Maximum Value: -0.000

Energy Intensity Test: Passed

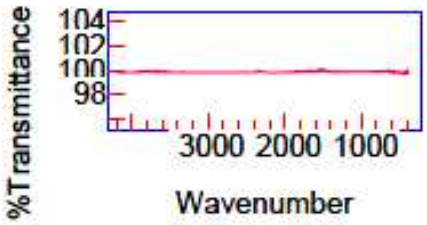

100% Line

Noise Level around 4000: 0.010

Noise Level around 2000: 0.006

Noise Level around 1000: 0.008

Noise Level around 500: 0.056

100% Line: Passed

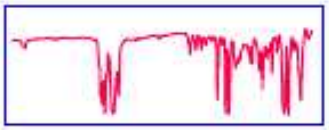

Polystyrene

Center of Gravity around 1028: 1027.648

Center of Gravity around 1601: 1601.726

Center of Gravity around 3060: 3059.778

Polystyrene: Passed

Results

Energy Intensity Test: Passed

Energy Shape Test: Passed

100% Line Noise Level Test: Passed

100% Line Flatness Test: Passed

Polystyrene Peaks Test: Passed

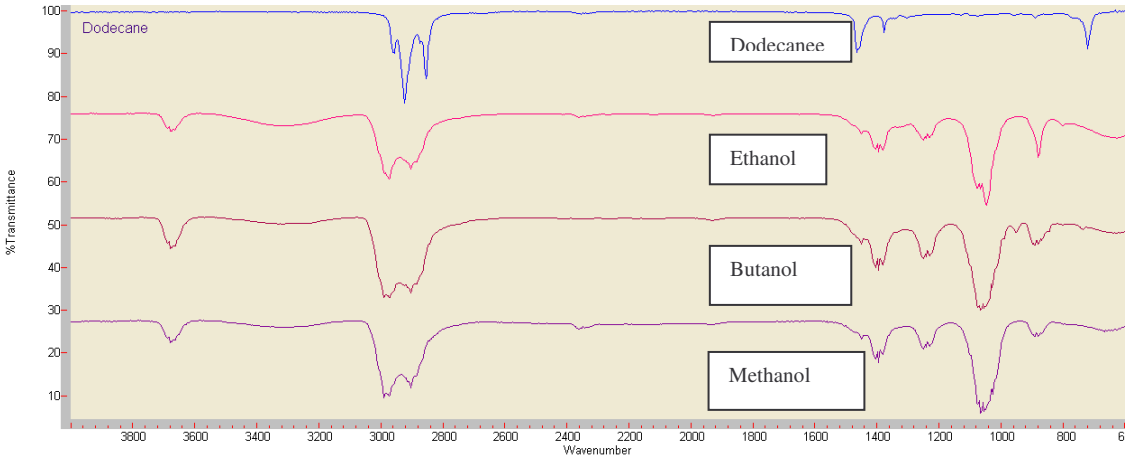

Analytical grade organic solvents stored with IR for quantifying purposes

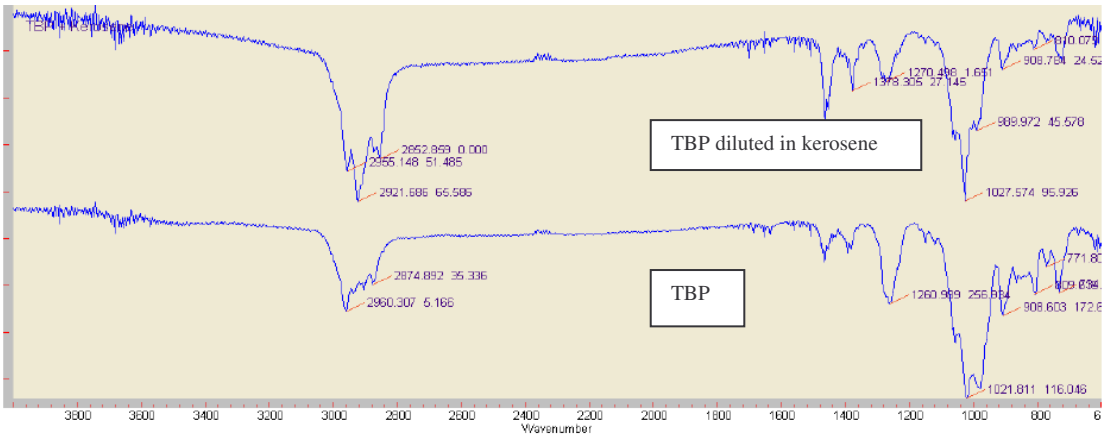

TBP analysed with IR

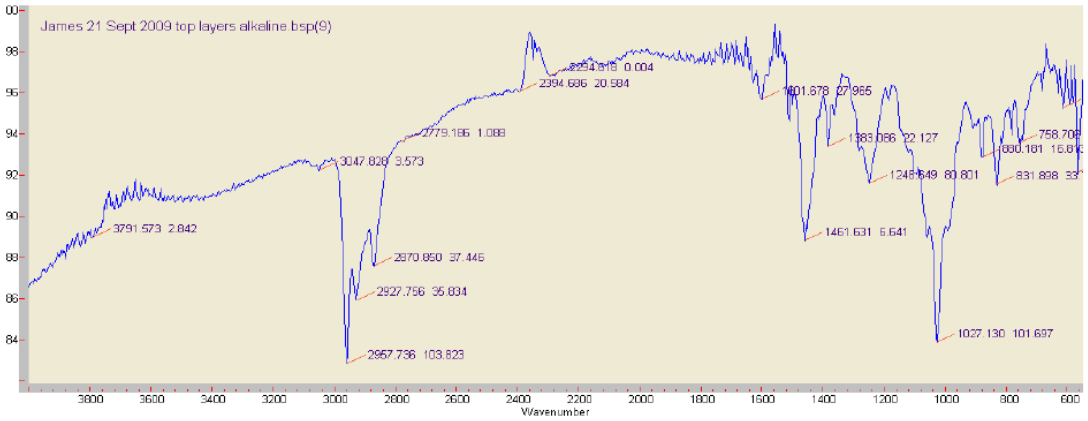

Top organic layer of TBP hydrolysed with alkaline hydrolysis

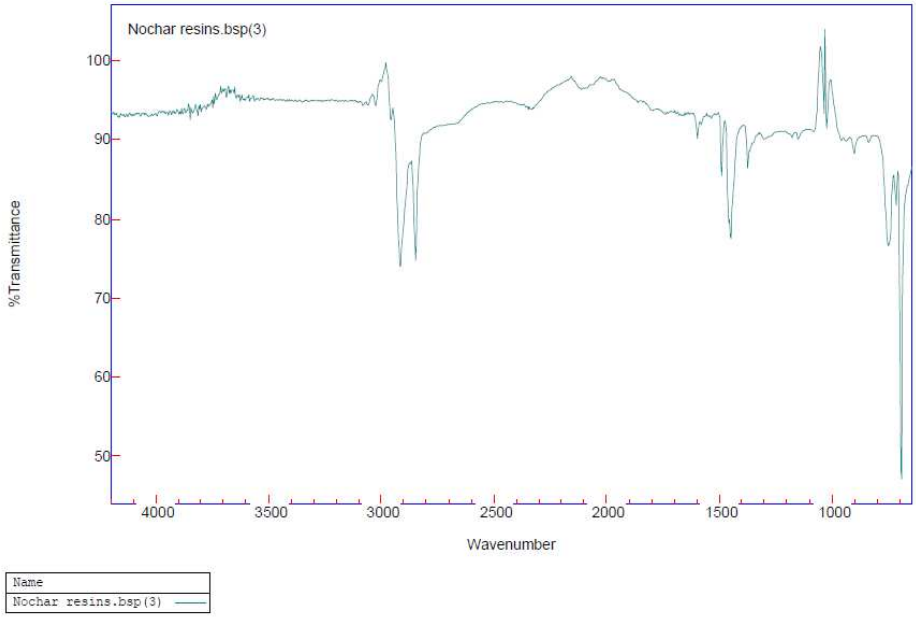

Noschar N910 resin analysed with IR

APPENDIX 10

The schematic representation of the FTIR gives a better understanding of how the instrument functions and also why one can change from a clear polystyrene film to a diamond attenuated reflective surface.

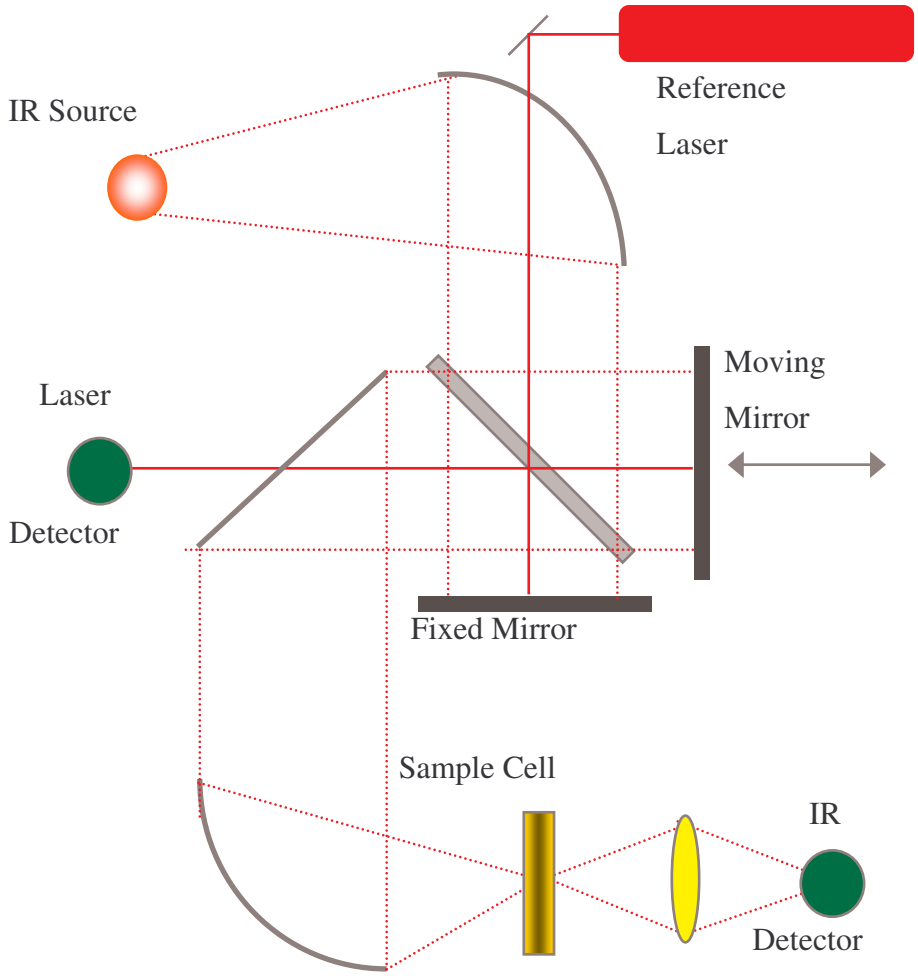

FTIR Schematic (Varian, 2004)

APPENDIX 11

The energy calibration for the gamma detector is crucial to ensure that the energies detected from the samples placed in the sample holder are correct and can be identified with the library.

```
Energy Calibration Report            2009/09/28 08:25:15 AM       Page  1

*****************************************************************************
*****       E N E R G Y   C A L I B R A T I O N   R E P O R T       *****
*****************************************************************************

     Detector Name:  DET01
     Sample Title:   20b

       *************  ENERGY CALIBRATION COEFFICIENTS  *************

              Energy Calibrate Performed on:  2009/09/01 10:16:06 AM
                     by:
              Energy Calibrate Type:          POLY

   Energy(keV) =   -20.937 +     1.899*ch +  0.00E+000*ch^2 +  0.00E+000*ch^3

       *************  SHAPE CALIBRATION COEFFICIENTS   *************

              Shape Calibrate Performed on:  2009/09/01 10:16:06 AM
                     by:

              FWHM     =    61.120  +  -1.492*E^1/2

              LOW TAIL =   3.1E+001 + -2.2E-002*E

****************     ENERGY CALIBRATION RESULTS TABLE     ****************

                   Centroid      Centroid         Energy
                   Channel       error            (keV )
                     74.14         0.43            121.78
                    192.68         0.13            344.28
                    410.02         0.38            778.90
                    763.04         1.20           1408.01

       *********     SHAPE CALIBRATION RESULTS TABLE      *********

             Energy     FWHM       FWHM         TAIL        TAIL
             (keV )     channels   error        channels    error
              121.78      7.49      0.93          14.39      1.00
              344.28     18.47      0.30          11.75      1.18
              778.90     39.48      0.96          20.62      2.75
             1408.01      0.83      0.29           0.04      0.03
Efficiency Calibration Report            2009/09/28 08:25:38 AM   Page  1
```

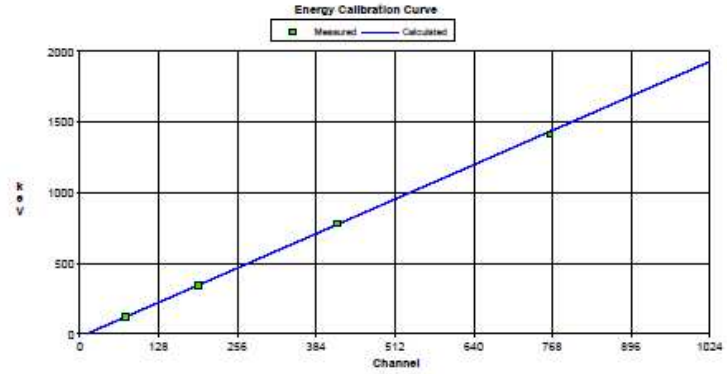

Datasource: C:\GENIE2K\CAMFILES\ULT\sample filter E.CNF
Energy = -2.094e+001 keV + 1.899e+000*Ch
FWHM = 6.112e+001 keV - 1.492e+000*E^1/2
Lo Tail = 3.068e+001 keV - 2.195e-002*E

****
**** E F F I C I E N C Y C A L I B R A T I O N R E P O R T *****
****

Detector Name: DET01
Sample Title: 20b

Geometry Description: 5ml
Efficiency Calibration Performed on: 2009/09/01 10:17:18 AM
by:
Geometry Type Used: DUAL

Efficiency Triplets
==========

Energy	Efficiency	Error
121.78	3.06E-001	1.07E-002
344.28	2.96E-001	1.00E-002
778.90	8.45E-002	4.53E-003

DUAL Efficiency Calibration Equation
==========

Single Equation Terms ->	Offset:	-23.759
	Slope:	8.592
	Quadratic:	-0.810
	Cubic:	0.000
	4th Order:	0.000
	5th Order:	0.000
	6th Order:	0.000
	7th Order:	0.000
	8th Order:	0.000
	9th Order:	0.000

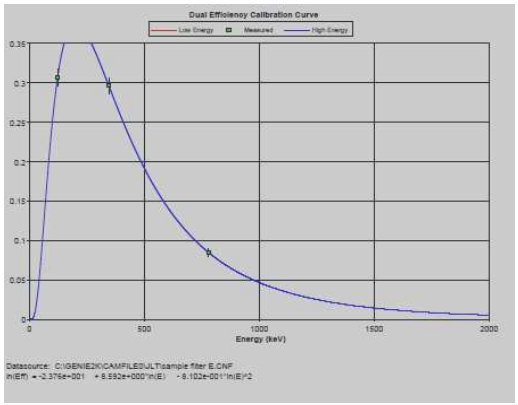

Datasource: C:\GENIE2K\CAMFILES\ULT\sample filter E.CNF
ln(Eff) = -2.376e-001 + 8.592e+000*ln(E) - 8.102e-001*ln(E)^2

APPENDIX 12

Trace amounts of TBP detected in the water used in the leaching tests were also analysed with the GC MS and only trace amounts of TBP were detected.

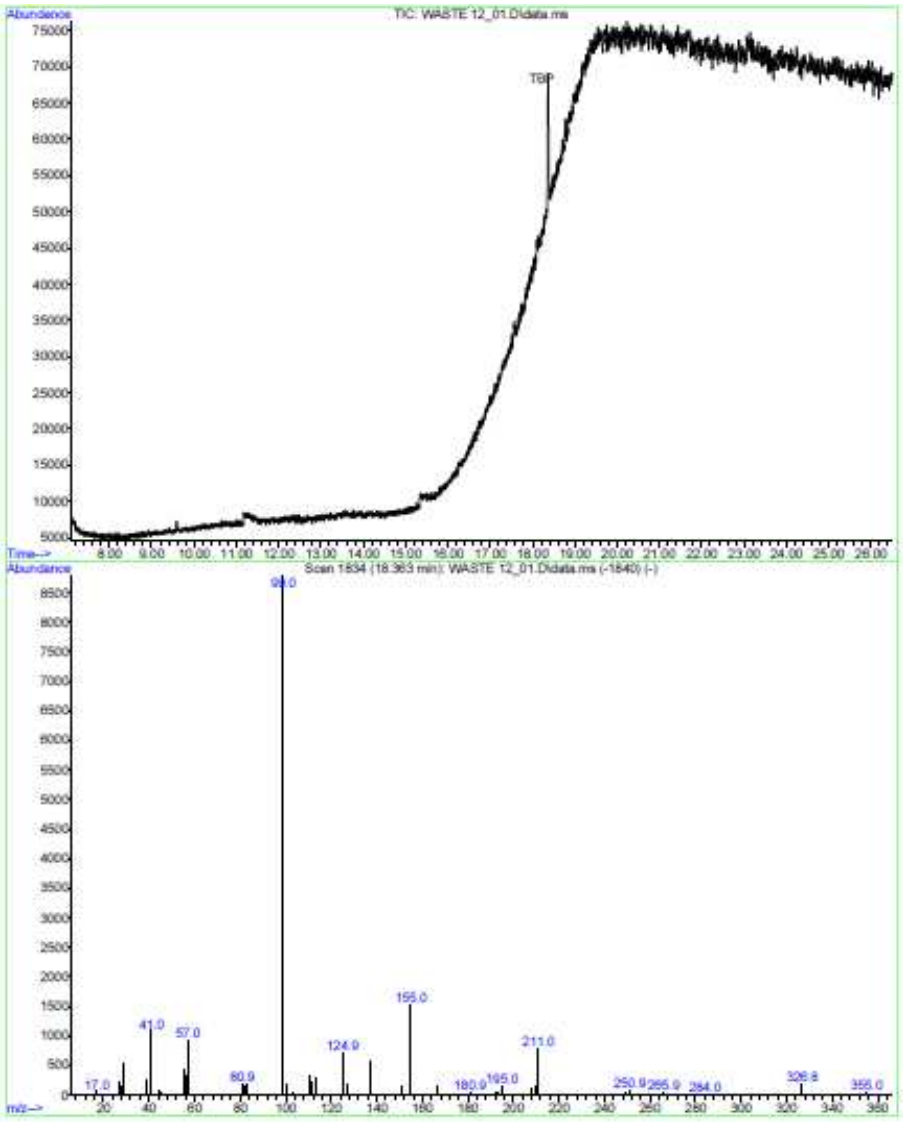

APPENDIX 13

UV VIS Uranium determination with Bromo-PADAP method also confirmed that no uranium was present in the deionised water used in the leaching experiments. This method is sensitive to ranges 0 to 2 ppm uranium.

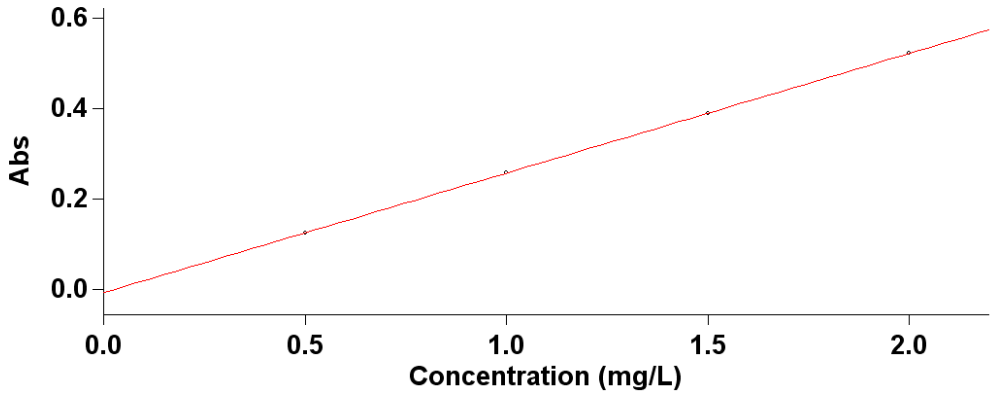

Sample	Concentration mg/L	F	Mean	SD	%RSD	Readings
1ppm						0.1948
						0.1947
	0.8		0.1946	0.0002	0.09	0.1944
1						0.0025
						0.0027
	0.0		0.0026	0.0001	2.22	0.0026
2						-0.0004
						-0.0009
	0.0		-0.0007	0.0003	-38.	-0.0008
3						-0.0001
						-0.0001
	0.0		-0.0001	0.0001	-57.	-0.0002

APPENDIX 14

Gamma Counter results for leaching tests confirmed that no activity was present in the deionised water used in the leaching experiments.

<table>
<tr><td>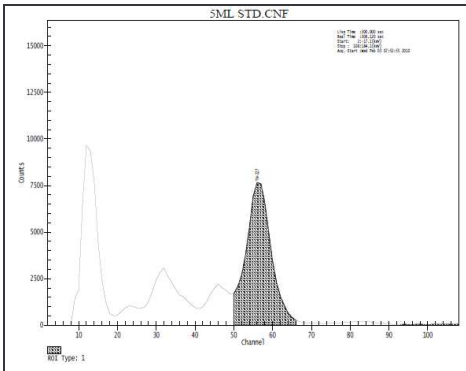
</td><td></td></tr>
<tr><td></td><td></td></tr>
<tr><td>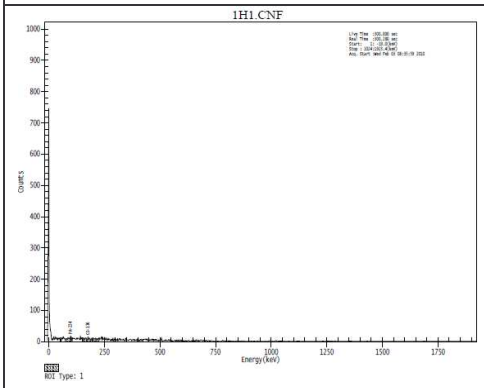
</td><td>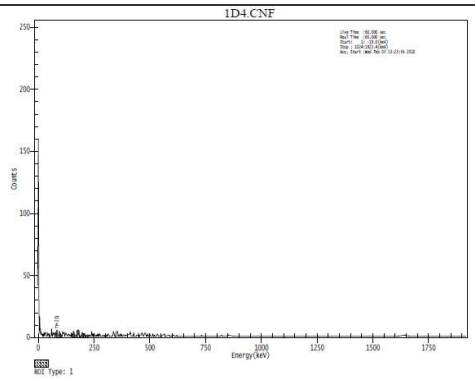
</td></tr>
<tr><td>Sample 1 after 1 hour</td><td>Sample 1 after 4 days</td></tr>
</table>

APPENDIX 15

	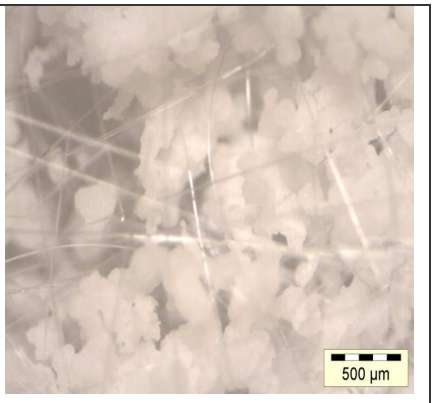
N910 resin	PVA fibres mixed with N910 Resin
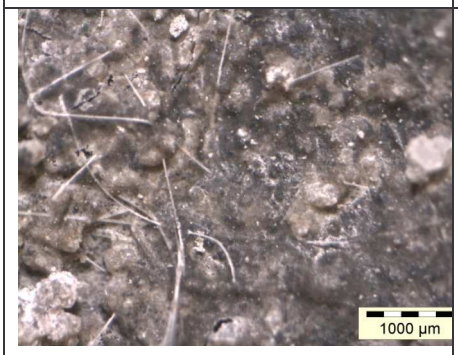	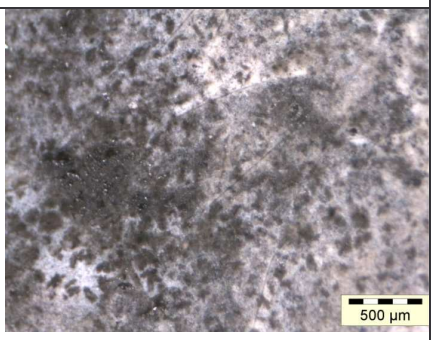
Cement mixed with Nochar and PAN fibre	Cement mixed with Nochar and PVA fibre

REFERENCES

Adamson, M. G., Hsu P. C., Hipple, D. L., Foster, K.G., Hopper, R. W. and Ford, T. D. (1998) Organic Waste Processing Using Molten salt Oxidation, Euchem Conference on Molten Salts France. June 27-July 3.

Alley, W. (1994) Regional Groundwater Quality, Van Nostrand Reinhold, New York, New York.

American Nuclear Society Standards Working Group, (1986) Measurement of the Leachability of Solidified Low Level Radioactive Wastes by a Short Term Test Procedure. ANSI/ANS-16.1-1986, Illinois, U.S.A.

Bentz, P. B., Ehen, A. M., Ferraris, F. C. and Garboczi, J. E. (2001) Sorptivity Based Service Life Predictions for Concrete Pavements, *International Society for Concrete Pavements*. September 9-13

Beyleveld, J. and Truter, W. (2005) Vaalputs National Radioactive Waste Disposal Facility: System Description and Probability Safety Assessment. Internal Necsa Report no VLP-PSA-01/0901, p. 30.

Bezerra, E. M., Joaquim, A. P and Savastano, H. (2004) Some Properties of Fibre Cement Composites With Selected Fibres. Pirassununga,SP, Brazil, 29 de Outobro, November 3.

Bolt, O. R. and Carrol, G. J. (1963) Radiation Effects on Organic Materials, Acedamic Press Inc., New York.

Brian S., Furniss, A. J., Hannaford, Peter W. G., Smith, A. R. and Tatchell, (1998) Vogel's Textbook Of Practical Organic Chemistry, Fifth edition.

Bruno, L. (1991) Ozone in water treatment: Application and Engineering: Cooperative Research, pp 11-55.

Coates, J. (2000) Interpretation of Infrared Spectra, A Practical Approach, Encyclopaedia of Analytical Chemistry, pp. 10815-10837.

Denes, F. C. Z. and Sorin, M. (2004) *Macromolecular Plasma-Chemistry*: An Emerging Field of Polymer Science, Prog.Polym. Sci. Elsevier, Vol 29, pp. 815–885.

EI-Dessouky, M.I., El-Aziz, M. M., Mossalamy, A. E. H. E. and Aly, H. F. (2001) Wet Oxidation of Spent Organic Waste Tributyl Phosphate / Diluents, *Journal of Radioanalytical and Nuclear Chemistry*, Volume 249, no 3, pp. 643-647.

European Nuclear Society, (2010) Info pool / Glossary http://www.euronuclear.org/info/encyclopedia/p/purex-process.htm, Date accessed, 12 July 2010.

Fernadez, J., Riu, J. and Garcai-Calvo, R. A. (2004) Determination Of Photo Degradation and Ozonation By Products of Linear Alkylbenzene Sulfonates By Liquid Chromatography and Ion Chromatography Under Controlled Laboratory Experiments, ELSEVIER, Talanta, pp. 69-79.

Fukasawa, T., Hajime, U. and Masami, M. (2001) Nuclear Fuel Cycle Technologies for a Long Term Stable Supply of Energy, Hitachi Review Volume 50, no 3.

Gomez, E., Amutha, R. D., Cheeseman, C.R., Deegan, D., Wise, M. and Boccaccini, A.R. (2009) Thermal Plasma Technology for Treatment of Wastes: A Critical Review, *Journal of Hazardous Materials*, Volume 161, pp. 614-626.

Gunale, T.L., Mahajani, V.V., Wattal, P.K. and Srinivas, C. (2009) Studies in liquid phase mineralization of cation exchange resin by hybrid process of Fenton dissolution followed by wet oxidation, *Chemical Engineering Journal*, Volume 149, pp. 371 – 377.

Horvath, M., Bilitzky, L. and Huttner, J., et al (1980) Ozone Monograph 20 Topics In Inorganic And General Chemistry, A Collection Of Monographs

Horwitz, E. P.and Schulz, W. W. (1986) Progress In Metal Ion Separation And Pre-Concentration, Journal of the Less Common Metals, Volume 122 pp 125-138.

IAEA, International Atomic Energy Agency, (1988) Immobilization of Low and Intermediate Level Radioactive wastes with Polymers, Technical Report Series no 289, Vienna.

IAEA, International Atomic Energy Agency, (2001) Combined Methods for Liquid Radioactive Waste Treatment, Technical Report Series no 1336, IAEA, Vienna.

Innis, P. (2004) Hazardous Waste Site Sampling Basics, Technical Notes 414, National Science and Technology Centre, Denver Colorado

International Atomic Energy Agency, (1992) Treatment and Conditioning of Radioactive Liquids, Technical Report Series no 656, IAEA, Vienna.

International Atomic Energy Agency, (1989) Options for the Treatment and Solidification of Organic Radioactive Waste, Technical Report Series no 294, IAEA, Vienna.

International Atomic Energy Agency, (2004) Predisposal Management of Organic Radioactive Waste, Technical Report Series no 427, IAEA, Vienna.

Judd, L. (2001) A Demonstration of Silver II for the Decontamination and Destruction of Organics in Transuranic Wastes, AEA Technology Engineering Services Inc, Sterling VA 20166, October.

Kelly, D. and Campbell, D. (2005) Proven Technologies for the treatment of Complex Radioactive Liquid Waste Streams; Us Department of Energy and International Case studies, Glasgow, Scotland.

Kevelam, J. (1999) Polymer-Surfactant Interactions, Aqueous Chemistry of Laundry Detergents, Thesis Rijksuniversiteit Groningen.

Kirsten, (1999) University of Wisconsin - Milwaukee, Environmental Health, Safety and Risk management Radiation Safety Program.

Kidd, S. and Bowers, J. S. (1995) Treatment of Mixed Waste Coolant, Lawrence Livermore National Laboratory, San Josde, CA, February.

Klasson, K., Tsouris, C. and Jones, S. (2002) Ozone Treatment of Soluble Organics in Produced Water, Petroleum Environmental Research Forum Projec*t* 98-04.

Manohar, S., Srinivas, C., Vincent, T., and Wattal, P. K. (1999) Management of Spent Solvents by Alkaline Hydrolysis Process, PERGAMON, Waste Management, Volume 19, pp. 509-517.

Meyer, A. (2006) Conditioning options for uranium contaminated Y-Plant oil, Necsa, GEA 1652.

Meyer, W. (2009) The Encapsulation of Possible Contaminated Oil Generated at the Compressors in a PBMR Plant, Internal Necsa Report.

Misra, S. K., Mahatele, A. K., Tripathi, S. C., and Dakshinamoorthy, A. (2009) Studies On Simultaneous Removal of Dissolved DBP and TBP As Well As Uranyl Ions from Aqueous Solutions by Using Micellar Enhanced Ultrafiltration Technique, Hydrometallurgy, Volume 96, pp. 47-51.

Morss, R. L., Edelstein, M. N. and Fuger, J. (2006) The Chemistry of the Actinide and Transactinide Elements, Springer Netherlands, pp. 253-698.

Nardi, L. (1989) Use of Gas chromatography in the study of the oxidative decomposition of spent organic solvents from reprocessing plants, ELSEVIER, *Journal of Chromatography*, Volume 463, pp. 81 - 93.

Paula, Yurkanis and Bruice, (2008) Organic Chemistry Fourth Edition, pp 1003-1007

Pente, S., Gireesan, P., Thorat, V., Katarani, V.G., Kaushik, C. P., Das, D. and Raj, K. (2008) Study of Different Approaches for Management of Contaminated Emulsified Aqueous Secondary Waste, Elsevier, Desalination Volume 232, pp. 206-215.

Phillips, R. (1983) Sources and Applications Of Ultraviolet Radiation, Academic Press, New York.

Raj, K., Prasad, K. K.and Bansal, N. K. (2005) Radioactive Waste Management Practices in India, ELSEVIER, *Nuclear Engineering and Design*, Volume 236, pp. 914-930.

Schwinkendorf, W. E., Musgrave, B. C. and Drake, R. N. (1997) Evaluation Of Alternative Non-Flame Technologies for Destruction of Hazardous Organic Waste, Lockheed Idaho National Engineering Laboratory, U.S. Department of energy, April.

Song, W., Ravindran, V. and Pirbazari M. (2008) Process Optimization Using A Kinetic Model for the Ultraviolet Radiation Hydrogen Peroxide Decomposition of Natural and Synthetic Organic Compounds in Groundwater, *Chemical Engineering Science*, Volume 63 pp. 3249-3270.

Sora, N. I., Pelosato, R., Botta, D. and Dotelli, G. (2002) Chemistry and Microstructure of Cement Pastes Admixed With Organic Liquids, *Journal of the European Ceramic Society*, Volume 22, pp. 1463-1473.

U.S. Army Corps of Engineers, (2001) Requirements for the Preparation of Sampling and Analysis Plans, Washington, DC 20314

Wagner, J. (1997) New and Innovative Technologies for Mixed Waste Treatment, University of Michigan, School of Natural Resources and Environment for EPA, Office of Solid Waste, August.